OPTIMIZING FIBER-REINFORCED LIGHTWEIGHT HIGH-STRENGTH CONCRETE: THE ROLE OF COCONUT SHELLS, GROUND GRANULATED BLAST-FURNACE SLAG, AND BASALT FIBER IN LOW CEMENT CONTENT MIXES

MUHAMMED TALHA ÜNAL

FACULTY OF ENGINEERING
UNIVERSITI MALAYA
KUALA LUMPUR

2024

OPTIMIZING FIBER-REINFORCED LIGHTWEIGHT HIGH-STRENGTH CONCRETE: THE ROLE OF COCONUT SHELLS, GROUND GRANULATED BLAST-FURNACE SLAG, AND BASALT FIBER IN LOW CEMENT CONTENT MIXES

MUHAMMED TALHA ÜNAL

THESIS SUBMITTED IN FULFILMENT OF THE REQUIREMENTS FOR THE DEGREE OF DOCTOR OF PHILOSOPHY

FACULTY OF ENGINEERING
UNIVERSITI MALAYA
KUALA LUMPUR

2024

UNIVERSITI MALAYA

ORIGINAL LITERARY WORK DECLARATION

Name of Candidate: **Muhammed Talha Ünal**

Matric No: **2037952/1**

Name of Degree: **Doctor of Philosophy**

Title of Project Paper/Research Report/Dissertation/Thesis ("this Work"):

Optimizing Fiber-Reinforced Lightweight High-Strength Concrete: The Role of Coconut Shells, Ground Granulated Blast-Furnace Slag, and Basalt Fiber in Low Cement Content Mixes

Field of Study: Concrete Materials

I do solemnly and sincerely declare that:

(1) I am the sole author/writer of this Work;
(2) This Work is original;
(3) Any use of any work in which copyright exists was done by way of fair dealing and for permitted purposes and any excerpt or extract from, or reference to or reproduction of any copyright work has been disclosed expressly and sufficiently and the title of the Work and its authorship have been acknowledged in this Work;
(4) I do not have any actual knowledge nor do I ought reasonably to know that the making of this work constitutes an infringement of any copyright work;
(5) I hereby assign all and every rights in the copyright to this Work to the Universiti Malaya ("UM"), who henceforth shall be owner of the copyright in this Work and that any reproduction or use in any form or by any means whatsoever is prohibited without the written consent of UM having been first had and obtained;
(6) I am fully aware that if in the course of making this Work I have infringed any copyright whether intentionally or otherwise, I may be subject to legal action or any other action as may be determined by UM.

Candidate's Signature   Date: 12.07.2024

Subscribed and solemnly declared before,

Witness's Signature   Date: 12.07.2024

Name:

Designation:

OPTIMIZING FIBER-REINFORCED LIGHTWEIGHT HIGH-STRENGTH CONCRETE: THE ROLE OF COCONUT SHELLS, GROUND GRANULATED BLAST-FURNACE SLAG, AND BASALT FIBER IN LOW CEMENT CONTENT MIXES

ABSTRACT

The demand for lightweight aggregate concrete (LWAC) has been growing in the construction industry due to its potential to reduce the dead weight of structures while maintaining strength, durability, and cost-effectiveness. This study proposes a method to design LWAC by integrating coconut shell (CS) as coarse lightweight aggregate and a high volume of wet-grinded ultrafine ground granulated blast furnace slag (UGGBS). The wet grinding of GGBS has shown great potential for providing high-volume cement replacement with reduced particle size and an improved hydration property while simultaneously decreasing the density in slurry form. Also, to increase the effectiveness of the hydration reactivity of UGGBS slurry, the ratios of GGBS powder and grinding media volumes to the grinding chamber volume were examined. To optimize the mix design of LWAC, a particle packing model was employed to estimate the packing density and void ratio of the concrete mixture. The study has demonstrated that optimizing the volume content of different CS and mining sand sizes can significantly improve packing density. It is observed that higher packing densities of the aggregate phase and the entire concrete mix lead to reduced void volumes, resulting in a less porous and more compacted concrete matrix. Furthermore, the inclusion of fines and powder content has proven to be an effective method for increasing packing density, which in turn enhances the void-filling capacity and strengthens the concrete. The optimal mix design was determined using the packing density method, and the impact of Basalt Fiber (BF) was investigated at varying levels (0%, 0.15%, and 1%). A comparative analysis was made between normal weight concrete (NWC) and the selected LWAC mixtures with different BF contents in

terms of cost, CO_2 emissions, saturated surface dry density, surface crack conditions, water absorption and porosity, sorptivity, compressive and flexural performances. The results revealed that the incorporation of UGGBS had a substantial positive impact on the mechanical properties of LWAC when BF was incorporated into the CS lightweight concrete mixture. Including 1% BF in the mix demonstrated superior mechanical and transport properties compared to non-fibrous LWAC, highlighting the significance of BF in enhancing the characteristics of high-strength LWAC. As a significant finding of this research, a grade 30 LWAC with a demoulded density of 1864 kg/m^3 containing only 284 kg/m^3 cement was produced. After considering all these approaches and implementations of green high-strength LWAC with a %40 reduction in cement, there are lower CO_2 emissions and reduced manufacturing costs, making it an alternative choice for production.

Keywords: Coconut shell; Wet grinding; Ground granulated blast furnace slag; Packing density; Compressive strength; Transport properties

MENGOPTIMALKAN KONKRIT RINGAN KEKUATAN TINGGI BERAT BERAT BERAT TINGGI: PERANAN TEMBUNG KELAPA, SLAG TUNGKU LETUP GROUND GROUND DAN FIBER BASALT DALAM CAMPURAN KANDUNGAN SIMEN RENDAH

ABSTRAK

Permintaan untuk konkrit agregat ringan (LWAC) telah berkembang dalam industri pembinaan kerana potensinya untuk mengurangkan berat mati struktur sambil mengekalkan kekuatan, ketahanan dan keberkesanan kos. Kajian ini mencadangkan satu kaedah untuk mereka bentuk LWAC dengan mengintegrasikan tempurung kelapa (CS) sebagai agregat ringan kasar dan sanga relau letupan berbutir halus (UGGBS) yang dikisar basah yang tinggi. Pengisaran basah GGBS telah menunjukkan potensi besar untuk menyediakan penggantian simen volum tinggi dengan saiz zarah yang dikurangkan dan sifat penghidratan yang lebih baik sambil pada masa yang sama mengurangkan ketumpatan dalam bentuk buburan. Juga, untuk meningkatkan keberkesanan kereaktifan penghidratan buburan UGGBS, nisbah serbuk GGBS dan isipadu media pengisaran kepada isipadu ruang pengisaran telah diperiksa. Untuk mengoptimumkan reka bentuk campuran LWAC, model pembungkusan zarah telah digunakan untuk menganggarkan ketumpatan pembungkusan dan nisbah lompang bagi campuran konkrit. Kajian telah menunjukkan bahawa mengoptimumkan kandungan volum CS yang berbeza dan saiz pasir perlombongan boleh meningkatkan ketumpatan pembungkusan dengan ketara. Adalah diperhatikan bahawa ketumpatan pembungkusan yang lebih tinggi bagi fasa agregat dan keseluruhan campuran konkrit membawa kepada pengurangan isipadu lompang, menghasilkan matriks konkrit yang kurang berliang dan lebih padat. Tambahan pula, kemasukan kandungan halus dan serbuk telah terbukti sebagai kaedah yang berkesan untuk meningkatkan ketumpatan pembungkusan, yang seterusnya meningkatkan kapasiti pengisian lompang dan menguatkan konkrit. Reka bentuk

campuran optimum ditentukan menggunakan kaedah ketumpatan pembungkusan, dan kesan Serat Basalt (BF) telah disiasat pada tahap yang berbeza-beza (0%, 0.15%, dan 1%). Analisis perbandingan telah dibuat antara konkrit berat normal (NWC) dan campuran LWAC terpilih dengan kandungan BF yang berbeza dari segi kos, pelepasan CO_2, ketumpatan kering permukaan tepu, keadaan retak permukaan, penyerapan air dan keliangan, daya serap, prestasi mampatan dan lentur. Keputusan menunjukkan bahawa penggabungan UGGBS mempunyai kesan positif yang besar terhadap sifat mekanikal LWAC apabila BF dimasukkan ke dalam campuran konkrit ringan CS. Termasuk 1% BF dalam campuran menunjukkan sifat mekanikal dan pengangkutan yang unggul berbanding LWAC bukan gentian, menonjolkan kepentingan BF dalam meningkatkan ciri-ciri LWAC berkekuatan tinggi. Sebagai penemuan penting penyelidikan ini, LWAC gred 30 dengan ketumpatan demoulded 1864 kg/m^3 yang mengandungi hanya 284 kg/m^3 simen telah dihasilkan. Selepas mempertimbangkan semua pendekatan dan pelaksanaan LWAC berkekuatan tinggi hijau ini dengan pengurangan %40 dalam simen, terdapat pelepasan CO_2 yang lebih rendah dan pengurangan kos pembuatan, menjadikannya pilihan alternatif untuk pengeluaran.

Kata kunci: Tempurung kelapa; Pengisaran basah; Sanga relau letupan berbutir tanah; Ketumpatan pembungkusan; Kekuatan mampatan

ACKNOWLEDGEMENTS

TABLE OF CONTENTS

LIST OF FIGURES

LIST OF TABLES

LIST OF SYMBOLS AND ABBREVIATIONS

LWAC	:	Light weight aggregate concrete
LWA	:	Light weight aggregate
NWC	:	Normal weight concrete
OPC	:	Ordinary portland cement
SSD	:	Saturated surface dry
ITZ	:	Interfacial transition zone
V_{GGBS}	:	GGBS volume
V_{GM}	:	Grinding media volume
V_{GC}	:	Grinding chamber volume
NCS	:	Normalized compressive strength
M40	:	Characteristic strength of 40 MPa after 28 days of casting
LWAC-Control	:	Packing density optimized mixture with no basalt fiber
LWAC-0.15%	:	Packing density optimized mixture with volume of 0.15% basalt fiber inclusion
LWAC-0.15%	:	Packing density optimized mixture with volume of 1% basalt fiber inclusion
HSLWAC	:	High strength light weight aggregate concrete
CS	:	Coconut shell
NWA	:	Normal weight aggregate
GGBS	:	Ground granulated blast furnace slag
BF	:	Basalt fiber
UGGBS	:	Ultrafine ground granulated blast furnace slag
ρw	:	Density of water
$\rho bulk$	:	Bulk density of the fresh mixture

τdry	:	Dry packing density
φwet	:	Wet packing density
uw	:	Volumetric water-to-solid ratio
Vp	:	Paste volume
CSC	:	Coconut shell concrete
SLWAC	:	Structural light weight aggregate concrete
CC	:	Conventional concrete
D_s	:	The smallest particle size
D_L	:	The largest particle size
a_t	:	The packing value of combined mix
a_i	:	The packing value of each particle class
k_s	:	Toufar model factor
k_d	:	Diameter ratio factor
q	:	The distribution component
d_{min}	:	Minimum particle size
d_{max}	:	Maximum particle size
$a_{i,j}$	:	The loosening effect coefficient
$b_{j,i}$	:	The wall effect coefficient
K	:	Compaction index
C	:	The real packing density
OPSC	:	Oil palm shell concrete
OPBC	:	Oil palm boiler clinker

CHAPTER 1: INTRODUCTION

1.1   Background

Globally, a substantial volume of concrete is manufactured annually. Normal-weight concrete (NWC) comprises four fundamental components: crushed stone, river sand, cement, and water. For construction of structural lightweight concrete, typically, lightweight aggregates serve as substitutes for both coarse and fine aggregate in the concrete mixture. The utilization of waste and by-products as renewable ingredients in concrete mixes has not only shown improvements in mechanical properties, durability, thermal resistance, but also aligns with the goals of sustainable development. Collivignarelli et al. (2020), Shao et al. (2023), Tao et al. (2023). Through the utilization of these materials, the construction industry can mitigate waste, foster sustainability, and concurrently maintain the quality and durability of concrete structures according to Gunasekaran & Kumar (2008), Pordesari et al. (2021) and Yaşar et al. (2004).

In contemporary construction practices, lightweight aggregate concrete (LWAC) has emerged as a pivotal and versatile material. To reduce the overall density, the incorporation of various mineral and plant-based LWAs into the concrete composition is a widely utilized technique. According to Pordesari et al. (2021), LWAC exhibits an oven-dried density ranging from 300 kg/m³ to 2000 kg/m³, accompanied by cube compressive strength varying between 1 MPa to 60 MPa. Yaşar et al. (2004) stated that the integration of LWAC contributes to a reduction in the dead weight of a building, thus leading to diminished cross-sections and steel reinforcement requirements for foundations, beams, and columns. Consequently, LWAC stands as a sustainable construction material, especially suited for structural applications in multi-story buildings.

Aggregates make up a major volume portion of concrete and have a significant impact on the material's fresh and hardened properties. According to Gunasekaran & Kumar (2008), natural aggregates face depletion from overexploitation, industrial and agricultural

waste emerge as a potential alternative source for construction materials. Agricultural wastes, available in vast quantities, present a viable and reliable substitute for crushed stone in concrete. CS, an agricultural byproduct, is abundantly accessible, particularly in tropical climates. Incorporating CS as an aggregate in concrete offers multiple advantages, including addressing landfill concerns and preserving natural resources, thereby contributing to environmental sustainability. Moreover, the use of CS aggregates in concrete leads to a reduction in weight compared to traditional concrete, resulting in an overall decrease in construction expenses.

The escalating global production of cement to meet the demands of advancing infrastructure suggests the enduring prominence of concrete as a favored construction material in the foreseeable future. However, statistical estimates according to Environment et al. (2018) indicate that a substantial increase in global cement output, expected to surge from 4.3 billion metric tonnes in 2015 to 6.1 billion metric tonnes by 2050). 2019 reports of the same statistics source stated that this growth is particularly pronounced in developed nations, with China accounting for nearly half of the global cement production. A primary environmental concern associated with concrete lies in the CO_2 emissions stemming from cement production. Berndt (2015) and Celik et al. (2015) stated that the manufacturing process of cement contributes significantly to CO_2 emissions, potentially constituting between 5-7% of global emissions. Therefore, it is vital to reduce the amount of cement used in concrete production. Sbia et al. (2017) noted that, beyond environmental and cost considerations, there is a motivation to limit both the heat of hydration and drying shrinkage in cement used for concrete materials, Kwan and Mora (2001) explained that these factors are linked to the cement paste content in concrete and can influence durability.

Liu et al. (2019), Ren et al. (2021), and Shen et al. (2020) noted that the steel industry generates GGBS, a glassy by-product renowned for its high calcium content. Recognized as one of the most efficient secondary cementitious materials, GGBS serves as a cement replacement, offering favorable mechanical properties and enhancing the durability of concrete. Importantly, GGBS has a low environmental impact. Chen et al. (2021), Xu et al. (2022), and Yang, Huang, He, et al. (2019) highlighted that its high pozzolanic reactivity contributes to reduced porosity, pore refinement, and inhibition of chloride ion transmission. Generally, LWAC with GGBS exhibits lower compressive strength than concrete without GGBS at early ages but demonstrates strength gains over time. Mo et al. (2015) indicated that the delayed hydration of GGBS is responsible for the observed decline in strength at early ages, followed by subsequent growth in strength at later stages. Yang et al. (2021) widely acknowledged that an optimal GGBS content in a mixture is around 25% by weight, as GGBS, with its relatively coarse particles, exhibits a low degree of early hydration.

Yang et al. (2021) and Yang et al. (2022) highlighted that the wet grinding process is an exceptionally effective method for the mechanical activation of GGBS. Yang et al. (2021) and Junjie Zhang et al. (2019) noted that this procedure effectively reduces particle size and surface defects, thereby enhancing the reactivity of GGBS. Furthermore, Yang et al. (2021) and Junjie Zhang et al. (2019) demonstrated the wet grinding process's ability to improve the microstructure of cement during the early stages of hydration. Yang, Huang, Su, et al. (2019) and Yang et al. (2021) revealed the significance of the wet grinding process as a valuable tool for enhancing both GGBS properties and cement hydration. Chelgani et al. (2019), Ogonowski et al. (2018), and Ozkan et al. (2009) established that wet grinding is more efficacious in reducing particle size compared to dry grinding. Consequently, Makaratat et al. (2010), Mehdipour and Khayat (2017), and Nazari and Riahi (2011) emphasized the positive impact of binder fineness and the resulting high packing density, when combined with cement, on the mechanical properties

3

of concrete.

Karbhari and Strassler (2007), Ünal et al. (2023), and Ünal and Şimşek (2021) stated that cementitious mixtures are inherently brittle, and fiber reinforcement can increase flexural and tensile strength, as well as improve toughness and fracture resistance. Additionally, fibers are becoming increasingly popular in the concrete industry due to their low environmental impact and cost-effectiveness during production. Sohail et al. (2020) noted that basalt fibers (BFs), derived from basaltic rocks constituting around 33% of the Earth's crust, offer the advantage of being readily abundant. Beyond accessibility and cost, Alcharchafche et al. (2022), Asil and Ranjbar (2022), Deák and Czigány (2009), Guler and Akbulut (2023), and Yıldırım and Özhan (2023) emphasized that BF exhibits superior chemical and mechanical properties when combined with cement paste and aggregates.

Sobolev and Amirjanov (2007), Wong and Kwan (2008), and Wong and Kwan (2014) noted that the packing parameters of granular materials consisting of solid particles greatly influence physical and mechanical properties. Chu (2019), Karadumpa and Pancharathi (2021), and Wang et al. (2019) suggested that understanding particle packing is crucial in industries using granular materials, and using particle packing models to assess packing density and void ratio can enhance both fresh and hardened concrete by reducing cement content and increasing solid mass. Mehdipour and Khayat (2018) pointed out that increasing packing density in the paste phase, aggregate phase, and overall concrete mix leads to reduced void volumes, which in turn necessitates less water and results in less porous, stronger, and more durable concrete over time, as supported by Abd Elrahman and Hillemeier (2014), Yoo et al. (2022), and Zhou et al. (2021).

Barksdale et al. (1991) and Zou and Yu (1996) explained that the packing density of particles is related to their sphericity, with higher sphericity leading to greater packing density. Kwan and Fung (2009) noted that sphericity acts as a measure of particle shape

and its ability to interlock tightly with other particles. Bogas et al. (2013), Chia and Zhang (2002), Kockal and Ozturan (2011), and Terzić et al. (2015) argued that the lower strength observed in lightweight aggregate concrete (LWAC) is due to the high porosity and low strength of the aggregates used. Kwan and Mora (2001), Kwan et al. (1999), Kwan and Fung (2009), and Mora and Kwan (2000) further highlighted that aggregate convexity influences packing, with concave sections causing challenges for filling and potentially reducing strength when particles are of comparable sizes. Reinforcing the weakest spots in the concrete matrix with fibers and filler significantly contributes to increased packing density and improved mechanical, durability, and transport properties, thus enhancing the use of waste coarse aggregates that may otherwise be less suitable for concrete.

This study delves into the synergistic effects of employing the packing density method for optimal mix design and integrating the wet grinding technique for UGGBS as a high-volume cement replacement. Additionally, the investigation explores the impacts of varying particle sizes on both coarse and fine aggregates, leading to the formulation of an optimal mix design based on overall packing density. The physical, mechanical and transport properties of the resulting mixture were thoroughly examined, taking into account the incorporation of BF at different volumes. Additionally, an evaluation was carried out to examine the environmental and financial consequences of the created mixture design in comparison to conventional normal weight M40 grade concrete.

1.2   Aims and Objectives

The study aims to produce a mixture design using packing density optimization to develop structural-grade concrete incorporating CS as a lightweight aggregate. Chapter 2 addresses the limitations of packing density optimization in determining the hydration level and strength development in hardened concrete and proposes an alternative approach for determining the optimum mix design. Furthermore, the objectives include conducting a comparative analysis between NWC and particle density optimized LWAC in terms of mechanical, durability, and transport properties by providing an approach

highlights the intention to evaluate the total cost and CO_2 emission. Based on the provided details, here is the research objectives are follows:

1. To explore the impact of optimization techniques on the development of structural concrete using CS aggregate.

2. To investigate the key parameters influencing the performance characteristics of slurry production processes for GGBS.

3. To compare and contrast the physical, mechanical, and transport properties of different concrete formulations to identify performance differentials

4. To assess the influence of fiber reinforcement on the mechanical and transport characteristics of LWAC.

1.3 Research questions

To accomplish the objectives of the current investigation, the following questions are posed:

1. How does packing density optimization contribute to the development of structural-grade concrete incorporating CS as a lightweight aggregate?

2. What are the key factors and their respective optimal levels in the wet milling process that contribute to the production of UGGBS slurry with superior performance characteristics?

3. What are the total costs and energy consumption associated with the production and use of NWC compared to packing density optimized LWAC, and how do they impact cost-effectiveness and environmental sustainability?

4. What is the optimal level of BF content that maximizes the mechanical strength and transport properties while minimizing the density of the lightweight aggregate concrete?

1.4   Significance of research

The advantages discussed below highlight the potential benefits of packing density approach in terms of physical properties, transport properties, mechanical properties, cost reduction, environmental impact, and sustainable resource utilization. One of the key advantages of using this approach is the expected lower cost and reduced CO_2 emissions for the production of 1 m^3 of concrete. By incorporating CS aggregates and supplementary cementitious materials such as GGBS, the amount of cement required in the concrete mixture can be significantly reduced. Cement production is known to have a significant carbon footprint, and by reducing the cement content, the overall environmental impact of concrete production can be mitigated. Moreover, the use of waste materials like GGBS contributes to a more sustainable and cost-effective concrete production process. Another advantage of the proposed approach is the potential reduction in the cross-section of structural members. Lightweight concrete, achieved through the incorporation of CS aggregates, has a lower density compared to traditional concrete. As a result, structural elements can be designed with reduced dimensions, leading to material savings and increased efficiency. This reduction in the cross-section can have a positive impact on the overall construction costs, as it requires less concrete and steel reinforcement, while maintaining the desired structural integrity.

High durability is a crucial characteristic of concrete structures, and the proposed approach offers the potential for enhanced durability. By reducing the amount of cement in the concrete mixture, the risk of excessive hydration is minimized. The optimized mix design with a lower cement content helps to mitigate this risk, resulting in high durability concrete that exhibits improved resistance to shrinkage and cracking. On the other hand, the use of waste materials, such as CS aggregates, in the production of LWAC can contribute to the protection of agricultural areas. CSs are abundantly available in tropical regions and are typically considered as waste. By utilizing these shells as aggregates, the

demand for natural aggregates can be reduced, thereby minimizing the environmental impact associated with quarrying activities. This approach promotes sustainable resource utilization and helps preserve natural resources, thus offering environmental benefits.

Importantly, this study addresses a gap in existing literature by meticulously examining the utilization of low cementitious and economically viable high-strength LWAC, integrating non-spherical waste aggregates through the packing density method. By doing so, it not only presents an innovative approach but also makes a substantial contribution to the realm of structural LWAC. This investigation is poised to offer valuable insights and practical implications, potentially revolutionizing the way lightweight aggregate concrete is utilized and engineered in various structural applications.

1.5   Thesis layout

The specified mix design follows analyzing each of the components of the concrete, which are coarse aggregate, fine aggregate, and concrete, separately and combined based on packing density method. The examination of each of the components groups was made based on a certain packing density testing method. Kwan et al. (2014), Li and Kwan (2014), Li et al. (2019), and Wong and Kwan (2005, 2008) stated that the wet condition test procedure is higher and more reliable than the dry condition for determining packing density in concrete mixtures. Pietsch (1997) identified 100 μ as the critical size, considering the stark difference between these two approaches. Wong and Kwan (2008) emphasized that dry methods are not recommended for particles smaller than 100 μ, as adhesion phenomena in fine materials (typically less than 100 μ) can lead to agglomeration and increased void content, which may result in underestimating overall packing density. Therefore, in this study, the dry packing density technique is used for coarse aggregates, while the wet packing density method is applied for fine aggregates.

The study basically consists of 3 phases. In the first step for phase A in determining

the mix design, CS aggregate was washed and purified from its fibers, dried in an oven at 100 °C. Two coarse aggregate sizes retaining 9.50-6.30 mm and 6.30-4.75 mm were sieved and proportioned by volume to provide the highest packing density to increase the compact structure and maximum solid ratio. Kwan et al. (Li et al., 2019) used the equations (1.1) and (1.2) to determine wet and dry packing density. The sample's bulk density (ρbulk) was used to compute the dry packing density (τdry) and the solid concentration (φwet) of the solution:

$$\tau dry = \frac{\rho bulk}{\rho\alpha R\alpha + \rho\beta R\beta + \rho\gamma R\gamma} \tag{1.1}$$

$$\varphi wet = \frac{\rho bulk}{\rho wuw + \rho\alpha R\alpha + \rho\beta R\beta + \rho\gamma R\gamma} \tag{1.2}$$

When calculating the dry packing density, the variables α, β, and γ stand for the cement, fine aggregate, and fiber, respectively. The densities of these three components are represented by ρα, ρβ, and ργ, and the volumetric ratios of these three components to the total solid materials content are denoted by Rα, Rβ, and Rγ. In addition, the volumetric W/S ratio, denoted as uw, and the density of water, ρw, are used for the computation of wet packing density.

The two coarse aggregate sizes underwent packing density tests at 5% volume intervals. Subsequently, another round of packing density testing was conducted between two volume ratios that exhibited the highest packing density, with intervals of 1%. This process aimed to refine precision when nearing the ideal content.. Due to the flaky and irregular shape of CS aggregate, it can be expected to have different void ratios than standard gravel aggregates with the same size groups. Barksdale et al. (1991) and Zou and Yu (1996) indicated that the packing density of particles is directly related to their sphericity, or how closely they resemble a perfect sphere. Kwan and Fung (2009) explained that the more spherical a particle is, the higher its packing density will be, as

this relationship measures the particle's shape and its ability to pack tightly with others. Bogas et al. (2013), Chia and Zhang (2002), Kockal and Ozturan (2011), and Terzić et al. (2015) pointed out that the low strength of lightweight aggregate concrete (LWAC) is often due to the high porosity and low strength of the aggregates used. However, Kwan and Mora (2001), Kwan et al. (1999), Kwan and Fung (2009), and Mora and Kwan (2000) noted that aggregate packing is also influenced by the convexity of aggregate particles, as concave sections are more difficult to fill, potentially reducing strength, especially when aggregate particles are of similar sizes. As a result, strengthening the weakest spots indicated in the concrete matrix significantly impacts increasing packing density and enhancing mechanical, durability, and transport properties. This method aims to increase the efficiency of waste coarse aggregates that are less suitable for use in concrete due to their physical properties.

The packing density of a fine aggregate, featuring a predetermined maximum size, is notably influenced by the presence of its finest component, which fills the voids between larger particles. The term fines (F) content pertains to the fraction of a material possessing particles smaller than 75 μ (F<75 μm), while powder (P) content refers to particles larger than 75 μ but less than 150 μ (75 μm <P<150μm). The third aggregate group (FA) encompasses particles larger than 150 μ but smaller than 4.75 mm (150 μm <FA<4.75 mm). A testing protocol was developed to examine the collective influence of these three distinct particle size categories on compaction density across different scenarios. During the second step of Phase A, the fine aggregate was subjected to mechanical sieving to categorize it into three size groups: aggregate A (<75 μm), aggregate B (75 μm <P <150 μm), and aggregate C (150μm<FA<4.75 mm). The specific gravity test of both coarse and fine aggregates conducted according to ASTM C128, and the wet packing density test results, expressed in volumetric ratios, were determined for the fine aggregate groups. Various combinations were analyzed based on increasing and decreasing particle size volumes, and the corresponding wet packing density results were examined. Afterwards,

optimal fine aggregate volume ratios were identified based on packing density values and preliminary test results. In the third step of Phase A, the volumetric ratios established for coarse and fine aggregates in the first two steps were defined, specific gravities of new aggregate groups were determined, and optimal volumetric ratios were fine-tuned based on preliminary test results. Figure 1.1 illustrates the underlying concept and rationale of the packing density method for achieving high strength by establishing a state of close packing among particles.
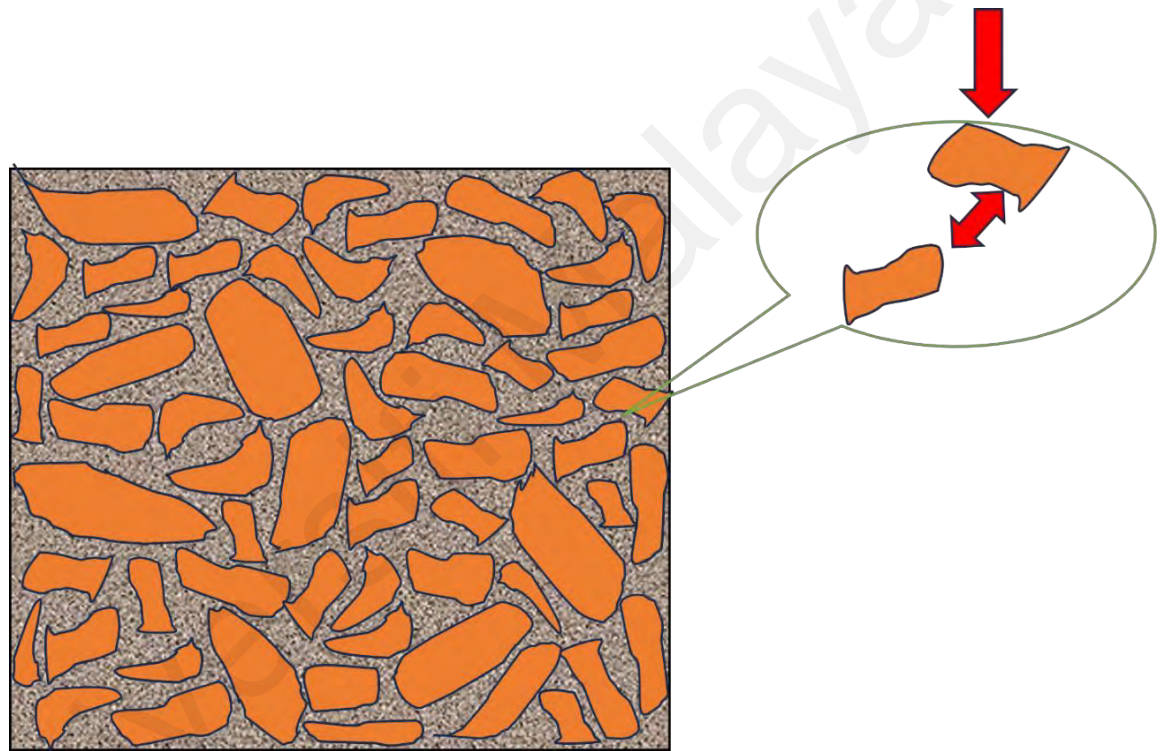
Figure 1.1: Close packing concept of packing density method

Phase B focused on the development of a high-efficiency paste incorporating cement and UGGBS slurry. This section emphasizes the fundamental concepts of low cement content and adoptable strength. The objective is to achieve elevated early and late strength by substituting UGGBS slurry for a high volume of the cement. In the initial step of Phase B, efforts were directed towards optimizing the preparation of UGGBS slurry under prevailing conditions. Investigations included determining the optimal binder-to-grinding media ratio by mass, and the ratio of material amount to total grinding capacity by volume variables. Next, the relationship between the compressive strength of pastes, by gradually

11

replacing cement with UGGBS slurry, and the wet packing density at equivalent proportions were examined. This analysis aimed to observe the efficiency of the cement-binder reaction in terms of the compressive strength-packing density relationship.

Phase C investigates into the process of filling the voids generated by the combination of aggregates with paste, as outlined in Phases A and B. The primary objective is to determine the optimal volume of paste (Vp). The research seeks to identify both theminimal volume of paste required to fill the voids between aggregate particles and an additional amount of paste that ensures sufficient workability. The optimal paste composition is characterized by achieving maximum efficacy in terms of minimal cement usage and reduced CO_2 emissions per unit of compressive strength. Consequently, this study defines the optimal mix design step by step, based on the theoretical foundation of high packing density and practical performance. The experiments in this study investigate various properties, including fresh-hardened density, water absorption and porosity, sorptivity, compressive strength, flexural strength, CO_2 emission, and cost-effectiveness. The overall framework of this paper is presented in Figure 1.2**.**
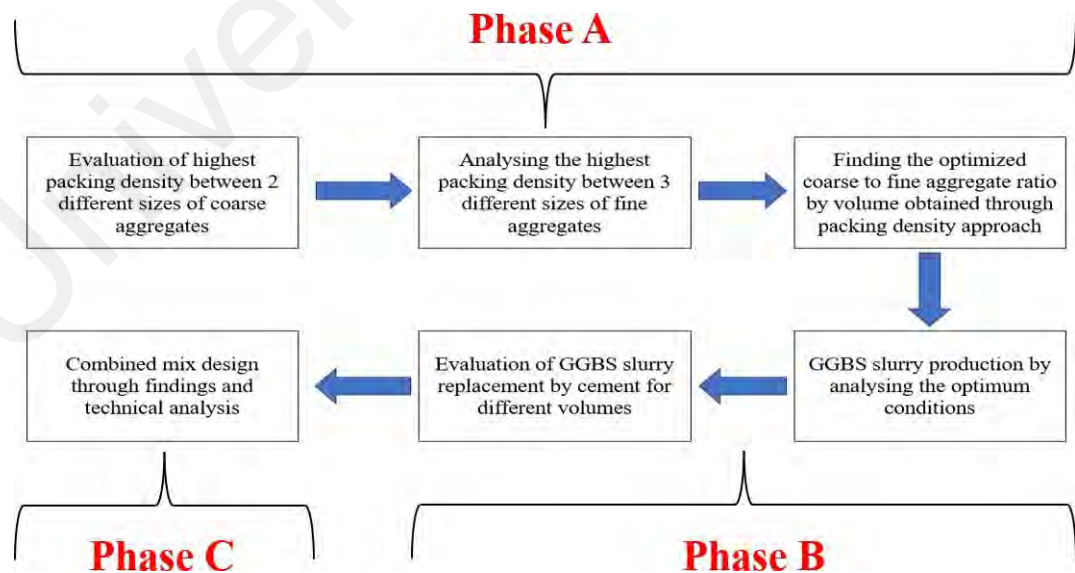
Figure 1.2: Research framework

CHAPTER 2: LITERATURE REVIEW

2.1   Introduction

Concrete is a highly prevalent construction material used in various types of structures. Without it, achieving structural integrity and stability in the building becomes challenging. In the modern era, despite the increasing variety of construction materials, cement and concrete have consistently maintained their status as the predominant choices for construction, owing to their widespread utilization in constructing diverse structures throughout every part of the world. Additionally, it is the sole primary construction material often manufactured at the location. Enormous structures, such as bridges, highways, walkways, and floors, are built using it. In brief, concrete is present wherever there is a structural plan. The utilization of concrete in contemporary buildings is of great importance, as the durability and steadfastness of structures rely on concrete. Furthermore, concrete is cost-effective and multifunctional in its applications. This construction material gained widespread popularity worldwide due to its exceptional flexibility and versatility.

The environmental impact of cement and concrete production is mostly attributed to their significant energy consumption. The manufacture of one ton of Portland cement necessitates a substantial quantity of energy, resulting in the emission of numerous tons of carbon dioxide into the environment. Moreover, the process of extracting raw materials like limestone and clay for cement manufacturing, together with coal for combustion, amplifies deforestation and leads to the depletion of topsoil. NWC consists of 90% stone components and 10% cement by weight. Annually, a substantial quantity of stone resources, such as sand, gravel, and fragmented materials, are utilized for the production of concrete.

Recently, there have been proposals for environmentally-friendly and sustainable methods of producing concrete. Industrialized countries have taken significant steps to improve concrete technology with the aim of preserving the planet for future generations. Pelisser et al. (2011) suggested that an effective approach to mitigating the detrimental environmental impact of the concrete industry and aligning it with the principles of sustainable development involves utilizing by-products and waste materials as ingredients in concrete, rather than relying on raw materials. Across various industries, including civil and structural engineering, concrete is increasingly recognized as an environmentally friendly and sustainable material. Prakash, Thenmozhi, Raman, Subramanian, et al. (2020) highlighted the numerous benefits of using waste materials in concrete, including reducing the demand for fresh resources, conserving natural materials, and addressing waste disposal issues. The use of alternative materials to replace natural aggregates contributes to a more environmentally friendly and sustainable ecosystem. Mehta and Monteiro (2014) also suggested that using agricultural waste and industrial by-products as substitutes for cement or aggregate can provide advantageous properties in concrete.

Although there have been many studies in literature about the usage of CS as an agro-based LWA in concrete mixture, further investigations are needed, as the use of CS in concrete is relatively new. Based on what has been studied in the literature, it is believed that significant progress can be made by studying and understanding the key features of CS and its properties. In addition, researchers can identify new research topics, allowing for exploration of innovative LWAC according to design, economic and environmental aspects.

Dardak (2021) and Subramani and Anbuvel (2016) pointed out that every part of the coconut palm tree, including the trunk, leaves, and even the interior of the fruit, can be used for many purposes, which is why the coconut tree is globally known as the "Tree of Life." This species of palm tree can thrive in diverse environments, even in the presence

of excessive salt, nutrient-depleted soil, or insufficient rainfall. However, optimal cultivation occurs in tropical and subtropical regions of Asia and East Africa, especially in hot, humid climates with sandy soil.

According to data from the Food and Agriculture Organization of the United Nations (2021), Indonesia is the world's leading producer of coconuts, followed by India, the Philippines, Brazil, and Sri Lanka. Coconut is commercially cultivated in about 35 countries, covering approximately 12 million hectares of land. Over 90% of coconut farms are small village-based operations occupying less than one hectare. In 2021, global coconut production reached 61,520,382 MT, representing a 1.0% decrease compared to the 62,159,626 MT produced in 2020. Gama et al. (2012) reported that Indonesia, India, and the Philippines account for around 70% of global copra production, while Indonesia and the Philippines are the primary exporters of coconut oil.

Table 2.1: Production of coconuts by country (MT)

Rank	Country/region	2020	2019	2018	2017	2016
1	Indonesia	16,824,848	17,074,536	17,100,000	17,200,000	17,400,000
2	India	14,695,000	14,682,000	16,413,000	11,166,772	11,344,306
3	Philippines	14,490,923	14,765,057	14,726,165	14,049,131	13,825,080
4	Brazil	2,458,839	2,348,663	2,345,400	2,210,139	2,634,396
5	Sri Lanka	2,233,600	2,468,800	2,098,400	1,960,000	2,408,800
6	Vietnam	1,719,415	1,677,044	1,571,709	1,499,228	1,469,960
7	Papua New Guinea	1,217,293	1,205,510	1,186,400	1,186,400	1,186,400
8	Mexico	895,291	908,302	926,400	927,200	925,600
9	Thailand	827,424	866,416	858,235	761,914	904,094
10	Malaysia	560,984	536,606	495,531	517,589	504,773

Dardak (2021) reported that Malaysia ranks among the top 10 coconut producers worldwide, with coconut being the fourth most significant industrial crop in the country, following palm oil, rubber, and paddy. The coconut plantation area in Malaysia grew from

84,609 hectares in 2016 to 85,630 hectares in 2020, with coconut production increasing from 504,773 MT in 2016 to 560,984 MT in 2020. This expansion is aimed at meeting the rising demands in both domestic and global markets. Additionally, the value of coconut commodities increased by nearly 20%, from RM555,250.00 (US$132,202.00) in 2016 to RM666,626.00 (US$158,720.00) in 2020.).

Senik (1995) noted that coconut meat can be processed into coconut cream powder, instant milk powder, and dried coconut. The coconut milk industry in Malaysia generates a substantial quantity of discarded CS, with many small-scale enterprises producing significant amounts of CS waste daily during the production of instant coconut milk. While CS disposal may not be the most urgent environmental concern, its lack of recycling will eventually lead to a waste management issue. Fauziah and Agamuthu (2009) highlighted that CS has a slow biodegradation rate due to its high lignocellulose content, which forms the primary structure of plant cell walls. This slow decomposition, which can take up to a decade, poses a challenge for agricultural waste management, as it adds strain on landfills. Datta et al. (2017) estimated that 80,000 metric tons of coconut waste are discarded annually, accounting for 6.7% of the total agricultural waste. In 2015, 2.843 million tons of solid waste were deposited in landfills, with 7,986.47 tons discarded daily. Fauziah and Agamuthu (2009) also mentioned that in the same year, 135 landfills were closed, leaving only 162 operational, and just four incinerators in use.

2.2 CS as aggregate

2.2.1 Origin of CS

The The coconut is often referred to as the "versatile tree," "man's most useful tree," "king of the tropical flora," and the "tree of life" due to its many practical uses. As Shahbandeh (2023) pointed out, the coconut tree is highly adaptable and provides humans with a wide range of resources, including food, fuel, medicine, cosmetics, industrial products, and even construction materials. CS can be used for charcoal production, while

the meat of mature seeds can be processed to extract coconut milk and oil. Recently, coconut milk has become popular among individuals following plant-based diets. Shahbandeh (2023) estimated that the global demand for coconut milk is expected to rise significantly, with market value projected to surpass 1.78 billion U.S. dollars by 2027, more than doubling its current value.

2.2.2 Physical properties of CS

Certain applications necessitate specific types of aggregate, as not all forms are appropriate for every use. Zhang and Gjorv (1990) highlighted that some LWAs have the potential to produce HSLWC. Therefore, a thorough investigation into the engineering properties of LWA is essential prior to its use in the concrete industry. The physical properties of CS aggregate directly influence the strength and durability of CSC. Figure 2.1 illustrates both intact and fragmented CS.

(a)   (b)
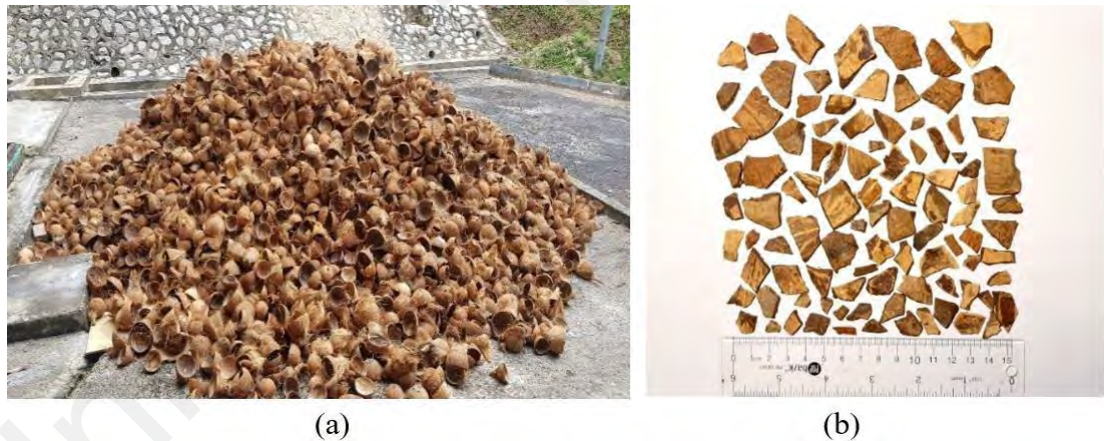
Figure 2.1: Different conditions of CS a) Discarded, b) Crushed

2.2.2.1 Specific gravity

According to Ahmad et al. (2007a), a material's specific gravity is the ratio of its density to water. A range of specific gravities has been reported for CS from 1.03 to 1.56, with Ealias et al. (2014) reporting the lowest specific gravity of 1.03, while Dangi and Soni (2017), Kumar and Kumar (2012), and Subramani and Anbuvel (2016) reported the highest specific gravity of 1.56. Several factors may have contributed to the wide variety

of specific gravities. Hemmings et al. (2009) reported that perlite, among other artificial LWAs, has a specific gravity ranging from 0.12 to 0.42, while Shafigh et al. (2014) found that LECA exhibits specific gravities between 0.51 and 1.18. Aslam et al. (2016) reported that OPBC is a natural LWA by-product and has a specific gravity ranging from 1.70 to 2.22. Although CS aggregates have a specific gravity within the range of other natural LWAs, they are 47–60% lighter than NWAs, 29–39% lighter than OPBC, but significantly heavier than those of perlite and LECA, respectively.

2.2.3   Chemical properties of CS

The chemical characteristics of the elements utilized in concrete mixtures are crucial for ensuring the high quality of the final product. The chemical features of each of these components impact the strength, durability, and other attributes of the concrete. Aggregates enhance the strength and durability of concrete, and the specific type and size of the aggregate will impact the strength and other properties of the concrete. Understanding both the physical and chemical properties of components is crucial to ensure their effective integration into the binder, hence achieving the intended outcomes.

Composition of CS aggregate is mainly composed of calcium carbonate, silica, and lignin. Calcium carbonate is the main component of CS aggregate, making up around 50-60% of the total composition. It is a white, powdery substance that is often found in nature, and it is a key component in the production of cement. Silica makes up around 15-20% of the aggregate, and it is a mineral that is composed of silicon and oxygen. It is an important component in the production of glass, and it also helps to strengthen the aggregate. Lastly, lignin makes up around 10-15% of the aggregate. It is a natural polymer that is found in plants, and it helps to bind the other components together. Weather resistance is enhanced by lignin content in composite materials. These components give the aggregate its strength, low density, and low cost, making it a popular choice for construction projects.

2.3   Physical properties of CS concrete

2.3.1   Workability

According to the guidelines established by the American Concrete Institute (ACI) in Standard 116R-90 (ACT 1990b), workability refers to the characteristic of freshly mixed concrete that determines how easily and consistently it may be mixed, placed, consolidated, and finished. Workability also describes the amount of effort required to manipulate a concrete mixture while minimizing the tendency for its components to segregate. Abimbola (2015) highlights that the strength of the material is influenced by various parameters, including the dimensions, form, surface roughness, and grading of the aggregates, the water-to-cement ratio, the inclusion of admixtures, and the proportion of the mixture.

The workability of CS concrete is notably improved due to the smooth surface on one side of the shells and the size of the CS particles used, as highlighted by Gunasekaran et al. (2014). Workability is assessed across five degrees, ranging from very low to high, as outlined by Neville and Brooks (2002). A detailed presentation of the degree of workability for the slump test is provided in Table 2.2.

Table 2.2: Degree of workability for different slump values

Degree of workability	Slump	
	mm	inch
Very low	0-25	0-1
Low	25-50	1-2
Medium	50-100	2-4
High	100-175	4-7

Xiaopeng (Xiaopeng, 2005) emphasize the need for careful consideration of workability in LWAC, noting differences compared to normal-weight aggregate concrete. LWAC tends to exhibit a lower slump and compacting factor for equal workability due to reduced gravitational work, as gravity has a lesser effect on lightweight aggregates.

Maintaining higher workability in LWAC increases the risk of segregation. Unlike normal-weight aggregate concrete, LWAC experiences a reverse phenomenon during higher slumps and excessive vibrations, where the mortar settles downward while the aggregate tends to float. This poses challenges for finishing operations on deck slabs and floors. To address these issues, the maximum slump is typically limited to 100 mm. The porous nature of lightweight aggregates leads to high and rapid water absorption. Dry aggregates absorb water quickly upon mixing, resulting in decreased workability. Thus, special attention must be paid to the moisture content of lightweight aggregates during mixing to maintain desired workability levels.

A research study conducted by Osei (2013) consistently shows that CSC is far more workable than NWC. True workability refers to the concrete's ability to be manipulated with greater ease throughout the mixing process. Gunasekaran et al. (2011) discovered that CSC can reach a slump value of up to 150 mm without any admixtures, and adding a low amount of admixture can lead to even higher slump values. Selwyn Babu and Mahendran (2014) focused on developing LWCs utilizing CS and natural sand as primary aggregates, observing a slump value ranging from 0 to 25 mm, while the compressive strength attained 27.2 MPa. Importantly, it should be noted that a low slump value does not necessarily imply lower compressive strength.

2.3.2   Hardened density

LWAC is a specialized concrete variant that incorporates LWAs to reduce density while maintaining adequate mechanical properties. The development of LWAC has garnered significant attention due to its potential to enhance structural performance, reduce dead loads, and improve energy efficiency in buildings and infrastructure, as highlighted by Junaid et al. (2022). Among the critical parameters influencing the properties of LWAC, the hardened density stands out as a pivotal characteristic governing its structural behavior and application suitability.

The hardened density of LWAC reflects its compactness and porosity, directly impacting its strength, durability, thermal properties, and overall performance. Achieving an optimal balance between reduced density and adequate strength is crucial in LWAC design to meet structural requirements while minimizing material usage and environmental impact. The quest for lightweight solutions in construction has spurred research efforts aimed at understanding the factors influencing the hardened density of LWAC and optimizing its performance in various applications.

Several factors influence the hardened density of LWAC, including the type and properties of LWAs, mix proportions, water-to-cement ratio, curing conditions, and incorporation of supplementary cementitious materials or chemical admixtures. Studies by Algaifi et al. (2022) and Eziefula (2018) elucidate the fundamental principles governing concrete technology, highlighting the importance of aggregate characteristics and mix design in determining concrete properties. SLWAC typically exhibits a hardened density ranging from 1400 to 2000 kg/m³, in contrast to the 2400 kg/m³ density observed for NWC. According to Neville and Brooks (2008), the density of LWC varies from 350 to 1850 kg/m³, while Clarke (2002) reported a range of 1200 to 2000 kg/m³ for LWC.

Researchers have studied the development of CSC by partially or wholly replacing NWA with CS as coarse aggregate. The resulting hardened density of CSC ranges between 1445 and 2529 kg/m³. Gunasekaran et al. (2011) found that LWC density ranged from 1865 to 2060 kg/m³, while SLWAC produced using CS aggregates fell within the range of 1930 to 1970 kg/m³, a density consistent with SLWACs under 2000 kg/m³.

Prakash et al. (2019) investigated the effects of replacing cement with 10 to 30% fly ash, demonstrating a reduction in concrete density. Their findings showed that incorporating CS as a coarse aggregate contributed to density reduction, with density decreasing as fly ash content increased. Prakash et al. (2020) further explored the

incorporation of polypropylene fibers into eco-concrete, composed of fly ash and CS coarse aggregate, resulting in decreased concrete density, thereby reducing dead weight and associated foundation and installation costs. Pordesari et al. (2021) explored the replacement of crushed granite with agro-based aggregates, leading to a decrease in density. The demoulded density of CSC and OPSC mixes decreased by 15.4% and 14.4% compared to NWC, respectively. The specific gravities of these aggregates directly influenced their densities, with CS and OPS concretes being 55.4% and 53.5% lighter than granite aggregate, respectively. NWC exhibited an air-dried density of 2341 kg/m³, significantly higher than CSC and OPSC mixes, resulting in reduced dead load for CSC and OPSC by 16.5% and 15.8%, respectively.

2.4 Mechanical properties of CS concrete

2.4.1 Compressive strength

Several factors contribute to the reduction of strength in concrete. These include the water-to-cement ratio, cement quality, curing effectiveness and temperature, aggregate grading, compaction level, testing age, as well as the effects of impact and fatigue as noted by Safiuddin et al. (2018). High-strength concrete tends to exhibit relatively brittle behavior, as evidenced by a significant descent in its stress-strain diagram following the peak stress point according to Feng et al. (2021). Understanding the compressive strength of LWAC is essential for assessing its structural feasibility and suitability in construction endeavors. LWAC provides a sustainable alternative to conventional concrete due to its reduced weight and enhanced thermal characteristics. Studying the variables that influence LWAC's compressive strength is key to enhancing its structural performance, longevity, and ecological footprint.

Multiple studies have investigated the compressive strength of LWAC, examining issues such as the type of lightweight aggregates, mix designs, curing processes, and the inclusion of extra components. The significance of lightweight aggregates in influencing

concrete characteristics is noted, particularly their capacity to decrease weight without compromising strength as highlighted by Akcay and Tasdemir (2009). Lu et al. (2022) emphasize the importance of accurate mix designs and quality control to achieve desired results in LWAC due to variability in compressive strength.

The effect of CS aggregate on the mechanical properties of concrete has been examined by various studies. Gunasekaran et al. (2011) investigated properties of LWAC by incorporating CS as coarse aggregates in concrete mixtures. They achieved a compressive strength range of 4.95 to 27.20 MPa by varying the water-to-cement ratio between 0.38 and 0.72. Similarly, Jackson et al. (2019) produced six different mix proportions with a constant water-to-cement ratio of 0.55. The control mix contained NWA, while the subsequent mixes replaced the NWA with CS in increments of 20%. The compressive strengths for mixes with 0%, 20%, 40%, 60%, 80%, and 100% CS were 30.6, 19.3, 13.2, 10.8, 10.19, and 7.9 MPa, respectively. Patel et al. (2015) conducted a study with the CS aggregates and replacement percentages, achieving a LWAC with a 0.48 water-to-cement ratio. Prakash et al. (2019) stated that using varying cement dosages from 357 to 510 kg/m³ and a constant CS aggregate amount of 331.5 kg resulted in compressive strength ranging from 26.4 to 30.7 MPa at 28 days.

Kanojia and Jain (2017) conducted an experiment to evaluate the impacts of substituting NWA with CS in concrete manufacturing. The study consisted of two portions. The initial segment assessed the effect of this replacement on the strength and density of concrete, while the second section aimed to calculate the extra quantity of cement needed to offset the decrease in concrete strength resulting from this substitution. Augmenting the concentration of CSs resulted in a decrease in compressive strength. Substituting 40% of NWA with CS decreased the 7-day compressive strength by 62.6% and the 28-day compressive strength by 21.5%. This substitution also decreased the density of the concrete by 7.47%. Reducing the water-to-cement ratio can help preserve

the strength of NWC and waste CSC. Increased waste CS concentrations necessitate a more significant decrease in the water-to-cement ratio and higher cement use..

Sekar (2016) conducted research aimed at developing environmentally friendly concrete using M sand as the fine aggregate, GGBS as a partial substitute for cement, and CS as the coarse aggregate. Through experimentation involving various mix designs and curing methods (including water, steam, and concealed curing), the study evaluated the mechanical properties and fracture toughness of CS-based concrete compared to other LWACs. The findings indicated that the fracture toughness and mechanical characteristics of CS-based concrete were comparable to those of other LWACs. Notably, concealed-cured CS concrete exhibited a significantly higher compressive strength of 27.4 MPa at 28 days compared to water- and steam-cured concrete, with compressive strengths of 23.5 MPa and 21.3 MPa achieved with cement densities of 401.35 kg/m³ and 264.91 kg/m³, respectively. Steam curing was found to reduce the strength of CS concrete due to the presence of CS retardants, rendering steam curing relatively ineffective. With a 25% GGBFS cement replacement, the compressive strength of water-cured, steam-cured, and concealed-cured CS concrete decreased by 8%, 7%, and 14%, respectively. Similarly, with a 50% GGBFS cement replacement, the compressive strength of water-cured, steam-cured, and concealed-cured CS concrete decreased by 26%, 24%, and 22%, respectively. Gunasekaran et al. (2013) investigated the failure patterns of CSC samples at both early and later stages of development. Up to 28 days of age, compression failure primarily stemmed from a bond failure occurring between the cement mortar and the CS aggregate, leading to the formation of cracks surrounding the CS aggregate. Beyond the 28-day mark, the bond between the components strengthened, allowing the crack path to propagate over the CS aggregates.

In general, the strength of concrete is influenced by factors such as inter-particle bonding, mortar permeability, mortar strength, and aggregate strength. However, the

smooth surface of CS aggregates diminishes the contribution of inter-particle connections to strength formation in CS concrete (Prusty & Patro, 2015). During compression tests, CS concrete exhibits a gradual failure process, with specimens retaining their shape post-failure without complete disintegration. In contrast, typical concrete experienced abrupt breakdown, resulting in complete specimen disintegration. The fibrous nature of CS concrete and the superior energy absorption capacity of CS aggregates, as indicated by their low impact and crushing values, primarily account for the slow failure observed in CS concrete (Prakash et al., 2021). This behavior proves advantageous for constructions requiring high impact resistance.

2.4.2 Flexural strength

Understanding the flexural strength of LWAC is critical for ensuring the structural integrity of concrete elements subjected to bending stresses. As a fundamental property, flexural strength is closely tied to the concrete's ability to resist bending and cracking, thereby enhancing its durability and safety. In the context of LWAC, flexural strength typically ranges within certain parameters relative to its compressive strength, reflecting the material's capacity to withstand bending loads.

The literature landscape surrounding LWAC, particularly with respect to flexural strength, highlights the significance of aggregate properties and mix designs. Unlike traditional concrete formulations, LWAC presents unique challenges and opportunities due to its reliance on LWAs for structural reinforcement. Investigating the mechanical behaviors and bonding dynamics of CS aggregates is crucial for comprehending their role in determining the flexural strength of LWAC. Studies exploring the flexural strength of LWAC have identified several key factors influencing its performance, including aggregate size, fiber reinforcement, and supplementary material incorporation. Notably, the integration of coconut fibers has emerged as a promising avenue for enhancing the flexural strength of LWAC, offering potential pathways for developing resilient and

sustainable concrete structures. As research in this field progresses, a deeper understanding of material composition, curing methodologies, and structural performance will be essential for optimizing the flexural strength of LWAC and unlocking its full potential in construction applications.

Various studies have delved into the flexural strength of concrete using CS as coarse aggregates, yielding diverse findings and insights. Gunasekaran et al. (2011) investigated the influence of water-to-cement ratios on CSC mixtures, resulting in flexural strengths ranging from 4.68 to 4.26 MPa, correlating to 17.53% to 16.42% of their compressive strengths. Similarly, Reddy et al. (2014) explored substitution levels of coarse aggregates with CSC, reporting flexural strengths from 5.36 MPa for 0% substitution to 2.4 MPa for 50% substitution. On the other hand, Selwyn Babu and Mahendran (2014) proposed a novel method for producing concrete using crushed dried CS, indicating that flexural strengths varied with substitution percentages. Additionally, Patel et al. (2015) observed decreased flexural strength with higher CS aggregate substitutions and studied the effects of aggregate size on flexural strength, noting reductions with larger sizes. Rajeevan and Shamjith (2015) explored the utilization of recycled CS as a coarse aggregate, reporting flexural strengths ranging from 2.28 to 3.32 MPa, with optimal substitution percentages favoring a 15% rate. Furthermore, Deepak et al. (2015) analyzed CSC mixtures with different levels of coarse aggregate substitution, highlighting decreasing flexural strength trends with increased substitution rates.

Sekar (2016) examined CSC mixtures with varying cement replacements, observing flexural strengths ranging from 4.92 to 6.52 MPa, emphasizing the impact of curing methods and cement substitution on flexural performance. Magrey et al. (2016) investigated the effects of waste glass and CS as aggregate replacements, noting flexural strength improvements with increased substitution levels.

Ravichandran (2017) explored the addition of fibers to CSC, leading to enhanced flexural strength, particularly with 1% fiber content. Moreover, Sekar and Kandasamy (2018) explored the optimization of coconut fiber addition to CSC and conventional concrete, noting significant flexural strength improvements with fiber inclusion. In a separate study, Prakash et al. (2020) incorporated polypropylene fibers into CSC mixtures, resulting in enhanced flexural strength and highlighting the potential of fiber reinforcement in improving structural performance. Gunasekaran et al. (2011) also discussed the fracture characteristics of CSC aggregates, suggesting their suitability as concrete aggregates despite inherent brittleness. These studies collectively contribute to understanding the multifaceted factors influencing flexural strength in CSC-based concrete mixtures.

2.4.3 Bond strength

For the purpose of ensuring the structural integrity of a building, the bond strength between concrete and embedded steel reinforcement is of utmost importance. CSC demonstrates a bond strength that is much superior to that of ordinary concrete due to the adhesive and fibrous characteristics of CS. In addition to significantly boosting binding strength, the uneven form and surface roughness of CS particles make it easier for them to interlock with one another. Additionally, the silica content of CSs contributes to the strengthening of the bond, which ultimately results in concrete that is more difficult to crack and of greater durability.

Experiments conducted by Gunasekaran et al. (2011) resulted in various water-to-cement ratios of CSC. The results of these experiments revealed that CSC specimens displayed bond strengths ranging from 3.56 to 7.49 MPa for plain bars and from 4.22 to 9.84 MPa for deformed bars. CSC's bond strength exceeded theoretical norms and was comparable to that of conventional concrete and other types of lightweight concrete, despite the bond strength decreasing with increasing bar size. Sekar and Kandasamy

(2018) explored the optimization of coconut fiber additions to both conventional concrete and concrete with CSC. They found that experimental bond strengths exceeded standard guidelines, with CSC samples showing bond strengths ranging from 4.01 to 7.7 MPa for plain bars and 3.98 to 9.57 MPa for deformed bars. Plain bars demonstrated continuous performance, whereas deformed bars failed suddenly following longitudinal cracks. Furthermore, plain bars displayed a higher bond strength than deformed bars. In general, the incorporation of coconut fiber resulted in an improvement in bond strength; however, a decrease was noted with an increase in bar diameter, which is consistent with the findings of previous experiments.

2.5   Transport properties of CS concrete

2.5.1   Porosity and water absorption

Porosity and water absorption capacity are two factors that have a substantial impact on the absorption property of concrete, which is an indicator of the material's durability. Porosity, which is dictated by the structure of the particle, has a significant impact on the water absorption characteristics of the particle. In comparison to NWAs, LWAs often have a larger porosity, which results in a significantlt more water absorption capacity. These disparities in absorption rates have important repercussions for the longevity and quality of structures made of concrete.

According to the findings of Polat et al. (2010) on LWACs formed from pumice and LECA aggregates, these LWACs exhibited increased water absorption rates due to the inherent properties of LWAs. The incorporation of LWAs into the concrete matrix introduces more capillaries and voids, facilitating water penetration into the matrix. During the concrete mixing process, CS aggregates, characterized by their porous shell structure, demonstrate a high capacity for water absorption. Even with their high water absorption capacity, the correct curing methods can reduce the amount of absorbed water and improve the internal curing process. Yerramala and Ramachandrudu (2012) noted

that incorporating CS and coir fibers into concrete resulted in increased water absorption capabilities, adding complexity to the dynamics of the absorption process. Furthermore, Kamal and Singh (2015) revealed that increasing the proportion of CS in concrete led to higher water absorption rates, impacting the material's long-term durability and performance. Given the direct correlation between the amount of CS present and the volume of water absorbed, careful consideration of concrete mix design and material selection is essential.

2.5.2   Permeability

The mechanisms governing the passage of liquids and gases through concrete are primarily influenced by its permeability. Permeable voids, which are tiny spaces between concrete aggregates, facilitate the movement of air and water, significantly contributing to the concrete's durability and weight reduction. Literature indicates that the size and shape of permeable voids are crucial factors influenced by the type of aggregate and water content during mixing. Larger voids generally enhance permeability; however, excessively large voids may compromise concrete strength and increase vulnerability to cracking. A study conducted by Yerramala et al. (2012) showed that replacing a portion of natural aggregates with CS significantly increased permeable voids, with 20% CS substitution leading to an 88% increase in voids compared to control concrete. Similarly, the addition of fly ash affected voids differently depending on whether it replaced cement or aggregates, demonstrating the nuanced interplay of materials in concrete mixtures. Further studies by Kamal and Singh (2015) confirmed that increasing the percentage of CS in concrete directly correlates with increased permeable voids, underscoring the role of aggregate composition in concrete permeability.

Supit and Shaikh (2015) demonstrated that incorporating fly ash reduced permeability voids by 6-11% compared to normal-weight concrete (NWC). This reduction in permeability is attributed to the finer pore structure resulting from fly ash inclusion, which

enhances concrete's resistance to liquid and gas penetration. Similarly, Prakash et al. (2020) demonstrated that incorporating fly ash in CSC mixes reduced permeability, particularly at later ages, due to fly ash's ability to restrict pore size and limit water absorption. This finding suggests that the choice of supplementary materials can significantly influence concrete permeability and the long-term durability of LWACs. Gunasekaran et al. (2015) highlighted the impact of curing conditions on permeability, showing that proper curing mitigated void formation, particularly in CSC.

2.5.3 Sorptivity

Sorptivity, which denotes concrete's ability to absorb and retain water, is a crucial determinant of concrete durability. It is influenced by concrete type, aggregate characteristics, and the curing process. Sorptivity testing provides insights into a concrete's pore structure and water absorption resistance. A sorptivity value below 0.1 mm/min$^{0.5}$ signifies high-quality concrete, as noted by Kareem et al. (2022). Studies have revealed varied sorptivity levels among different concrete types and compositions. For instance, certain concretes exhibited sorptivity values ranging from 0.12 to 0.18 mm/min$^{0.5}$, with increased values correlating with higher percentages of CS material..

Gunasekaran et al. (2015) observed that CSC exhibited sorptivity values ranging from 0.095-0.104 mm/min$^{0.5}$ under different curing conditions, comparable to other LWA types. The low sorptivity of CSC can be attributed to a low water-to-cement ratio, which enhances compaction and reduces pore size, thus limiting water absorption. Prakash et al. (2020) noted a decrease in sorptivity with the addition of fly ash in CSC mixes, indicating improved aggregate interfacial transition. Sorptivity values declined with increased fly ash content, resulting in sorptivity levels comparable to those of other LWAs. Mo et al. (2016) reported that the inclusion of fly ash and silica fume in mixes led to lower sorptivity values, attributed to a mortar matrix with a low water-to-binder ratio. Enhanced compaction and improved aggregate-matrix interface further reduced sorptivity,

promoting concrete durability. Additionally, the filling ability of silica fume and fly ash improved the interfacial transition zone, further reducing sorptivity in OPSC concrete.

2.6 CS as aggregate

The phenomenon of particle packing has garnered significant attention from academics across multiple disciplines for more than a century. This interest can be attributed to its important role in determining the characteristics of materials produced in various industrial sectors, including ceramics processing, as noted by Reed (1995), and powder metallurgy, as highlighted by Smith (2003). The behavior of concrete mixes is influenced by the arrangement of constituent particles, which contributes to the packing of these particles. Extensive research conducted over several decades has demonstrated that the arrangement of particles in the concrete system significantly impacts the rheological characteristics of concrete mixes, as shown by De Larrard (1999), Kwan (2000), Lange et al. (1997), Powers (1969), Roshavelov (2005), and Xie et al. (2002). Nevertheless, existing research remains inadequate for precise quantification and forecasting of the packing density and rheology of cement paste, mortar, and concrete. This rationale has led to calls for increased focus on particle packing in recent years. The subsequent discussion will elucidate how a deeper understanding of the packing in concrete particle systems can facilitate the optimization of mix compositions, resulting in enhanced performance without incurring additional expenses.

The packing density, referring to the ratio of solid volume to bulk volume in a closely packed state, is a fundamental characteristic that describes the features of numerous granular systems, as highlighted by Oliviera et al. (1996) and Reed (1995). Concrete is a granular system composed of cementitious ingredients and aggregates. The packing density of the solid elements in concrete significantly impacts numerous performance aspects. For example, if the cementitious materials are packed more densely, flowability increases, even with the same amount of water, or a lower water-to-cementitious material

ratio can enhance strength and durability while maintaining the same flowability, as noted by Kwan and Wong (2008) and Li et al. (2017). Conversely, if the aggregate is packed more densely, workability increases, even with the same volume of paste, or a smaller volume of paste can improve dimensional stability while maintaining the same workability, as indicated by Li et al. (2017) and Powers (1969).

The phenomena of loosening occur when there is a predominance of coarse particles, as illustrated in Figure 2.2 (a), whereas the wall effect arises when there is a predominance of fine particles, as indicated in Figure 2.2 (b), according to Wong et al. (2013). Furthermore, Figures 2.2 (c) and (d) demonstrate the presence of a wedging effect due to the prevalence of both coarse and fine particles. The differential in size between fine and coarse particles causes the loosening, wall, and wedging effects, which are collectively referred to as a size ratio. Several particle packing models have been devised to account for the diverse structural effects. Furnas (1931), Powers (1969), Aim and Goff (1968), Toufar et al. (1976), Goltermann et al. (1997), and Dewar (1986) introduced the concepts of loosening and wall effects, which are today recognized as crucial principles in packing theories. The principles of particle packing have led to the classification of packing concepts into discrete and continuous models, as depicted in Figure 2.3. Discrete packing describes systems that consist of two or more distinct particle size classes packed together. The discrete models can be categorized into linear and nonlinear model approaches, as indicated by Liu et al. (2020), and are also depicted in Figure 2.3.

a — Loosening effect

b — Wall effect

c — Wedging effect — **Coarse particles are dominant**

d — Wedging effect — **Fine particles are dominant**
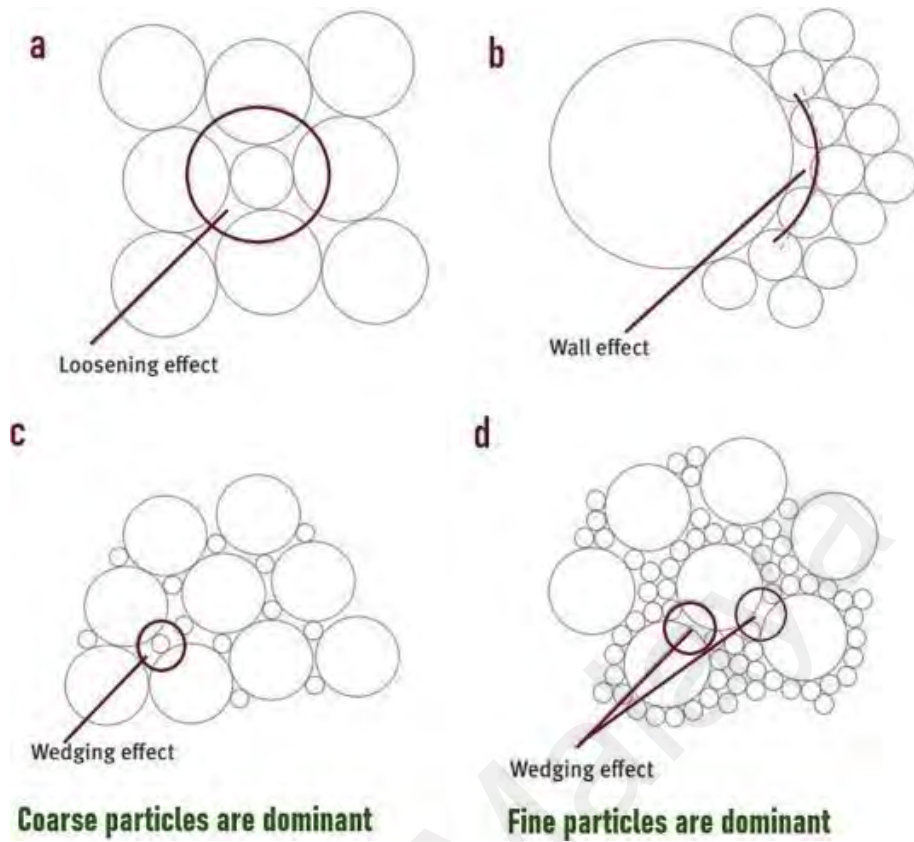
Figure 2.2: Structural effects of particle packing concept (a) Loosening effect (b) Wall effect (c) & (d) Wedging effect
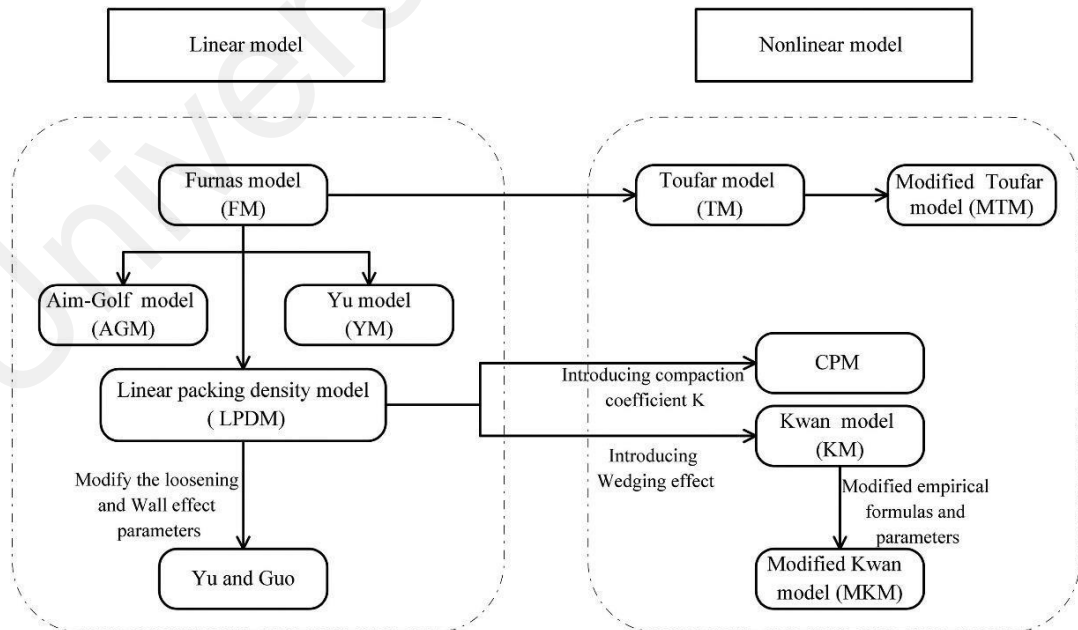
Figure 2.3: Summary of Particle Packing Model

2.6.1   Linear packing models

2.6.1.1   Furnas model

The approach is based on the work conducted by Furnas (1931), who researched materials used in mortar and concrete construction, building upon earlier studies by Feret, Fuller, Abrams, Talbot, and others. However, Furnas focused on mathematically formulating the laws rather than relying on empirical relationships, as noted by Brewe and Myers (2005). Based on his methodology, the upper limit for the density of uniformly sized particles when closely packed is roughly 60%. In addition, when smaller particles are placed between the larger particles, they occupy 60% of the remaining empty space. Consequently, the initial step involves packing particles of significant size until they occupy 60% of the total volume. Subsequently, smaller particles are added to cover the remaining 40% of spaces between the large particles, resulting in an approximate density of 84%. When three different sizes are available, medium-sized particles occupy the empty spaces inside the larger particles, while small particles fill the gaps between the medium and big particles. This arrangement results in a packing density of around 94%. While the packing density may appear remarkable, it is challenging to attain. In order to maximize packing efficiency, Furnas suggests that the ratio of particle sizes should ideally be infinitely large, however a more practical approach would be to have a ratio beyond 100:1. Due to the infrequent occurrence of this ratio in practical scenarios and the rarity of pure monosized distributions, achieving such high packing densities is seldom fulfilled. Furnas further extended his theory to encompass class sizes denoted by the variable "N," which represents a continuous distribution. This distribution is analogous to discrete distributions where the class ratios tend towards a 1:1 ratio, forming a geometric progression. He observed that the ratio of mass or volume between any two consecutive sieves should be constant. As a result, he developed the Cumulative Percent Finer Than (CPFT) curve by Equation (2.1):

$$\frac{CPFT}{100\%} = \frac{r^{\log D} - r^{\log D_S}}{r^{\log D_L} - r^{\log D_S}}$$

(2.1)

Where; ratio of the volume of particles on one sieve to the volume on the next smaller sieve (r), the particle size (D), the smallest particle size (D_S), and the largest particle size (D_L). The value of r fluctuates across many distributions, however it consistently hovers around 1.1. This method for continuous particle size distribution is an expansion of his approach for the discrete case involving many components. According to this theory, particle size distributions that conform to this curve will achieve the highest feasible level of density when packed. The issue arises when the larger particles reach their maximum packing density, leaving insufficient empty spaces to accommodate the smaller particles. Figure 2.4 illustrates the arrangement of circles packed into a square, using the Furnas paradigm. Despite the appearance of dense packing, there were not enough open areas to pack the requisite particles. Figure 2.5 illustrates the identical arrangement of particles within an open-ended container, emphasizing those particles that lacked sufficient space, as described by Funk and Dinger (2013).
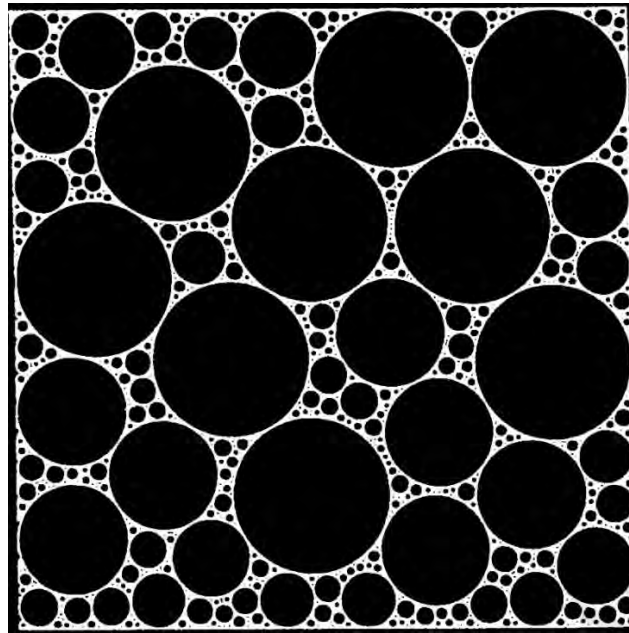
Figure 2.4: Particle packing according to the Furnas model
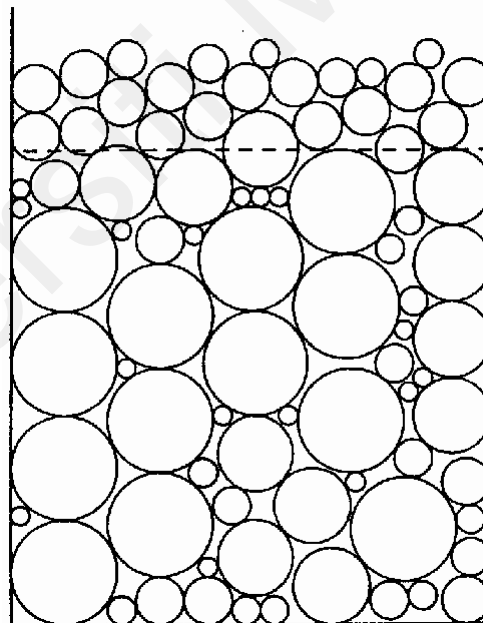
Figure 2.5: Particle packing of larger classes according to Furnas, illustrating particles that could not fit into the pack

Furnas (1929) developed a binary methodology focusing on the loosening and wall effect. However, the forecasted value of the Furnas model was found to be imprecise for a progressively increasing fine-to-coarse particle size ratio. As the particle size ratio increases, the interaction between particles becomes more pronounced. Despite this, the

Furnas model does not account for particle interactions, which affects the accuracy of its predictions.

2.6.1.2 Aim and Goff model

The packing density of fine aggregate is disrupted when a single coarse particle is present within a matrix of fine aggregate. This leads to larger voids forming around the contact points between the particles. Aim and Goff explored this phenomenon, known as the wall effect, and introduced a correction factor to accurately evaluate the density of binary mixtures. To address inconsistencies in phenomena such as loosening and the wall effect, Kwan and Wong (2008) introduced the wedging effect. In the presence of coarse particles, fine particles tend to interfere with the arrangement of the coarse particles by wedging themselves between them, rather than simply filling the voids. However, in situations where fine particles are predominant, the wedging effect occurs when certain coarse particles are placed close to each other, preventing the formation of a complete layer of fine particles. According to Wong et al. (2013), this results in the creation of additional empty spaces between large particles. Consequently, a 3-parameter particle packing model was developed, incorporating the wedging effect as a key component.

2.6.1.3 Linear packing density model

The Furnas model, a Linear Packing Density Model, was further developed by Stovall et al. (1986) and De Larrard (1999) through two significant advancements. Fennis (2011) expanded the two-component model by incorporating several components and introducing geometric interactions among particles, as represented by Equation (2.2):

$$a_t = Minimum_{i=1}^{n} \left\{ \frac{a_i}{1-(1-a_i)\sum_{j=1}^{i-1} g(j,i)r_j - \sum_{j=i+1}^{n} f(j,i)r_j} \right\}$$ (2.2)

Where;

a_i is the packing value of each class, in this case, fine and coarse material. a_t represents the packing value of the combined particle mix. The functions g(j, i) and f(i, j) depict the interaction between particles, specifically related to the concept of the minimum value.

The packing density of a binary mixture, estimated using the Linear packing density model, is always determined by the lesser of the two a_t values. When the radius of the smaller particles is significantly greater than the radius of the bigger particles, it is not possible to completely fill the voids of the larger particles. This is because there is insufficient space to accommodate all the smaller particles. The Linear Packing Density Model is only applicable when the diameter of one particle size is significantly greater than the diameter of the smaller particle size. Failure to meet this criteria will result in the packing density of the binary mixture being influenced by the diameter ratios of the size classes. As a result of interaction, the ideal grading curve is altered, resulting in each mixture achieving its unique ideal composition.

Because it reliably predicts packing densities for multiple types of particles, the Linear Packing Density Model is well-suited for use with real-world concrete mixes. The packing densities of each class and the distribution of particle sizes in the mixture are taken into account in the analysis. Indirectly, the parameter a_t incorporates the impact of particle morphology and surface properties. Interaction formulas f(i, j) and g(j, i) are computed relations based on the packing density of two-component mixtures and are crucial to the model's performance. This is in agreement with the theory that the interactions between the system's smaller size categories can be ignored. Because of its construction and the equations used, the model is theoretically sound and robust.

Incorporating particle-surface force interactions into the model for ecological concrete applications is made possible through the use of interaction formulas.

2.6.2 Nonlinear packing models

2.6.2.1 Toufar and modified toufar model

A model was developed by Toufar et al. (1976) to determine the optimal configuration of binary mixes with ratios ranging from $0.22 < d_1/d_2 < 1.0$. Because of how the model was constructed, smaller particles with diameter d_1 will be unable to fit between larger particles with diameter d_2 when the diameter ratio exceeds 0.22. Because of this, the packing density (k_d) should be defined as the ratio of the two particle classes' diameters. Furthermore, the statistical probability of the space between bigger particles that is unoccupied by smaller particles was investigated by Toufar et al. (1976). Theoretically, a factor k_s is produced when the fine particles are put one by one between exactly four of the coarse particles, as described by Fennis-Huijben (2011).

The Equations from (2.3) to (2.6) below indicate the total packing density according to Toufar model.

$$a_t = \frac{1}{\frac{r_1}{a_1} + \frac{r_2}{a_2} - r_2(\frac{1}{a_2}-1)k_{dks}} \tag{2.3}$$

$$k_d = \frac{d_2-d_1}{d_1+d_2} \tag{2.4}$$

$$k_s = \frac{1+4x}{(1+x)^4} \tag{2.5}$$

$$x = \left(\frac{r_1}{r_2}\right)\left(\frac{a_2}{a_1(1-a_2)}\right) \tag{2.6}$$

The variable x is employed as a contributing component in the computation of k_s.

In the absence of interaction, the values of k_d and the packing density align with the Furnas model when r_1 is significantly larger than r_2 and when r_1 is significantly less than r_2. However, subsequent comparisons with the experiment indicate that this model predicts that the packing density of a sample of coarse particles remains unchanged when a modest quantity of fine particles is introduced to the mixture of coarse particles. This is because it is assumed that each particle is situated within a confined region, delimited by four larger particles. However, Fennis (2011) made an adjustment to the k_s expression due to the impracticality of this behavior, as explained by Equations (2.7) and (2.8):

$$k_s = \frac{0.3881x}{0.4753}, \qquad \text{For } x < 0.4753 \tag{2.7}$$

$$k_s = 1 - \frac{1+4x}{(1+x)^4}, \quad \text{For } x \geq 0.4753 \tag{2.8}$$

Modified Toufar is a useful model for calculating packing density when only a few input variables can be used. Furthermore, it is more user-friendly in comparison to other packing models, which tend to be more intricate. Nevertheless, employing this approach to calculate the packing density of multi-component mixtures sometimes results in underestimations of the packing density. The deviation from the predicted packing density increases as the number of size categories rises, as noted by Fennis (2011).

2.6.2.2 Compressible packing model

The initial attempt to predict packing density using the Solid Suspension Model, introduced by Sedran et al. (1994), faced limitations, particularly regarding the concept of reference viscosity (used as a measure of the system's compaction level) and the inadequate mathematical formulation of interaction functions, as highlighted by De Larrard and Sedran (1999). The concept of the compaction index "K" was later added in the CPM model to represent the compaction energy. This model enables the prediction of

the actual packing density of a mixture including multiple granular classes based on the compactness of each individual class in one dimension and the energy involved in the arrangement process. The actual packing density is contingent upon the level of compaction energy applied. The relationship between the actual packing density "C" of a mixture of aggregates and "K" is defined by the equation provided in Equation 2.13. In addition, de Larrard (2000) developed simplified formulas (Equation (2.9) and Equation (2.11)) for the granular interaction coefficients (a and b) after calibrating the CPM using several sets of experimental data.

$$K = \sum_{i=1}^{n} \frac{K_i}{1} = \sum_{i=1}^{n} \frac{y_i}{\beta_i} : (\frac{1}{C} - \frac{1}{\gamma_i}) \tag{2.9}$$

$$a_{i,j} = \sqrt{1 - \left(1 - \frac{d_j}{d_i}\right)^{1.02}} \tag{2.10}$$

$$b_{j,i} = 1 - \left(1 - \frac{d_i}{d_j}\right)^{1.5} \tag{2.11}$$

Within the context of the CPM framework, it is feasible to estimate the packing density by first determining the coefficients a and b. These coefficients are calculated based on the void index at the boundaries of coarse and fine grains dominance, together with the coefficient K. These characteristics were calibrated using binary mixtures of aggregates with various compositions, including both crushed and rolled aggregates, according to research by De Larrard (2000) and Lecomte et al. (1997). The discrepancy between measured and predicted packing densities following calibration was no more than 0.77% for rolled aggregates and 1.71% for crushed aggregates, as noted by De Larrard (2000).

Various models and computational approaches have been proposed to enhance the accuracy of packing density predictions, with contributions from Dewar (1986), Reisi and Nejad (2011), and Toufar et al. (1976). Several authors, including Kwan et al. (2013) and Roquier (2016), have suggested novel interaction parameters. Roquier (2016) introduced the "interference effect," which arises when a high density of coarse grains causes fine

grains to become trapped in the narrow spaces between them. Despite numerous efforts to improve packing density predictions, the CPM (Compressible Packing Model) remains one of the most accurate and user-friendly models, as demonstrated by Jones et al. (2002) and Moutassem (2016). In a study conducted by Moutassem (2016), nine packing density models were tested, and it was found that the CPM accurately predicts the packing density of granular mixtures commonly used in concrete.

2.6.2.3   Modified Andreassen and Andersen packing model

Andreassen expanded on Fuller's theory, investigating the size distribution for particle packing using a continuous method and deriving the equation for optimal packing. In this hypothesis, the smallest particles are infinitesimally small, as explored by Das et al. (2021). To achieve high compactness, Andersen (2020) recommended using a value of q ranging from 0.21 to 0.37, depending on factors such as the desired workability and the type of concrete, such as conventional concrete, roller-compacted concrete, high-strength concrete, or reactive powder concrete, as outlined by Saidi et al. (2020). As the exponential q value rises, so does the proportion of coarse materials, whereas a decrease in the q value results in more fine particles, as discussed by Banerjee (1998).

According to Andreasen model in Equation (2.12) below,

$$CPFT = \left(\frac{d}{D}\right)^q x\ 100 \tag{2.12}$$

q=0.21-0.33.

Nevertheless, the Andreassen model is inadequate for achieving optimal packing when dealing with granular materials that have a significant level of fineness ($<250\ \mu m$). Fuller and Thomson proposed that the true size distribution should encompass both the largest and smallest particle sizes. Consequently, Equation (2.13) was derived based on the Modified Andresen and Andreasen model.

Based on the Modified Andreassen model,

$$CPFT = \left(\frac{d - d_{min}}{d_{max} - d_{min}}\right)^q x\ 100 \qquad (2.13)$$

d = Size of the particle.

d $_{min}$ = Minimum particle size.
d $_{max}$ = Maximum particle size,
q = the distribution exponent.

The amount of water and viscoelasticity-modifying additives, such as admixtures, to be included in the mixture can be determined based on q, which is influenced by the volume of fine particles and affects the water demand and water-holding capacity of the mixture, as explained by Goltermann et al. (1997). These theories assist in identifying factors that govern material behavior and illustrate how changes in these factors can impact the effectiveness of concrete.

2.7   Summary of research gaps in the literature

The advantages discussed highlight the potential benefits of the packing density approach, particularly in terms of physical properties, transport properties, mechanical performance, cost reduction, environmental impact, and sustainable resource utilization. A key advantage is the anticipated lower cost and reduced CO_2 emissions for producing 1 m³ of concrete. By incorporating CS aggregates and supplementary cementitious materials such as ground granulated blast-furnace slag GGBS, the cement content in concrete mixtures can be significantly reduced. Given that cement production is a major contributor to carbon emissions, lowering the cement content mitigates the environmental impact of concrete production. Additionally, using waste materials like GGBS enhances the sustainability and cost-effectiveness of concrete.

This study addresses a key research gap by thoroughly exploring the use of low-cementitious, economically viable, high-strength LWAC, integrating non-spherical waste

aggregates through the packing density method. This innovative approach contributes significantly to the field of structural LWAC, offering new insights and practical applications that may transform the way lightweight aggregate concrete is designed and employed in various structural contexts.

CHAPTER 3: MATERIALS AND METHOD

3.1 Materials

The Ordinary Portland Cement (OPC) used in this research was supplied by Tasek Corporation Berhad-Cement Industry of Malaysia. The OPC adhered to Type I Portland cement specifications, conforming to the ASTM C 150-05 standard. The cement exhibited a specific gravity of 3.14 and a specific surface area of 3510 cm^2/g.

GGBS is primarily composed of alumino-silicates, calcium silicates and other bases, is a non-metallic substance. Its composition encompasses both amorphous and crystalline components. The cementitious properties of GGBS are largely attributed to its glassy composition, with the glass component comprising approximately 85% to 90% of its content, as noted by Gong and White (2016). The detailed physical and chemical compositions of the GGBS used in this study can be found in Table 3.1.

This study employed CS obtained as waste material from a local manufacturer, as illustrated in Figure 3.1. The CS, originating from the co-processing of various coconut species, display thicknesses ranging from 2 to 8 mm. After undergoing the crushing process, the resultant shells exhibit a flaky and irregular morphology. The physical and mechanical properties of CS coarse aggregate and BF utilized in this study are presented in Table 3.2 and Table 3.3, respectively.

Table 3.1: Physical properties and chemical compositions of GGBS

Specific gravity		Specific surface (m^2/kg)		
2.89		410-450		
CaO (%)	SiO_2 (%)	Al_2O_3 (%)	MgO (%)	Fe_2O_3 (%)
40.54	36.17	11.49	8.75	1.13

Table 3.2: Physical and mechanical properties of CS aggregate

Bulk Density (Loose)(kg/m³)	Bulk Density (Compacted)(kg/m³)	Specific Gravity (kg/m³)	Water absorption (%)		
			15 min	1 hour	24 hour
583	657	1032	12.8	19	27.3

Table 3.3: Physical and mechanical properties of BF (information from the manufacterer)

Length (mm)	Diameter (μ)	Specific weight (kg/m³)	Tensile strength (N/mm²)	Elastic modulus (N/mm²)	Ultimate Elongation (%)
12	15	2600	2000	93,000	3

Figure 3.1: CS and BF used in the study

The fine aggregate employed in this study possessed a maximum grain size of 4.75 mm. To facilitate separation into 3 selected sizes, as detailed in the previous section, mechanical sieving was applied to the fine aggregate. The resulting portions are designated as aggregates A, B, and C, as outlined in Table 3.4.

Table 3.4: Three size classes of mining sand

Size class	Sieve size range	
	Lower sieve size (sieve retained on)	Upper sieve size (sieve passed through)
A	-	75 μm
B	75 μm	150 μm
C	150 μm	4.75 mm

3.2   Experimental testing methods

Water absorption and porosity tests were carried out following ASTM C 642-06 (2006), and the sorptivity test was conducted in accordance with ASTM C 1585-04 (2004). Compressive and flexural strengths were assessed using ASTM C39-14a (2005) and ASTM C78 (2009), respectively. Following the demolding of cube samples and cylinders 24 hours after casting and obtaining fresh density results, they were cured in water until the age of testing. For saturated surface dry (SSD) and compressive strength tests, the specimens underwent curing periods at 1-, 7-, and 28-days, each consisting of three cube specimens for every mix design with dimensions of 100 x 100 x 100 mm. Flexural strength testing was conducted at 28 days only for three beam specimens with dimensions of $100 \times 100 \times 500$ mm. Compressive and flexural strength tests employed a constant loading rate of 5 kN and 0.0675 kN per second, respectively. The flowchart outlining the research is depicted in Figure 3.2. The flowchart illustrates the process of producing HSLWAC through the integration of waste materials and the packing density approach. The process begins with the utilization of waste CS aggregates, which are used as an eco-friendly alternative to natural aggregates. These shells, typically considered waste, help reduce the environmental impact of aggregate extraction. Additionally, mined sand undergoes a grinding process to create fine particles, contributing to a more efficient particle distribution and enhanced packing density in the concrete mix. The goal is to minimize voids, leading to improved strength and durability.

The core of the process focuses on achieving maximum packing density, as shown by the graph in the center, which optimizes the aggregate mixture by adjusting particle sizes and volume ratios. This improves the mechanical performance of the concrete while reducing the cement content. Wet-milled GGBS is incorporated as a supplementary cementitious material, further reducing the cement required and lowering CO_2 emissions. GGBS not only contributes to the environmental sustainability of the concrete but also enhances its durability and strength.

The result of this process is HSLWAC, a concrete with improved physical, transport, and mechanical properties, while also being cost-effective and environmentally friendly. The optimized mix design reduces cement use, leading to lower production costs and a smaller carbon footprint. This approach addresses the identified research gap by exploring the benefits of integrating non-spherical waste aggregates and supplementary materials into lightweight concrete, promoting sustainability in construction.
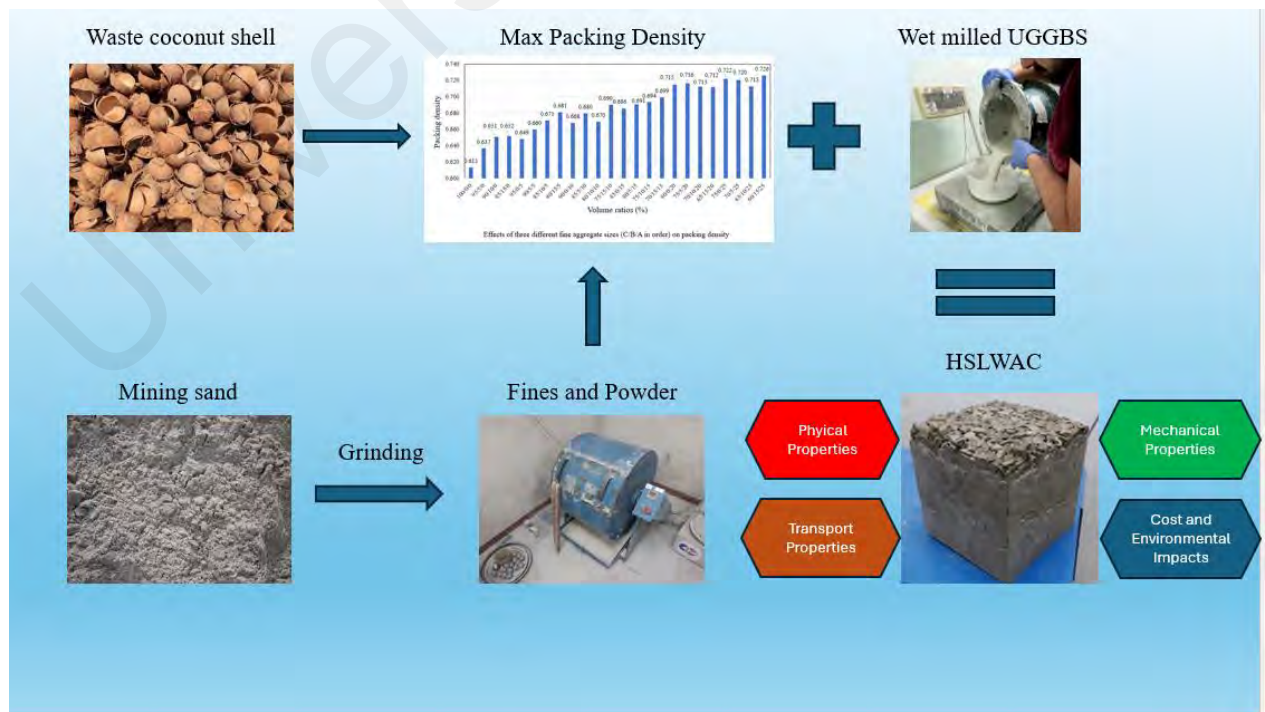
Figure 3.2: Research flowchart

3.3 Developing the mix design

3.3.1 Optimum combination of CS aggregates

Coarse aggregate makes up around 70% of concrete volume, and any changes in critical factors such as aggregate gradation and rheology significantly influence the flow characteristics and hardened properties of concrete, as discussed by Roussel et al. (2005), Zhang et al. (2016), and Jingbin Zhang et al. (2019). Notably, the use of graded coarse aggregate has been shown to reduce both the yield stress and viscosity of concrete compared to using single-sized coarse aggregate, as observed by Hu and Wang (2011) and Westerholm et al. (2008). The optimal grading of coarse aggregate enhances filling capacity, thereby reducing the amount of cement paste required to achieve a desired consistency, as explained by Meddah et al. (2010). This reduction occurs due to the decreased need for cement slurry to fill the gaps between the coarse aggregates, as identified by Feys et al. (2009) and Hu and Wang (2007, 2011).

This study focused on determining the optimal combination of selected CS aggregates in two different sizes, considering both their loose and compacted dry packing densities. In the initial phase, volume ratios were adjusted at 5% intervals to assess the impact on packing density. Subsequently, the final volumetric ratios were determined based on achieving the highest packing density between the two mixes, with adjustments made at 1% intervals. As illustrated in Figure 4.1., the highest two packing density values of CS aggregate volume mixes was determined to be 20/80 and 15/85 for the aggregate sizes of 9.50-6.30/6.30-4.75 mm for 5% intervals. However, for greater precision of packing density values, another dry packing density procedure with 1% intervals was followed and 18/82 were found and chosen to be the optimum volume ratios for coarse aggregate based on both Figure 4.1. and Figure 4.2..
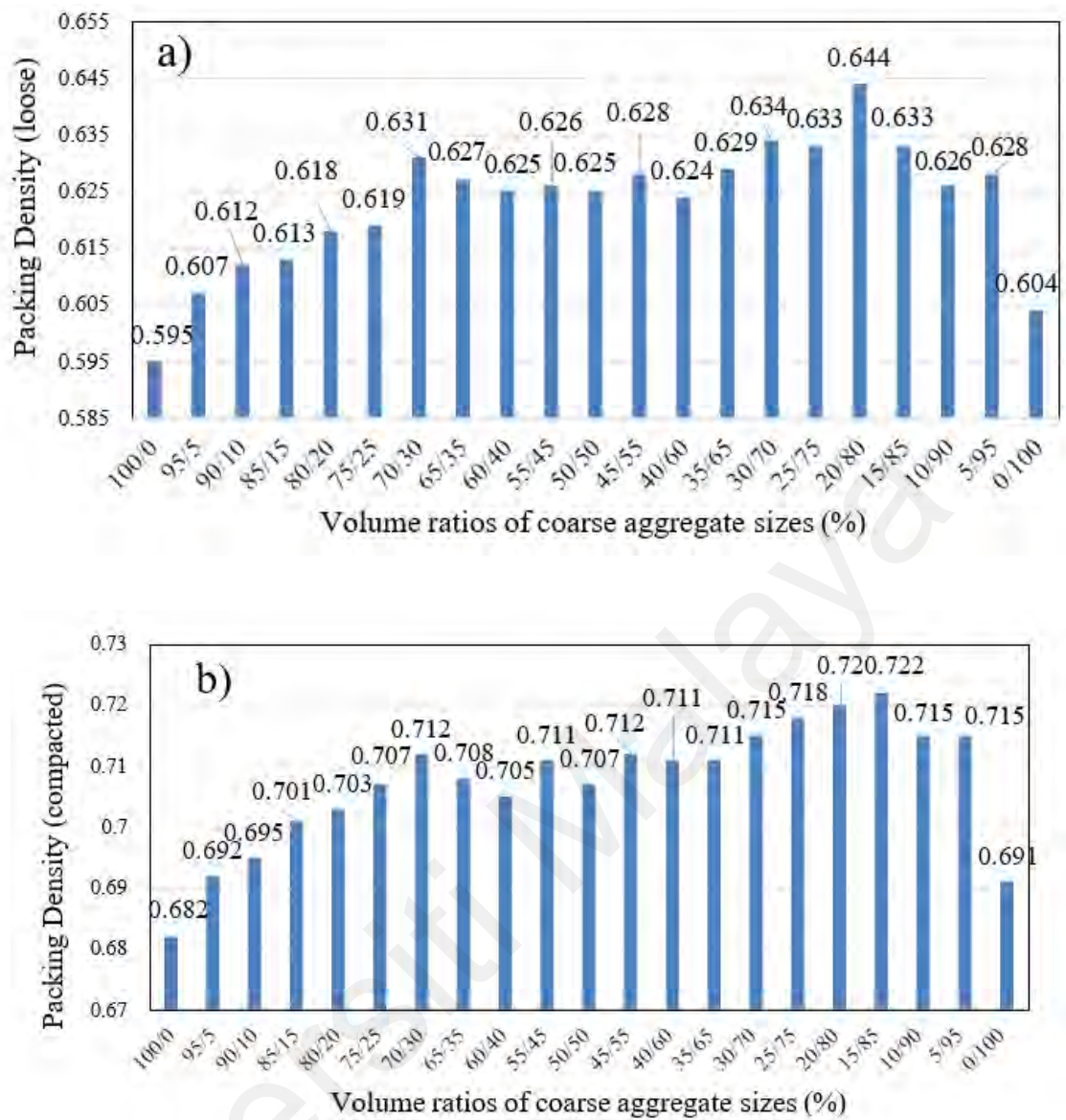
Figure 4.1: Effect of volume ratios of CS aggregate sieve sizes (9.50-6.30/6.30-4.75) on packing density for a) loose b) compacted
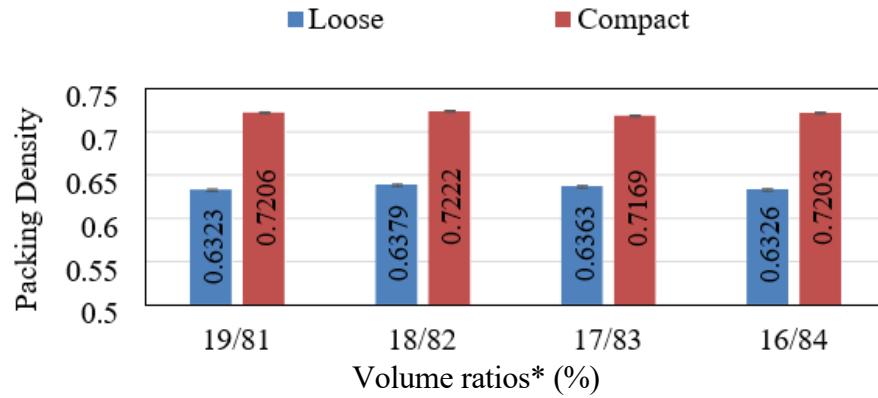
Figure 4.2: Optimum volume percentages for %1 interval

The results revealed from Figures 4.1 and 4.2 that both loose and compacted packing densities increased with the higher ratio of the smaller aggregate size. However, the upward trend diminished after a specific rate of volumetric substitution of 6.30–4.75 mm aggregate size with 9.50–6.30 mm. For compacted packing method, a 6% and 4.5% increase was observed from volume ratios 100/0 (all aggregates retain sieve sizes between 9.50-6.30 mm) and 0/100 (all aggregates retain sieve sizes between 6.30-4.75 mm) to optimum volume ratios 18/82 mixture. An insignificant rise in packing density (0.02%) was observed for the experiment of 1% intervals, from 20/80 to 18/82 volume ratios. The flaky-concave structure of coconut shell (CS) aggregates, which modifies the void structure, may also contribute to the decline in packing density as aggregate size increases, as suggested by Kusumawardani and Wong (2020).

3.3.2 Fine aggregate composition

The microstructure of concrete is critical in determining its workability, strength, durability, and transport properties, as noted by Mukharjee and Barai (2014). Despite the potential benefits in terms of performance, cost reduction, and property enhancement from increasing fines content in concrete, certain standards (ASTM, 2002; BS-EN-12620, 2002) impose restrictions on the allowable amounts. However, some studies have indicated that the fines content can be increased up to 25%, as observed by Oliveira et al. (2020). Recent years have also seen stricter regulations on river sand dredging due to

environmental concerns and risks to riverbank stability, as highlighted by Chow et al. (2013). Consequently, this led to a severe scarcity of river sand, prompting the construction industry to seek viable substitutes. Mining sand has emerged as a potential alternative to river sand in construction projects. Although mining sand offers a cost-effective option as a fine aggregate replacement, there is a common concern that its higher fine content may result in excessive water demand, making it less workable for concrete.

During this stage of Phase A, two distinct fine aggregate sizes, namely Aggregate B (75 µm <P <150 µm) and A (<75 µm) , were replaced with Aggregate C (150<FA<4.75) at various volume ratios to achieve the maximum packing density, as illustrated in Figure 4.3. Compacted wet packing densities for various volume combinations were determined using Equation (1.2). Numerous combinations were scrutinized, and the mixture with the highest solid content was identified as the optimum fine aggregate mix. The water-to-solid (V_w/V_s) volumetric ratio was maintained constant at 0.35 for all mixtures. According to the results presented in Figure 4.3., it was observed that packing density exhibited a significant increase with the rise in powder and fine content.
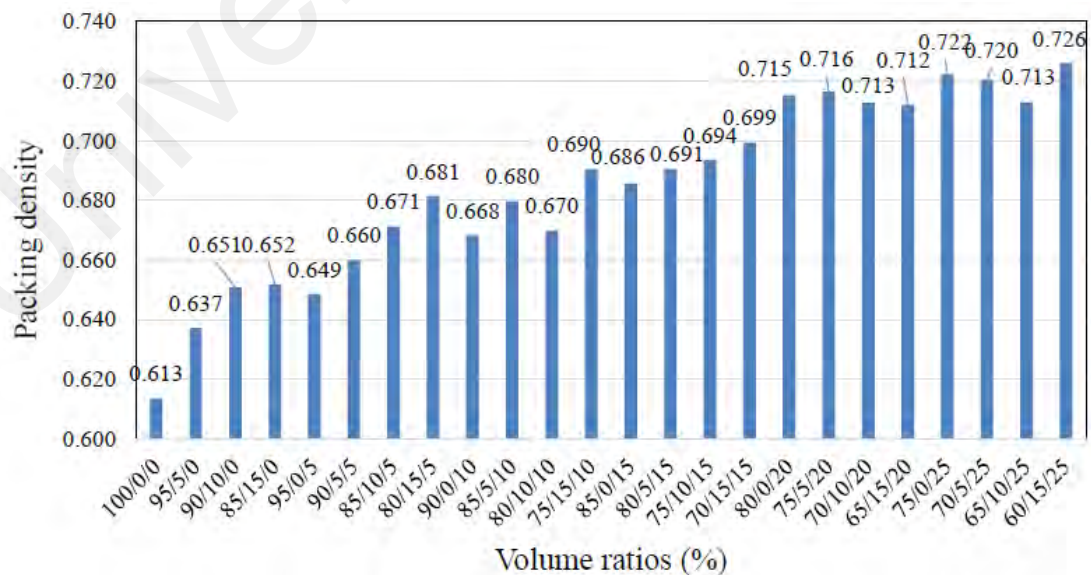
Figure 4.3: Effects of three different fine aggregate sizes (C/B/A in order) on packing density

Specifically, upon the inclusion of powders and fines, the packing density of the mixture demonstrated a notable 18% increase at volume proportions of 60/15/25 compared to 100/0/0 volume ratios. Remarkable packing density rises can be observed from the results for each fine and powder content volume increase. To emphasize its importance, the increase of the packing density 95/5/0 mixture is 4% compared to the 100/0/0 mixture, in which 5% of the powder content was added. This increase was observed to be 6% for the 95/0/5 mixture. While this increment raised to up to 16% for the case where the fines content increased up to 20%, it remained at the same level around 25% fines content. The primary reason for this enhancement is that powders and fines can occupy voids that would otherwise be filled by water or air. As a result, the composition of 60/15/25 proportions was selected as the optimal fine aggregate blend.

3.3.3 Coarse to fine aggregate composition

The unique shape and characteristics of CS aggregates can significantly affect the microstructure and interfacial transition zone (ITZ) when compared to traditional granite aggregates, as discussed by Bari et al. (2021) and J. Wang et al. (2020). The irregular shape of CS aggregates introduces variability within the concrete matrix, leading to a distinct microstructure, as indicated by J. Wang et al. (2020). This irregularity may result in reduced interlocking between particles and increased porosity within the CS aggregates, as observed by Aziz et al. (2022). Consequently, the ITZ between the CS aggregates and the surrounding cement paste may exhibit distinct characteristics compared to the ITZ formed with granite aggregates, as suggested by Ejaz et al. (2022). The irregular surface of CS aggregate may contribute to a reduced contact area and weaker bond strength with the cement paste. To address these challenges, proper mix design optimization and the incorporation of suitable admixtures or surface treatments can be employed. These measures can improve the overall bond strength and load transfer capabilities between CS aggregates and the surrounding matrix.

As depicted in Figure 4.4, there is an obvious trend that as the fine aggregate/CS coarse aggregate ratio decreases (indicating a higher proportion of CS aggregate), the packing density values tend to increase. At a ratio of 100/0 (only fine aggregate), the packing density is 0.698. However, as the CS aggregate content increases, the packing density generally rises until it reaches a peak value of 0.796 with 14% increase at a ratio of 25/75 (25% fine aggregate, 75% CS aggregate) then this ratio reduces to 8% from its peak for 10/90 mixture.
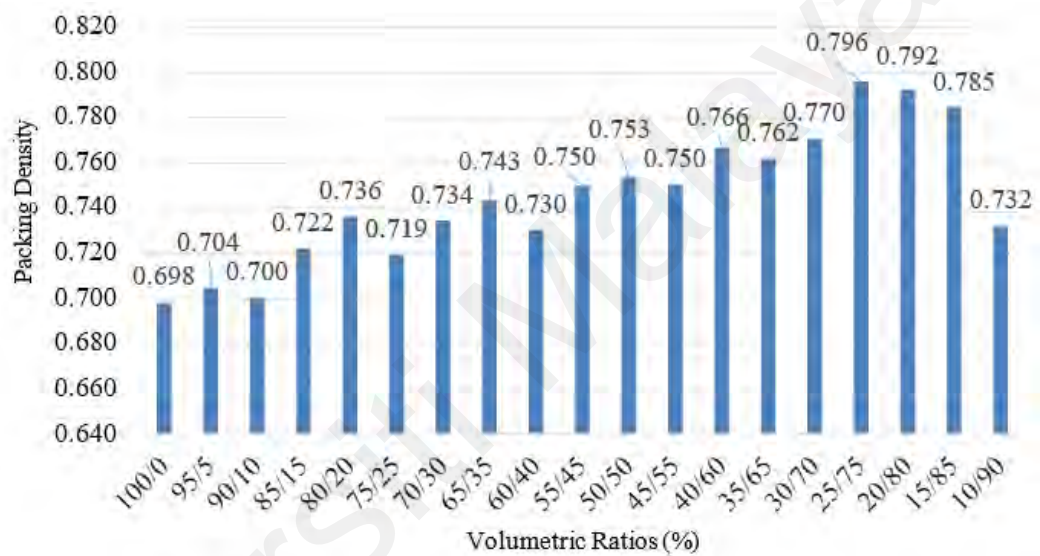
Figure 4.4: Effect of volumetric ratios of aggregates (Fine aggregate/Coarse aggregate in order) on packing density values

The variations in packing density with different fine aggregate/CS aggregate volume ratios can be explained by factors such as particle shape, as highlighted by Kwan and Fung (2009), particle size distribution, as discussed by A. K. Kwan and H. Wong (2008), interlocking and compaction effects, noted by Mora and Kwan (2000) and Wong and Kwan (2005), and porosity, as reported by Chen et al. (2020). The irregular shape and inherent porosity of CS aggregates hinder the efficient arrangement of particles, leading to lower packing density compared to more angular or rounded fine aggregates, as suggested by Matias et al. (2013). Achieving optimal packing density necessitates careful consideration of the proportions, particle sizes, and shape characteristics of aggregates in the concrete mixture. Proper mix design and optimization are essential to address these

variations and ensure the desired properties of the concrete are attained. Before proceeding to the next step of arranging the binder composition, the volume ratio of fine aggregate to CS coarse aggregate was determined to be 25/75.

3.3.4 Preparation of UGGBS slurry

The wet-grinding process utilizes advanced technology to refine the fineness of solid particles in a liquid medium, as explained by Tan et al. (2021), Yang et al. (2021), and Yang et al. (2020). To maintain a water-to-powder GGBS ratio of 0.3, polycarboxylate-based superplasticizers were employed as dispersants at 1% of the total solid mass.

In the first step of Phase B, the investigation focused on the impact of the binder-to-grinding media ratio by mass and the ratio of the material amount to the grinding chamber capacity by volume for efficiency of reactivity of UGGBS slurry. Consequently, the processing of three distinct UGGBS slurry mixes was examined based on varying binder-to-grinding chamber volume (V_{GGBS}/V_{GC}) and grinding media-to-grinding chamber volume ratio (V_{GM}/V_{GC}) within the rotating chamber. Steel grinding media, each with a mass of 400 g, a volume of 47.67 cm^3, and a rotating chamber volume of 4785 cm^3, were employed as processors. The blending of GGBS powder, water, and superplasticizer, underwent milling at a rotation frequency of 50 Hz for a duration of 1.5 hours, resulting in the production of UGGBS slurry. The wet milling process and the equipment used are depicted in Figure 4.5.. The density of the processed UGGBS was measured at 2000 kg/m^3. 7-day normalized compressive strength (NCS) test results for paste mixtures with identical UGGBS slurry mass replacement and water-to-binder ratios are detailed in Table 4.1.
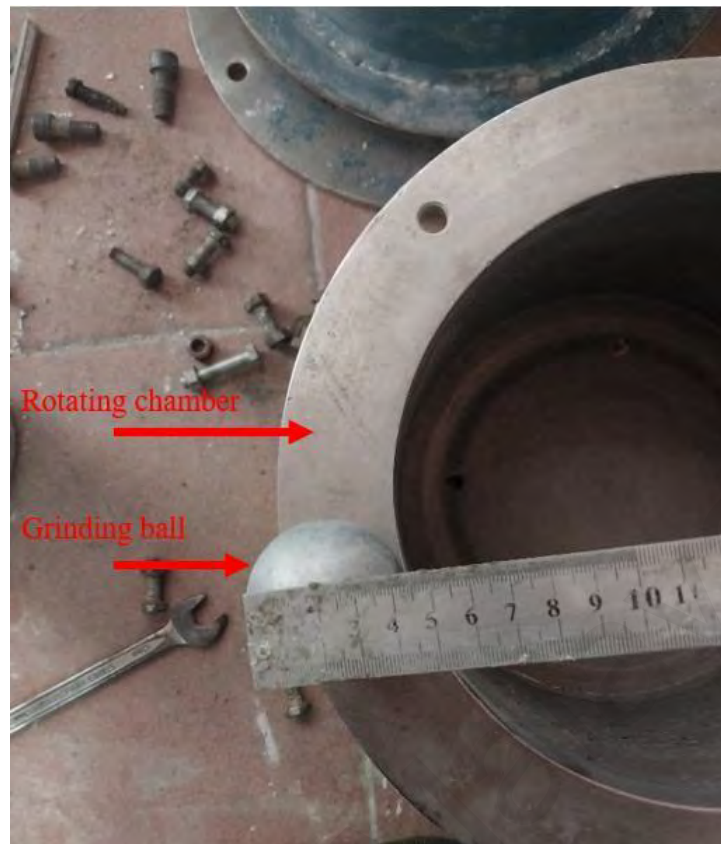
Figure 4.5: The wet milling procedure equipments

Table 4.1: The effect of GGBS and grinding media volume on the compressive strength of cement pastes

No	V_{GGBS}/V_{GC}	V_{GM}/V_{GC}	Cement (kg)	UGGBS slurry (kg)	Water (kg)	7 days NCS
1	0.052	0.04	1103	400	451	126
2	0.052	0.05	1103	400	451	110
3	0.079	0.05	1103	400	451	100

In the process of producing UGGBS slurry through wet grinding, a comprehensive assessment was conducted to evaluate the impact of different conditions on the resulting properties. Three distinct scenarios were examined, characterized by varying ratios of GGBS volume to the grinding chamber volume of the rotating chamber, namely 0.052, 0.052, and 0.079. Additionally, the volume of grinding media in relation to the volume of

the rotating chamber was also assessed with ratios of 0.04, 0.05, and 0.04 for the seperate conditions. The primary performance indicator considered in this evaluation was the NCS of the conditions compared to a reference condition with 100 (where the lowest strength is represented by 100). The determined NCS values were 126, 110 and 100 for the three conditions for cement-included hardened pastes. It can be concluded from Table 4.1 that the conditions with V_{GGBS}/V_{GC} and V_{GM}/V_{GC} at 0.052 and 0.04, respectively, were determined optimal and selected for the production of UGGBS slurry.

In comparative analysis, an increase in V_{GGBS}/V_{GC} was associated with a reduction in the compressive strength of the resulting slurry. This phenomenon can be attributed to the likelihood of a higher average particle size resulting from the decreased free-fall distance of the grinding media. Consequently, the grinding process may have been less efficient in reducing particle size and enhancing the reactivity of the GGBS particles. Similarly, an increase in the V_{GM}/V_{GC} ratio was also correlated with a decrease in strength. This can be explained by the larger volume of grinding media causing heightened interaction between the grinding balls, thereby diminishing the speed and impact of the free balls on the grinding process. However, this reduced the efficiency of the grinding process, leading to a lower compressive strength in the cement paste, as observed by He et al. (2006) and Patino et al. (2022).

3.3.5 Binder

Replacing cement with wet-grinded UGGBS slurry offers a promising strategy to reduce cement content in concrete production. This substitution is implemented in 10% increments by cement volume, as described by Li, Fang et al. (2022), Yang et al. (2021), and Yang et al. (2022). UGGBS slurry contains finely divided particles with pozzolanic properties, enabling them to participate actively in hydration reactions. Incorporating UGGBS slurry into concrete increases the reactivity of fine particles, leading to additional hydration products and improved strength and performance in the concrete matrix, as

highlighted by Li, Lei et al. (2022) and Yang et al. (2021). This substitution not only reduces cement usage but also takes advantage of the supplementary cementitious properties of GGBS, improving workability, durability, and reducing the heat of hydration in the concrete, as discussed by Wang et al. (2022) and Zhu et al. (2023).

Furthermore, the incorporation of UGGBS slurry as a partial replacement for cement aligns with sustainable construction practices by effectively repurposing an industrial waste material and reducing the environmental impact associated with cement production. Striking a reasonable balance involves carefully adjusting the UGGBS slurry content to ensure cost-effectiveness and sustainability while maintaining the desired engineering properties of the concrete. In Compared to regular GGBS, UGGBS demonstrates a notable ability to accelerate the hydration process, particularly in the early stages, as noted by Pyo and Kim (2017). After wet grinding, UGGBS exhibits properties that enable self-hydration, further enhancing its reactivity and improving the interfacial contact area between particles, which leads to improved mechanical characteristics, as described by Wang et al. (2018). UGGBS, with its finer particle size compared to GGBS, leads to a pronounced filling effect. Moreover, smaller particles exhibit increased reactivity, leading to the production of a greater quantity of hydration products and consequently contributing to increased strength. This phenomenon can be attributed to the reduced particle size and the homogeneous distribution achieved in GGBS particles through the implementation of the wet grinding technique. This specific procedure enhances the interfacial contact area among particles, which in turn improves mechanical characteristics, as observed by Wang et al. (2018). Figure 4.6. illustrates that the NCS, which considers control paste with no UGGBS slurry replacement (100/0) represents 100, tends to decrease slightly as the volume of UGGBS slurry replacement increases. For the ratios of 95/5, 85/15, and 75/25, the NCS remains relatively close to the 100/0 mix ratio. However, at the ratio of 65/35, there is a slightly decreasing trend in the NCS. Noticeably, at the ratio of 55/45, a more pronounced reduction is observed, with the NCS

dropping to 88.73. This suggests that a higher volume of UGGBS slurry replacement (45%) can lead to a moderate decrease in compressive strength compared to the 100/0 mix.
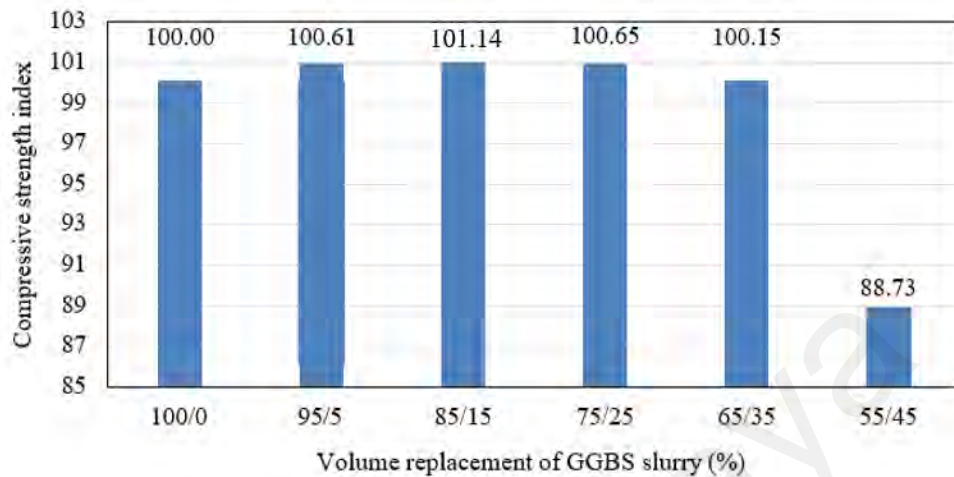
Figure 4.6: The effect of GGBS slurry replacement on the compressive strength of cementitious pastes

Considering these findings, it is important to carefully assess the trade-off between the potential benefits and the slight reduction in compressive strength when considering a high volume of UGGBS slurry replacement in concrete mixtures.

3.3.6   Finalized mix design and casting

The casting phase represents a pivotal stage in concrete production, exerting a substantial influence on the quality and ultimate performance of the end product. Commencing the process, the UGGBS slurry underwent wet grinding for a duration of 1.5 hours. The critical step of continuous stirring significant to prevent the segregation of GGBS particles to the bottom and the initiation of the self-hydration process, ensuring a uniform distribution of UGGBS slurry throughout the mixture. Given the high water absorption capacity of CS aggregates, standing at 27% for the first day, an additional pre-treatment step becomes imperative. This involves immersing the aggregates in water for a duration of one day to mitigate their capacity for excessive water absorption. Subsequently, the aggregates were subjected to a drying process until reaching a saturated surface-dry condition until the last 30 minutes of the mixing process. This drying interval

is important in preventing water evaporation from the voids within the CS aggregates.

To maintain a consistent water/binder ratio during the casting process, coarse CS aggregates and fine aggregates from mining sand are pre-mixed for a duration of 5 minutes. This preliminary mixing stage effectively addresses potential water demand and flowability concerns arising from the increased water absorption of the fine content. Following the pre-mixing of aggregates, OPC is introduced and dry-mixed for an additional 2 minutes, ensuring the complete integration of cement particles within the mixture. Subsequently, half of the UGGBS slurry and water are gradually incorporated into the mix, with each component undergoing mixing for 2 minutes. This gradual addition and careful mixing contribute to achieving a homogeneous mixture where UGGBS and water are evenly dispersed throughout the concrete blend.

Finally, the controlled addition of BF to the mixture is performed gradually to ensure a well-distributed integration. This procedural measure holds significant importance in elevating the mechanical attributes of the concrete while simultaneously mitigating the potential issues of fiber clustering or agglomeration. By meticulously implementing this optimized casting process, the inherent challenges linked to GGBS segregation from UGGBS slurry, self-hydration, water absorption by CS aggregates, and overall flowability are effectively addressed. The outcome is a concrete mix characterized by improved homogeneity and enhanced performance metrics, rendering it well-suited for diverse applications. Detailed specifications of the mixtures' design are elucidated in Table 4.2.

Table 4.2: Finalized mix designs following packing density method (kg)

Mix design code	Cement	GGBS slurry	Fine aggregate	Crushed stone	CS 9.50 - 6.30 mm	6.30 - 4.75 mm	BF	Free Water	SP
M40	487	-	913	805	-	-	-	198	-
LWAC-Control	284	307	390	-	82	374	-	43.5	8
LWAC-0.15%	284	307	390	-	82	374	4	43.5	8
LWAC-1%	284	307	390	-	82	374	23	43.5	8

CHAPTER 4: RESULTS AND DISCUSSION

4.1   Concrete properties with developed mix design

4.1.1   Fresh density and particle packing

Figure 4.7. shows the results of fresh density and packing density values of the studied mixtures. As depicted in the figure, M40 grade concrete has the highest fresh density at 2390.5 kg/m³, highlighting the significant impact of crushed stone aggregate on density, especially when compared to mixtures using only CS aggregate replacement. However, its packing density, standing at 0.794, suggests a potential inefficiency in the arrangement of solid particles. In contrast, the LWAC- Control mix, characterized as UGGBS slurry-replaced non-fibrous concrete, exhibits a lower fresh density of 1792.4 kg/m³ with a 25% decrease but compensates with a relatively higher packing density of 0.887.

The incorporation of BF follows a consistent trend, resulting in increased fresh density across all mixes. LWAC-0.15% demonstrates a fresh density of 1821.6 kg/m³ , while the LWAC-1% mix achieves a fresh density of 1855.1 kg/m³ with 24% and 22% reduction compared to M40 grade concrete, respectively.

	M40	Control	0.15%	1%
Fresh Density (kg/m3)	2390.5	1792.4	1821.6	1855.1
Packing Density	0.794	0.887	0.901	0.915
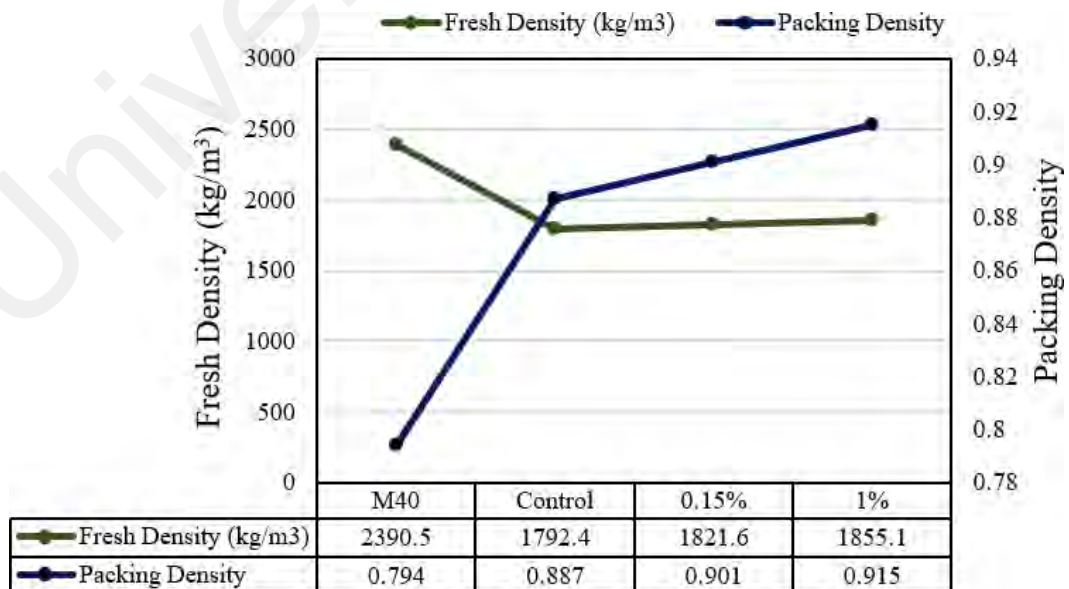
Figure 4.7: Fresh and packing density values of mixtures

The addition of BF further enhanced the packing efficiency for fibrous mixes. The mix with 0.15% BF resulted a packing density of 0.901, and the 1% BF-added mix achieves an even higher packing density of 0.915. These findings indicate that the inclusion of BF fosters a more effective arrangement of solid particles within the mixture, leading to increased packing density. The impact of fiber type on enhancing packing density is clearly illustrated by Chu et al. (2019) in Figure 4.8. The incorporation of BF as flexible fibers consistently raised both fresh and packing densities in all concrete mixtures. This improvement in density values signifies the valuable role of BF in enhancing the overall density and packing efficiency of concrete mixes, potentially leading to improved mechanical and durability characteristics.
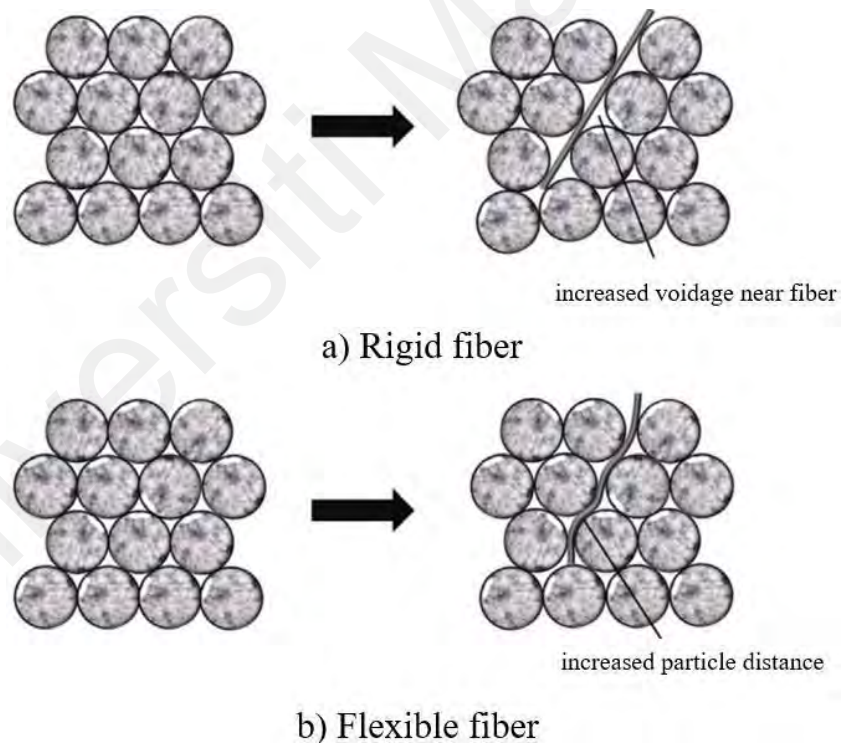
Figure 4.8: Illustration for the effect of rigid and flexible fibers on packing density

4.1.2 Saturated surface dry density and surface crack

Table 4.3 presents the fresh and SSD density results of M40 and LWAC mixtures at 1-day, 7-day, and 28-day, highlighting the impact of CS aggregates and BF inclusion.

Table 4.3: Density of concrete mixes in different ages (kg/m³)

Mix	Fresh Density	Demoulding day (1 day)	7-day SSD	28-day SSD
M40	2390	2394	2431	2452
LWAC-Control	1792	1800	1826	1880
LWAC-0.15%	1822	1830	1858	1906
LWAC-1%	1855	1864	1883	1922

In the case of M40, the fresh density is recorded at 2390 kg/m³, which increases slightly to 2394 kg/m³ on the demoulding day and then to 2431 kg/m³ at 7 days under saturated surface dry (SSD) conditions. By 28 days, the SSD density increases further to 2452 kg/m³. These consistent and gradual increases in density are typical of conventional concrete and can be attributed to ongoing hydration and the densification of the concrete matrix as moisture is absorbed during curing. The relatively high density of M40 is indicative of the use of standard aggregates, which are more compact and less porous than lightweight alternatives.

In contrast, the LWAC mixtures, which incorporate CS aggregates, exhibit significantly lower densities at all stages. For LWAC-Control, the fresh density is measured at 1792 kg/m³, which slightly increases to 1800 kg/m³ on the demoulding day and further to 1826 kg/m³ at 7 days SSD. By 28 days, the density reaches 1880 kg/m³, still significantly lower than M40. The lower density in LWAC can be directly linked to the porous nature of the CS aggregates. These aggregates, being less dense and more permeable than conventional aggregates, result in a more lightweight concrete mix. The smaller increases in density over time, compared to M40, suggest that the internal voids within the lightweight aggregates limit the overall densification process, even as hydration proceeds.

The addition of BF slightly increases the density of LWAC mixtures, though the effect is still relatively modest. For LWAC-0.15%, the fresh density is 1822 kg/m³, which rises to 1830 kg/m³ on the demoulding day, 1858 kg/m³ at 7 days SSD, and 1906 kg/m³ by 28 days SSD. Similarly, for LWAC-1%, the fresh density starts at 1855 kg/m³, increasing to 1864 kg/m³ on the demoulding day, 1883 kg/m³ at 7 days SSD, and 1922 kg/m³ at 28 days SSD. The progressive increases in density with the addition of BF indicate that the fibers help improve the overall packing density of the matrix, likely by filling microvoids and enhancing the bond between the cement paste and the aggregates. The fact that LWAC-1% shows the highest densities at each stage suggests that the effect of BF is more pronounced with a higher percentage of fiber addition.

However, it should be noted that even with the incorporation of BF, the LWAC mixtures remain significantly less dense than M40, which is expected due to the lightweight nature of the aggregates used. The increase in density observed with BF inclusion is relatively modest, with the difference between LWAC-Control (1880 kg/m³ at 28 days) and LWAC-1% (1922 kg/m³ at 28 days) being only 42 kg/m³, or about 2.2%. This suggests that while BF has a positive effect on increasing density, the dominant factor controlling the density of LWAC mixes remains the lightweight aggregates themselves, whose porous structure limits the overall potential for densification. This aligns with existing literature, which typically categorizes lightweight concrete as having densities lower than 2000 kg/m³ according to EN 206-1 (2013). When examining the 1-day demolded density, it becomes evident that all mixtures show a slight increase compared to their fresh densities.

After 28 days of water curing, minor cracks were observed on the surface of the CS aggregate-replaced concrete samples, as depicted in Figure 4.1.. These cracks may be attributed to autogenous shrinkage, which is the uniform reduction of internal moisture

due to cement hydration. Autogenous shrinkage is particularly noticeable in high-strength concrete, where the water-to-cement ratio is often below 0.42, as first noted by Powers and Brownyard (1946). However, the presence of cracks becomes less severe with the increasing volume of fibers, suggesting that BF reinforcement contributes to reducing internal matrix stress through the bridging effect within the microstructure. This reinforcement potentially helps maintain structural properties by preventing decomposition, as shown by Guo et al. (2023).
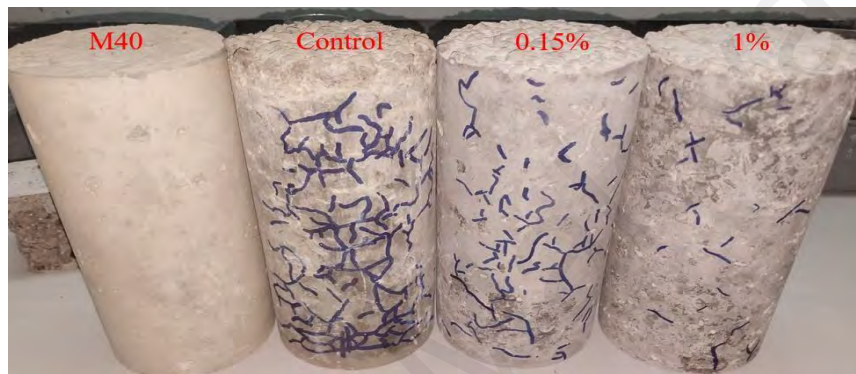
Figure 4.9: Surface crack propagation of concrete samples after water curing at 28 days

4.1.3 Water absorption and porosity

Previous studies, including those by Jiang et al. (2014), Kabay (2014), and Li et al. (2023), have demonstrated that BF is effective in lowering the water absorption of concrete mixtures. This reduction in absorption is attributed to the improved compactness of the concrete, which consequently decreases water permeability. Water absorption of CS aggregate concrete samples showed a similar increases in the range of 260-286%, compared to granite aggregate concrete. Alike trend is evident when examining the volume of permeable voids.

Table 4.4. presents the detailed results of water absorption and volume of permeable voids for the mixtures.

Table 4.4: Water absorption, and volume of permable void values of mixtures

Mix	Water Absorption (%)	Volume of Permeable Voids (%)
M40	3.87	9.19
LWAC-Control	14.96	27.13
LWAC-0.15%	14.92	26.88
LWAC-1%	13.95	25.56

From the data provided, the water absorption for LWAC-Control is 14.96%, while for M40, it is significantly lower at 3.87%. This substantial difference can be attributed to the materials used. The dense, impermeable nature of conventional aggregates in M40 results in lower water absorption, whereas the CS aggregates in the LWAC mixtures contribute to the higher absorption due to their porous structure. The more than 10% difference between the two (M40 vs. LWAC-Control) clearly demonstrates the significant influence of aggregate selection on water absorption.

The introduction of BF into LWAC mixtures results in a marginal reduction in water absorption. For LWAC-Control, water absorption is 14.96%, which decreases slightly to 14.92% with 0.15% BF and to 13.95% with 1% BF. While the changes are small, the decrease in water absorption can be attributed to the effect of BF in enhancing the packing density, thereby reducing the porosity of the matrix. However, the reduction remains minimal, likely due to the dominant influence of the lightweight CS aggregates, which inherently exhibit higher porosity and continue to govern the water absorption behavior.

The volume of permeable voids follows a similar trend. M40 demonstrates the lowest value at 9.19%, correlating with its low water absorption. In contrast, LWAC-Control exhibits a much higher value at 27.13%, largely due to the porosity of CS aggregates. This high permeable void content suggests a greater potential for fluid penetration, which could negatively affect the durability of the structure over time.

When BF is incorporated, the volume of permeable voids shows a slight reduction. With 0.15% BF, the volume decreases to 26.88%, and with 1% BF, it further decreases to 25.56%. The reduction, although slight, indicates that the fibers contribute to filling some voids within the concrete matrix, enhancing the packing density and reducing overall porosity. The decrease from 27.13% in LWAC-Control to 25.56% in LWAC-1% reflects a 1.5% improvement, which could have beneficial effects on long-term durability, particularly by reducing fluid ingress. Even a small reduction in permeable voids could slow the penetration of deleterious substances like chlorides and sulfates, thus potentially extending the service life of the structure.

However, the modest nature of these reductions suggests that the primary factor influencing the water absorption and void content remains the porous CS aggregates. Despite BF's ability to improve the microstructure and reduce porosity, the overall absorption and void behavior is still predominantly governed by the lightweight nature of the aggregates. The reduction in water absorption and permeable voids, while statistically significant, is not sufficient to drastically alter the overall performance of the LWAC mixtures in these aspects.

4.1.4 Sorptivity

The sorptivity test results from 1 to 24h reveal distinctive differences in absorption rates among various concrete mixes for earlier and later ages. Figure 4.10. illustrates the water sorptivity test results for all mixes. Specifically at 1 minute for LWAC-Control concrete, a 1351% rise was observed compared to M40 concrete, which is a significantly high sorptivity value, highlighting its inferior resistance to immediate water penetration. The LWAC-Control mix exhibits remarkably high sorptivity at these early time intervals, indicating its susceptibility to rapid water ingress. The 0.15% and 1% BF-added mixes demonstrate intermediate sorptivity values with a 465% and 358% rises compared to M40

concrete, respectively, suggesting that the inclusion of BF contributes to reducing early water absorption rates. This trend revealed itself by having a 275%, 197% and 66% increases for LWAC-Control, LWAC-0.15% and LWAC-1% mixtures compared to M40 concrete, respectively, in 24 hour duration.

As evident in the figure, the sorptivity values of M40 concrete remain consistently low. Notably, the mix incorporating 1% BF displays a noteworthy decreasing trend for sorptivity. Over time, sorptivity values of LWAC-1% mix exhibit a gradual decline, converging toward those observed for M40 concrete. Additionally, both the LWAC-0.15% and LWAC-1% formulations show significant reductions in sorptivity compared to the LWAC-Control mix during both testing intervals. This may be due to BF's filler effect, which blocks capillary pathways and offers sustained protection against water penetration, as reported by Lu et al. (2022) and Yıldırım and Özhan (2023). Furthermore, the contrast in sorptivity between early and late-age results is more pronounced in the LWAC-Control mix than in the BF- added mixes. This implies the critical role of BF reinforcement in sustaining consistently lower sorptivity values over time. Overall, the findings underscore the significant role of BF in reducing sorptivity, with particular emphasis on the 1% BF-added mixture, which achieves sorptivity values akin to those of M40-grade concrete. These findings contribute to the understanding of how BF incorporation can effectively control sorptivity, offering valuable insights for enhancing the durability and performance of concrete structures.
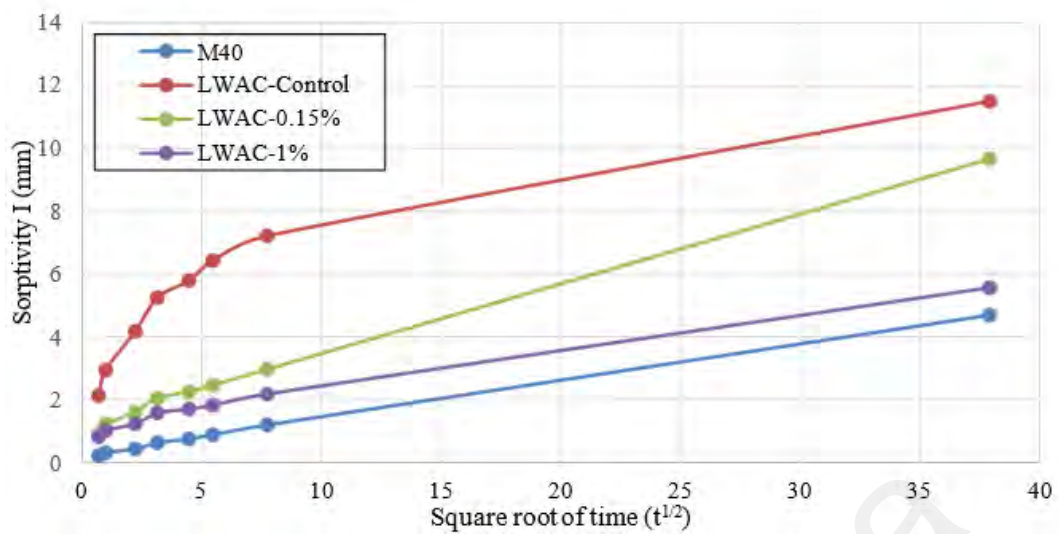
Figure 4.10: Sorptivity test results by square root of time

4.1.5   Compressive strength

The 1-, 7-, and 28-day compressive strengths of tested specimens are shown in Figure 4.11.. Notably, a significant increase in 1-day compressive strength was observed in the UGGBS slurry-replaced mixtures. The 1-day compressive strength of the LWAC-Control, LWAC-0.15% and LWAC-1% mixes are 49%, 49% and 61% of M40 concrete. Insignificant early compressive strength difference between LWAC-Control and LWAC-0.15% mixtures due to the low fiber content of BFs which is lower compared to that of LWAC-1%. The results also align with Wu et al. (2019) that low fiber content has negligible impact on early compressive strength of LWACs. All packing density-optimized LWAC mixtures exhibit significant strength development even after just one day of curing. This behavior differs from the findings of Lv et al. (2015) and Shafigh et al. (2016), who discussed high cement content LWAC mixtures. The increased packing density of UGGBS slurry with cement and the optimized coarse-fine aggregate combination likely contribute to this early-age strength development. These findings align with studies conducted by Yang et al. (2021) and Zhang et al. (2020), which attribute accelerated early-age strength development to the material's activation efficiency.
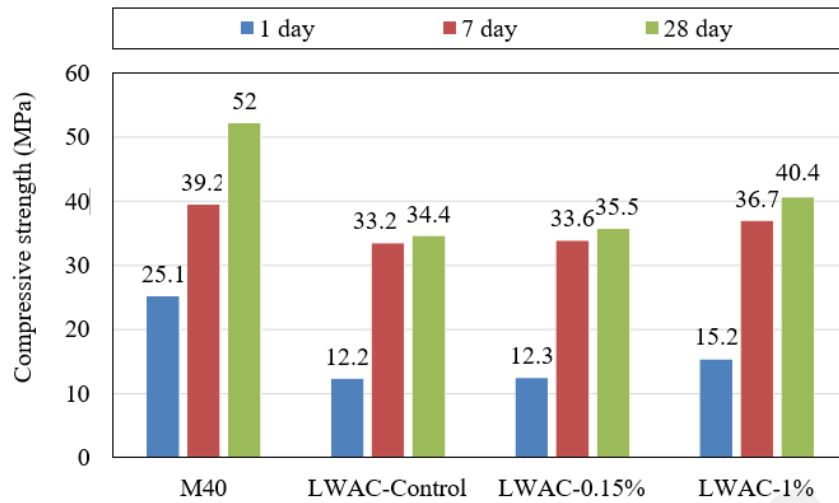
Figure 4.11: Compressive strength results of mixtures at different curing days

The 7-day compressive strength shows a similar pattern compared to 1-day results, where the UGGBS slurry-replaced LWAC-Control, LWAC-0.15% and LWAC-1% mixtures had 85%, 86%, and 94% of compressive strength of M40 concrete. The results imply that these mixtures have the potential to attain strength levels comparable to traditional concrete within a relatively short curing period. he relatively higher compressive strength of LWAC mixes compared to existing literature can also be linked to the increased fines content, which reduces total porosity, improves compactness, and enhances microstructural development, as noted by Cheng et al. (2017). Thus, the strength enhancement in LWACs is not solely due to hydration reactions but also the grain size distribution, which promotes particle interlocking within the matrix, as indicated by Jiang et al. (2018). Moreover, the addition of BF contributes to this strength increase, which may be due to its reinforcing effects and its role in enhancing packing density, as noted by Arora et al. (2018), Khan et al. (2022), and Wang et al. (2020). These outcomes revealing that BF incorporation can develop both the early- and long-term strength of concrete.

The remarkable early-age strength attributes of UGGBS slurry-replaced mixtures are further highlighted by Yang et al. (2021). This strength development can be attributed to

the combined effects of UGGBS and CS aggregates, which improve packing density in both the mortar phase, as indicated by Kwan and Wong (2008), and the aggregate phase, as shown by Kwan et al. (2014). The incorporation of BF further increases both early-age and long-term strengths, positioning these mixtures as promising contenders for diverse concrete applications. These results represent the importance of optimizing packing density, aligning with insights from the existing literature regarding early-age strength development in concrete.

Results of investigated mixtures revealed that the 28-day compressive strengths of M40 concrete exhibit a higher development compared to other concretes, characterized by its conventional composition with higher cement content, exhibits a steady and consistent development in strength, resulting in a final compressive strength of 52 MPa. However, despite demonstrating comparable early-age strength, the UGGBS slurry-replaced LWAC-Control mixture shows a relatively lower 28-day strength of 34.4 MPa. This difference may be due to the prolonged pozzolanic reaction of GGBS, resulting in slower strength gain after the first 7 days, as noted by Yazıcı et al. (2009) and Yu et al. (2015). However, with the introduction of BF, particularly evident in the 1% BF mixture, a noticeable enhancement in 28-day strength is observed (40.4 MPa). With the addition of BF reinforces the tension of capillary pores induced by water evaporation, thereby mitigating the formation of microcracks. In the long term, the compressive strength of BF-reinforced concrete tends to surpass that of non-fibrous concrete, as indicated by Wang et al. (2020). Moreover, as can be seen from the above results, the influence of packing density remains significant in shaping the 28-day strengths of these mixtures. It is important to state that negligible increase in strength was observed between the 7th and 28th days for the LWAC-Control, LWAC-0.15% and LWAC-1% concrete mixtures with a 4%, 6% and 10% rises, respectively.

4.1.6 Flexural strength

The 28-day flexural strength of mixtures are presented in Figure 4.12.. The flexural strength results at the 28-day illustrate the influence of involving BF in concrete. M40 concrete resulted a flexural strength of 7.1 MPa, additionally, the LWAC-Control mix demonstrated a marginally lower flexural strength of 7.0 MPa, where the flexural strength of the LWAC-Control mix is notably comparable to that of the M40. Adding 0.15% and 1% of BF rose the flexural strength by 33.80% and 59%, respectively. The previous studies also revealed that inclusion of BFs enhanced the flexural strength of cementitious LWAC composites. In a study conducted by Zeng et al. (2021) flexural strength of BF reinforced concrete specimens increased compared to non- fibrous control mixtures in 0.5%, 1.0%, and 1.5% volume fractions.
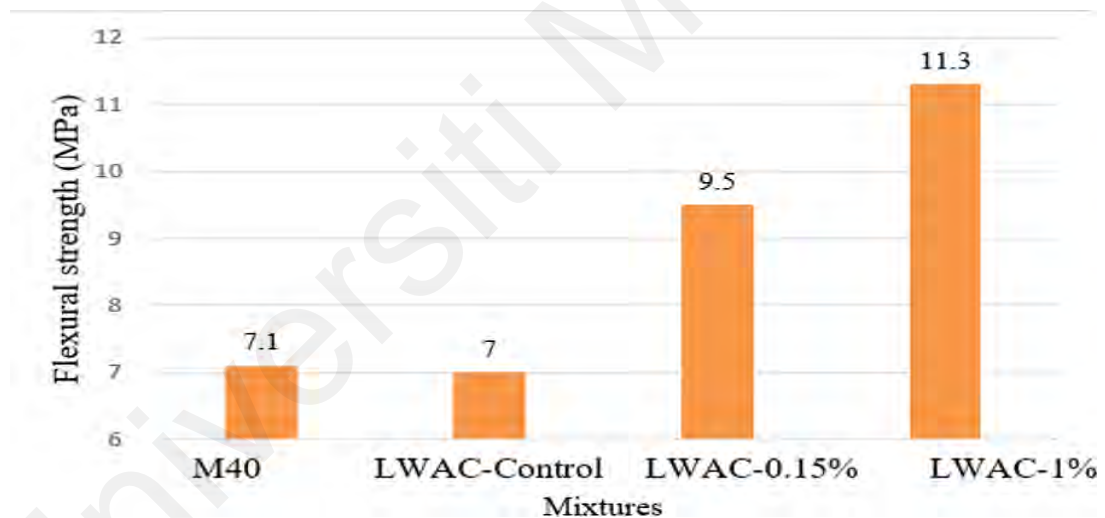
Figure 4.12: 28 day flexural strength values of mixtures

Figure 4.13. illustrates the crack propagation in the mixtures following the flexural strength test. Notably, all mixtures, except the one containing 1% BF, exhibited a single crack on the surface of specimen. In contrast, the presence of a double crack in the mixture with 1% BF signifies a bridging effect of the BF, which enhances the bending crack resistance and ductility of LWAC, as observed by Alaskar et al. (2021), Lian et al. (2022), and Lyu et al. (2021). This effect results in the transfer of load energy through the BF,

providing a positive impact on the structural concrete. Furthermore, the substantial increase in flexural strength observed in the BF-added mixtures indicates the potential for further enhancing the mechanical properties of lightweight structural concrete. These findings indicate that incorporating BF, in conjunction with sustainable mix designs, can be a promising strategy for constructing eco-friendly yet robust structures with improved flexural strength.

Figure 4.13: Crack propagation of concrete samples after the flexural strength test

4.1.7 Effect of packing density on physical, transport and mechanical properties of concrete

The correlation values presented in Table 4.5 offer valuable insights into the relationship between packing density and various critical properties of concrete. Packing density stands out as a fundamental parameter for evaluating concrete quality, particularly concerning its long-term structural integrity. The correlation values indicate a strong positive correlation between packing density and compressive strength, as well as flexural strength, with correlation coefficients of 0.991 and 0.939, respectively. This suggests that an increase in packing density correlates with a corresponding increase in both compressive and flexural strengths, highlighting the crucial role of effective particle packing in enhancing the material's mechanical performance.

Conversely, packing density exhibits a strong negative correlation with water absorption, porosity, and sorptivity, with correlation coefficients of -0.885, -0.931, and -

0.977, respectively. These negative correlations imply that as packing density increases, the water absorption, porosity, and sorptivity of the concrete decrease. This suggests that a denser packing of concrete particles results in reduced permeability and increased resistance to moisture ingress are essential attributes for the durability and extended service life of concrete structures.

In summary, the correlation values signifies the crucial role of packing density in influencing various critical properties of concrete, emphasizing its significance in designing and assessing high-performance and LWAC mixtures for construction applications.

Table 4.5: Correlation values between packing density and relevant properties of mixtures

	SSD	Compressive strength	Flexural strength	Water absorption	Porosity	Sorptivity
Packing Density	0.991	0.939	0.996	-0.885	-0.931	-0.977

4.1.8 Economic and ecological sustainability

Assessing green building materials considers economic benefit and carbon emissions as important factors. Although the LWAC mixed with high-volume UGGBS demonstrates comparable compressive strength with the addition of 1% BF to M40 at 28 days, it is essential to consider the manufacturing costs and carbon footprint.

Table 4.6 provides a comprehensive assessment of individual and cumulative CO_2 emissions and a cost analysis for various components and mixtures. These component unit values were derived through a thorough evaluation, incorporating life cycle assessment and sustainability studies, with references provided.

Table 4.6: Carbon footprint and manufacturing cost of green LWAC with high volume UGGBS slurry

Component		CO₂ emission (kg/t)	Cost ($/t)	28 days compressive strength (MPa)
Cement		930[Wu et al., 2018]	87.3 [Wu et al., 2018]	-
UGGBS slurry		298.87[Yang et al., 2021]	60 [Yang et al., 2021]	-
Filler		0.063[Zulcão et al., 2020]	120[a]	-
BF		0.85[Pavlović et al., 2022]	1000[b]	-
Aggregate	Granite Aggregate	-	76.3[Ohemeng & Ekolu, 2020]	-
	Lightweight aggregate	-	19[Ohemeng & Ekolu, 2020]	-
Mix				
M40		452.91	103.95	52
LWAC-Control		365.76	67.38	34.4
LWAC-0.15%		369.16	71.38	35.5
LWAC-1%		385.31	90.38	40.4
	a,b: The data provided has been sourced from the current market values			

The cost of various mixtures has been computed based on the information in the Table 4.6. Additionally, the expenses and carbon emissions associated with LWAC when blended with high-volume UGGBS slurry have been determined. The inclusion of high-volume UGGBS into LWAC yields substantial cost savings and a reduction in carbon emissions.

Table 4.7: Comparison of the current study's mix design and compressive strength results with previous literature

Sample code	Cement dosage (kg)	Binder	CS amount (kg)	Hardened density (kg/m³)	Compressive Strength (MPa)	Reference
1%	284	UGGBS slurry (%40)	456	1864	40.4	This study
C-100	450	N/A	450	1905	29.81	(Aziz et al., 2022)
M11	510	N/A	331.5	1970	26.7	(Gunasekaran et al., 2011)
OPSC	450	Fly Ash (10%)	302	1954	40.8	(Pordesari et al., 2021)
CCS100	400	N/A	616.9	1689	18.8	(Liu et al., 2023)
M10	408	GGBS (%20)	331.5	N/A	23	(Kumar et al., 2019)

Compared to M40 concrete, the LWAC-Control sample exhibits a decrease of 35.2% in cost and 19.2% in CO_2 emissions. When adopting a performance-oriented approach with a 1% BF addition, these values stand at 13% and 14.9%, respectively. Notably, only a 22% decrease in compressive strength after 28 days was observed for the 1% BF concrete mix, despite a 40% reduction in cement volume.

Table 4.7 provides a comparison between the current study and previous research regarding the components used in their mix designs and the compressive strength obtained. Earlier investigations employing CS as coarse aggregates exhibited lower strength levels and required higher cement dosages. The use of high volumes of CS with improved mechanical characteristics emphasizes the importance of the packing density method for the matrix. Furthermore, the wet grinding technique for GGBS enhanced hydration properties by reducing particle size, facilitating the formation of a reliable binder between coarse and fine aggregate particles. The specific gravity of lightweight coarse aggregate in a dry state, which ranges between one-third and two-thirds of that of normal-weight aggregate, meets the criteria for achieving a 28-day compressive strength of at least 17 MPa as outlined by the ACI (2003). Furthermore, HSLWAC can exceed 40 MPa, as indicated by Lu (2023), while maintaining a unit weight of 1120-1920 kg/m³, consistent with the ACI (2003) guidelines. Consequently, all LWAC mixes classified as SLWAC can be defined also as HSLWAC, particularly the LWAC-1% mix, as noted by Lu (2023).This implies that through careful selection of supplementary materials and systematic mix design optimization, it is feasible to strike a balance between eco-friendliness and structural reliability.This study not only offers a novel approach to address challenges faced by the cement industry but also serves as inspiration for developing cost-effective, low-cement-content, high-strength LWAC with a greener profile.

CHAPTER 5: CONCLUSIONS AND RECOMMENDATIONS FOR FUTURE WORK

5.1   Summary of research

This study presents an innovative approach to enhance the physical, mechanical and transport properties of LWAC production. The research methodology involved an investigation integrating experimental tests and numerical methods.

The procedure for the particle packing concept employed in this study followed a meticulous step-by-step approach to optimize the packing density of LWAC. The investigation began by systematically assessing combinations of two different CS aggregate sizes. By experimenting with various combinations, the aim was to identify the combination that yielded the highest packing density. Once the optimal combination of CS aggregate sizes was determined, a similar process was undertaken for the fine aggregate component, comprising three different sizes. Mining sand was subjected to dry milling to produce fines and filler sizes, aimed at increasing solid content and packing density for mix design optimization.

Following the selection of the combination with the highest packing density for both coarse and fine aggregates, the next step involved determining the volume ratio between the combined coarse and fine aggregates. This ratio played a crucial role in achieving the desired packing density for the LWAC mixture. The remaining void spaces were allocated for the combined cement and UGGBS slurry paste, which also included water and superplasticizer inclusions. In the process of producing UGGBS slurry through wet grinding, experiments were conducted to increase the hydration reactivity of the slurry. The investigation focused on assessing the impact of two key variables: the binder-to-grinding media ratio and the ratio of the material amount to the grinding chamber capacity. Three distinct UGGBS slurry mixes were prepared, each varying in binder-to-

grinding chamber volume (VGGBS/VGC) and grinding media-to-grinding chamber volume ratio (VGM/VGC) within the rotating chamber. This method aimed to refine the fineness of solid particles within a liquid environment, enhancing the reactivity of the UGGBS slurry. Furthermore, the study investigated the impact of BF reinforcement with different volume replacements on the properties of LWAC

Once the mix design was defined, a comprehensive evaluation of the physical, mechanical, and transport properties of the optimized LWAC was conducted. A careful consideration was given to material properties and mix design parameters to increase the efficiency. The specimens were subjected to various tests such as compressive and flexural strength, fresh and hardened density, fresh particle packing density, water absorption, porosity, and sorptivity. The LWAC specimens were compared against M40 grade concrete, providing a benchmark for performance evaluation. Additionally, the cost of production and environmental impacts associated with the production of the LWAC were analyzed and compared to conventional concrete mixtures.

The results of the experimental tests and numerical methods provide valuable insights into the structural performance and potential applications of LWAC in construction. By optimizing mix designs and incorporating innovative materials like CS, UGGBS, and BF, it is possible to produce high-strength LWAC with reduced environmental impact and manufacturing costs.

5.2   Findings and conclusions

Given the significant emphasis on sustainability and resilience, numerous studies in recent years have explored into understanding the behavior of LWAC using different types of LWAs and reinforced by different fibers. Moreover, endeavors have been undertaken to explore the effectiveness of employing the packing density method to improve and optimiz mix design of LWACs. This research attempted to optimize mix

design of LWAC using CS as coarse LWA and BF as reinforcement through packing density method. The following conclusions can be drawn based on the results of this study.

1. Packing density optimization has been identified as an effective method for enhancing the physical, mechanical and transport properties of short and long-age LWAC.

2. The study has demonstrated that varying the volume content of different CS sizes can significantly improve both loose and compacted packing density. Loose and compacted packing densities increased with the higher ratio of the smaller aggregate size. However, the upward trend diminished after a specific rate of volumetric substitution of 6.30–4.75 mm aggregate size with 9.50–6.30 mm. For compacted packing method, a 6% and 4.5% increase was observed from single size of larger and smaller particle sizes to optimum volume ratios 18/82 (9.50-6.30/6.30-4.75 mm) mixture.

3. The inclusion of fines and powder content has proven to be an effective method for increasing packing density, which in turn enhances the void-filling capacity. The results show a significant increase in packing density with the addition of powders and fines. At a volume proportion of 60/15/25, there was an 18% increase compared to 100/0/0 ratios.

4. As the proportion of CS coarse aggregate increases, the packing density generally rises until it peaks at a ratio of 25/75 (25% fine aggregate, 75% CS aggregate), showing a 14% increase. Subsequently, the packing density decreases after this peak by 8% for the 10/90 mixture.

5. The wet grinding of GGBS has shown great potential for providing high-volume cement replacement with reduced particle size and an improved hydration property while simultaneously decreasing the density in slurry form. According to the

varying ratios of GGBS volume to the grinding chamber volume, and the volume of grinding media, optimal conditions for UGGBS slurry production were determined as V_{GGBS}/V_{GC} and V_{GM}/V_{GC} ratios of 0.052 and 0.04, respectively based on the normalized compressive strength results.

6. The highest fresh density is observed in M40 grade concrete at 2390.5 kg/m³, while the lowest fresh density is found in the LWAC-Control mix at 1792.4 kg/m³. Conversely, the LWAC-Control mix demonstrates the highest packing density of 0.887, indicating efficient particle arrangement, while M40 grade concrete exhibits the lowest packing density at 0.794.

7. The 1-day compressive strengths of the LWAC-Control, LWAC-0.15%, and LWAC-1% mixes are 49%, 49%, and 61% of M40 concrete, respectively, indicating substantial early-age strength development even with low cement content. Furthermore, the 28-day compressive strength of the BF-reinforced LWAC-Control mixture shows a noticeable enhancement, particularly in the 1% BF mixture, suggesting the reinforcing effects of BF and the significance of packing density in long-term strength development. Notably, the 1% BF mixture achieves a 28-day compressive strength of 40.4 MPa, categorizing it as HSLWAC according to literature.

8. The flexural strength results at the 28-day mark demonstrate the impact of incorporating BF into concrete. While M40 concrete achieved a flexural strength of 7.1 MPa, the LWAC-Control mix showed a marginally lower strength at 7.0 MPa, comparable to M40 concrete. However, the addition of 0.15% and 1% BF increased flexural strength by 33.80% and 59%, respectively, highlighting the reinforcing effects of BF on lightweight concrete. Notably, crack propagation analysis revealed a bridging effect of BF in the 1% BF-added mixture, enhancing bending crack resistance and ductility of lightweight aggregate concrete.

9. Including 1% BF in the mix demonstrated superior mechanical and transport properties compared to non-fibrous LWAC, highlighting the significance of BF in enhancing the characteristics of high-strength LWAC. With the addition of 1% BF, an 18% increase was observed compared to the LWAC without fiber.

10. The correlation values reveal a strong positive relationship between packing density and compressive strength (0.991) as well as flexural strength (0.939), indicating that higher packing density corresponds to increased mechanical performance. Conversely, packing density demonstrates strong negative correlations with water absorption (-0.885), porosity (-0.931), and sorptivity (-0.977), suggesting that denser packing reduces permeability and enhances resistance to moisture ingress, crucial for concrete durability.

11. The LWAC-Control mixture exhibits a 35.2% reduction in cost and a 19.2% decrease in CO_2 emissions compared to M40 concrete, demonstrating the economic and environmental benefits of incorporating high-volume UGGBS slurry. Furthermore, the LWAC-1% mix, despite a 40% reduction in cement volume, achieves a compressive strength of 40.4 MPa.

12. The findings suggest that optimizing packing density through various means such as CS sizes, fines and powder contents, and wet grinding of GGBS and BF reinforcement holds promise for achieving enhanced physical transport and mechanical strength properties. Further research is warranted to explore and refine these techniques, ultimately advancing the engineering properties of LWAC.

This study introduces a novel approach to the production of HSLWAC by integrating non-spherical waste aggregates, specifically CS, through the packing density method. The innovation lies in the utilization of waste materials such as CS and GGBS, which not only reduces the environmental impact of concrete production but also enhances its sustainability by minimizing cement content. By optimizing the aggregate mix design for maximum packing density, the study achieves improved physical, transport, and

mechanical properties, while simultaneously lowering production costs and carbon emissions. This novel approach allows for the reduction of structural member cross-sections without compromising the structural integrity of the concrete, leading to material savings and further cost efficiency.

Moreover, the incorporation of CS aggregates addresses a critical environmental issue by reducing the demand for natural aggregates and mitigating the negative effects of quarrying. The use of these waste materials offers a sustainable solution to waste management in tropical regions, contributing to the preservation of natural resources. This study's innovative integration of waste aggregates through the packing density method presents a significant advancement in the field of structural lightweight concrete, providing valuable insights for future research and practical applications. By addressing a key gap in the literature, this research offers a transformative approach to lightweight concrete design, potentially reshaping its use in structural engineering and promoting more sustainable construction practices.

5.3   Recommendation for future work

1. Future research should explore advanced techniques for further optimizing packing density in lightweight aggregate concrete (LWAC), including investigating the impact of different combinations and types of fines, powders, and aggregate sizes on packing efficiency.

2. To enhance the sustainability and performance of LWAC mixtures, further research is needed to explore alternative pozzolanic materials, such as fly ash or silica fume, in combination with GGBS.

3. There is a need for comprehensive studies examining the long-term durability and performance of LWAC reinforced with BF, including assessing its resistance to environmental factors such as freeze-thaw cycles and chemical exposure.

4. Further exploration of cost-effective and sustainable mix designs for LWAC, particularly those incorporating high-volume UGGBS slurry, could lead to the development of greener construction practices with reduced environmental impact and enhanced economic viability.

REFERENCES

Abd Elrahman, M., & Hillemeier, B. (2014). Combined effect of fine fly ash and packing density on the properties of high performance concrete: An experimental approach. *Construction and Building Materials, 58*, 225-233.

Abimbola, S. K. (2015). *Effect Of Water Cement Ratio On The Strength Of Concrete Having Crushed Cow Bone As Partial Replacement Of Fine Aggregate* Department Of Building, College Of Environmental Sciences And Management].

ACI213R. (2003). Guide for structural lightweight-aggregate concrete.

Aim, R. B., & Le Goff, P. (1968). Effet de paroi dans les empilements désordonnés de sphères et application à la porosité de mélanges binaires. *Powder technology, 1*(5), 281-290.

Akcay, B., & Tasdemir, M. A. (2009). Optimisation of using lightweight aggregates in mitigating autogenous deformation of concrete. *Construction and Building Materials, 23*(1), 353-363.

Alaskar, A., Albidah, A., Alqarni, A. S., Alyousef, R., & Mohammadhosseini, H. (2021). Performance evaluation of high-strength concrete reinforced with basalt fibers exposed to elevated temperatures. *Journal of Building Engineering, 35*, 102108.

Alcharchafche, M. A. S., Al-mashhadani, M. M., & Aygörmez, Y. (2022). Investigation of mechanical and durability properties of brick powder-added White Cement composites with three different fibers. *Construction and Building Materials, 347*, 128548.

Algaifi, H. A., Shahidan, S., Zuki, S. S. M., Ibrahim, M. H. W., Huseien, G. F., & Rahim, M. A. (2022). Mechanical properties of coconut shell-based concrete: Experimental and optimisation modelling. *Environmental Science and Pollution Research*, 1-16.

Arora, A., Aguayo, M., Hansen, H., Castro, C., Federspiel, E., Mobasher, B., & Neithalath, N. (2018). Microstructural packing-and rheology-based binder selection and characterization for Ultra-high Performance Concrete (UHPC). *Cement and Concrete Research, 103*, 179-190.

Asil, M. B., & Ranjbar, M. M. (2022). Hybrid effect of carbon nanotubes and basalt fibers on mechanical, durability, and microstructure properties of lightweight geopolymer concretes. *Construction and Building Materials, 357*, 129352.

Aslam, M., Shafigh, P., & Jumaat, M. Z. (2016). Oil-palm by-products as lightweight aggregate in concrete mixture: a review. *Journal of Cleaner Production, 126*, 56-73.

ASTM, C. (2002). Standard Specification for Concrete Aggregates. *ASTM International*(11 pp).

ASTMC33. (2002). Standards Specification for Concrete Aggregates. *ASTM International*.

ASTMC39-14a. (2005). "Standard Test Method for Compressive Strength of Cylindrical Concrete Specimens. *ASTM International*.

ASTMC78. (2009). "Standard Test Method for Flexural Strength of Concrete (Using Simple Beam With Third-Point Loading)". *ASTM International*.

ASTMC642-06. (2006). Standard test method for density, absorption, and voids in hardened concrete. *Annual Book of ASTM Standards*.

ASTMC1585-04. (2004). Standard Test Method for Measurement of Rate of Absorption of Water by Hydraulic-Cement Concretes. *ASTM International*.

Aziz, W., Aslam, M., Ejaz, M. F., Ali, M. J., Ahmad, R., Raza, M. W.-u.-H., & Khan, A. (2022). Mechanical properties, drying shrinkage and structural performance of coconut shell lightweight concrete. *Structures*,

Banerjee, S. (1998). *Monolithic refractories: a comprehensive handbook*. World Scientific.

Bari, H., Safiuddin, M., & Salam, M. A. (2021). Microstructure of structural lightweight concrete incorporating coconut shell as a partial replacement of brick aggregate and its influence on compressive strength. *Sustainability, 13*(13), 7157.

Barksdale, R. D., Kemp, M. A., Sheffield, W. J., & Hubbard, J. L. (1991). Measurement of aggregate shape, surface area, and roughness. *Transportation Research Record*(1301).

Berndt, M. (2015). Influence of concrete mix design on CO2 emissions for large wind turbine foundations. *Renewable Energy, 83*, 608-614.

Bogas, J. A., Gomes, M. G., & Gomes, A. (2013). Compressive strength evaluation of structural lightweight concrete by non-destructive ultrasonic pulse velocity method. *Ultrasonics, 53*(5), 962-972.

Brewe, J. E., & Myers, J. J. (2005). Particle size optimization for reduced cement high strength concrete. *Proceedings of the PCI-NBC on Bridges for Life*.

BS882. (1992). Aggregates For Concrete.

BS-EN-12620. (2002). Aggregates for concrete. *British Standards Institution*.

BSEN206. (2013). Concrete — Specification, performance, production and conformity.

Celik, K., Meral, C., Gursel, A. P., Mehta, P. K., Horvath, A., & Monteiro, P. J. (2015). Mechanical properties, durability, and life-cycle assessment of self-consolidating concrete mixtures made with blended portland cements containing fly ash and limestone powder. *Cement and Concrete Composites, 56*, 59-72.

Chelgani, S. C., Parian, M., Parapari, P. S., Ghorbani, Y., & Rosenkranz, J. (2019). A comparative study on the effects of dry and wet grinding on mineral flotation separation–a review. *Journal of Materials Research and Technology, 8*(5), 5004-5011.

Chen, J., Ng, P. L., Chu, S., Guan, G., & Kwan, A. (2020). Ternary blending with metakaolin and silica fume to improve packing density and performance of binder paste. *Construction and Building Materials, 252*, 119031.

Chen, Q., Ma, R., Li, H., Jiang, Z., Zhu, H., & Yan, Z. (2021). Effect of chloride attack on the bonded concrete system repaired by UHPC. *Construction and Building Materials, 272*, 121971.

Cheng, S., Shui, Z., Sun, T., Yu, R., Zhang, G., & Ding, S. (2017). Effects of fly ash, blast furnace slag and metakaolin on mechanical properties and durability of coral sand concrete. *Applied Clay Science, 141*, 111-117.

Chia, K. S., & Zhang, M.-H. (2002). Water permeability and chloride penetrability of high-strength lightweight aggregate concrete. *Cement and Concrete Research, 32*(4), 639-645.

Chow, R. K., Yip, S. W., & Kwan, A. K. (2013). Processing crushed rock fine to produce manufactured sand for improving overall performance of concrete. *HKIE Transactions, 20*(4), 240-249.

Chu, S. (2019). Effect of paste volume on fresh and hardened properties of concrete. *Construction and Building Materials, 218*, 284-294.

Chu, S., Jiang, Y., & Kwan, A. (2019). Effect of rigid fibres on aggregate packing. *Construction and Building Materials, 224*, 326-335.

Collivignarelli, M. C., Cillari, G., Ricciardi, P., Miino, M. C., Torretta, V., Rada, E. C., & Abbà, A. (2020). The production of sustainable concrete with the use of alternative aggregates: A review. *Sustainability, 12*(19), 7903.

Dangi, V., & Soni, K. (2017). Improving The Engineering Properties Of Reinforced Concrete Modified With Coconut Shell Aggregates.

Das, B. B., Barbhuiya, S., Gupta, R., & Saha, P. (2021). Recent Developments in Sustainable Infrastructure: Select Proceedings of ICRDSI 2019. Springer.

Datta, R., Kelkar, A., Baraniya, D., Molaei, A., Moulick, A., Meena, R. S., & Formanek, P. (2017). Enzymatic degradation of lignin in soil: a review. *Sustainability, 9*(7), 1163.

De Larrard, F. (1999). Concrete mixture proportioning: a scientific approach. CRC Press.

De Larrard, F. (2000). Structures granulaires et formulation des bétons.

De Larrard, F., & Sedran, T. (1999). Une nouvelle approche de la formulation des bétons. Annales du BTP,

Deák, T., & Czigány, T. (2009). Chemical composition and mechanical properties of basalt and glass fibers: a comparison. *Textile Research Journal, 79*(7), 645-651.

Deepak, T. J., Jalam, A., Loh, E., Siow, Y. T., Nair, S., & Panjehpour, M. (2015). Prognostication of Concrete Characteristics with Coconut Shell as Coarse Aggregate Partial Percentile Replacement. *International Journal of Scientific Research in Science, Engineering and Technology, 1*(5), 45-50.

Dewar, J. (1986). Ready-mixed concrete mix design. *Municipal Engineering, 3*(1), 35-43.

Ealias, A. M., Rajeena, A., Sivadutt, S., John, L., & Paul, A. (2014). Improvement of Strength of Concrete with Partial Replacement Of Course Aggregate With Coconut Shell and Coir Fibres. *Journal of Mechanical and Civil Engineering, 11*, 16-24.

Ejaz, M. F., Aslam, M., Aziz, W., Khalil, M. J., Ali, M. J., Raheel, M., & Ahmed, A. (2022). Coconut shell waste as an alternative lightweight aggregate in concrete-A review. *Advances in Materials Research, 11*(4), 299-330.

Environment, U., Scrivener, K. L., John, V. M., & Gartner, E. M. (2018). Eco-efficient cements: Potential economically viable solutions for a low-CO2 cement-based materials industry. *Cement and Concrete Research, 114*, 2-26.

Eziefula, U. G. (2018). Developments in utilisation of agricultural and aquaculture by-products as aggregate in concrete–a review. *Environmental Technology Reviews, 7*(1), 19-45.

Fauziah, S. H., & Agamuthu, P. (2009). Sustainable household organic waste management via vermicomposting. *Malaysian Journal of Science, 28*(2), 135-142.

Feng, M., Wang, Z., & Wu, L. (2021). Experimental study on high-strength concrete, ultrahigh-strength concrete and corresponding mortar under triaxial compression. *Arabian Journal for Science and Engineering, 46*(11), 11179-11194.

Fennis-Huijben, S. A. A. M. (2011). Design of ecological concrete by particle packing optimization.

Feys, D., Verhoeven, R., & De Schutter, G. (2009). Why is fresh self-compacting concrete shear thickening? *Cement and Concrete Research, 39*(6), 510-523.

Food and Agriculture Organization of the United Nations. (2021). *Production Quantity; Items – Coconuts; Years – 2020 + 2019 + 2018 + 2017 + 2016*. FAOSTAT.

https://en.wikipedia.org/wiki/List_of_countries_by_coconut_production#cite_no te-FAO-pdf-3

Funk, J. E., & Dinger, D. R. (2013). *Predictive process control of crowded particulate suspensions: applied to ceramic manufacturing*. Springer Science & Business Media.

Furnas, C. (1931). Grading aggregates-I.-Mathematical relations for beds of broken solids of maximum density. *Industrial & Engineering Chemistry, 23*(9), 1052-1058.

Furnas, C. C. (1929). *Flow of gases through beds of broken solids* (Vol. 307). US Government Printing Office.

Gama, M., Gatenholm, P., & Klemm, D. (2012). *Bacterial nanocellulose: a sophisticated multifunctional material*. CRC press.

Goltermann, P., Johansen, V., & Palbøl, L. (1997). Packing of aggregates: an alternative tool to determine the optimal aggregate mix. *Materials Journal, 94*(5), 435-443.

Gong, K., & White, C. E. (2016). Impact of chemical variability of ground granulated blast-furnace slag on the phase formation in alkali-activated slag pastes. *Cement and Concrete Research, 89*, 310-319.

Guler, S., & Akbulut, Z. F. (2023). Workability, physical & mechanical properties of the cement mortars strengthened with metakaolin and steel/basalt fibers exposed to freezing-thawing periods. *Construction and Building Materials, 394*, 132100.

Gunasekaran, K., Annadurai, R., & Kumar, P. (2013). Study on reinforced lightweight coconut shell concrete beam behavior under flexure. *Materials & Design (1980-2015), 46*, 157-167.

Gunasekaran, K., Annadurai, R., & Kumar, P. (2015). A study on some durability properties of coconut shell aggregate concrete. *Materials and Structures, 48*(5), 1253-1264.

Gunasekaran, K., & Kumar, P. (2008). Lightweight concrete using coconut shells as aggregate. Proceedings of the ICACC-2008. International conference on advances in concrete and construction, Hyderabad, India,

Gunasekaran, K., Kumar, P., & Lakshmipathy, M. (2011). Mechanical and bond properties of coconut shell concrete. *Construction and Building Materials, 25*(1), 92-98.

Gunasekaran, K., Ramasubramani, R., Annadurai, R., & Chandar, S. P. (2014). Study on reinforced lightweight coconut shell concrete beam behavior under torsion. *Materials & Design, 57*, 374-382.

Guo, Y., Pan, H., Shen, A., Zhao, Z., Wu, H., & Li, Z. (2023). Fracture properties of basalt-fiber-reinforced bridge concrete under dynamic fatigue loading. Structures,

He, M., Wang, Y., & Forssberg, E. (2006). Parameter effects on wet ultrafine grinding of limestone through slurry rheology in a stirred media mill. *Powder technology, 161*(1), 10-21.

Hemmings, R. T., Cornelius, B. J., Yuran, P., & Wu, M. (2009). Comparative study of lightweight aggregates. World of Coal Ash (WOCA) Conference,

Hu, J., & Wang, K. (2007). Effects of size and uncompacted voids of aggregate on mortar flow ability. *Journal of advanced concrete technology, 5*(1), 75-85.

Hu, J., & Wang, K. (2011). Effect of coarse aggregate characteristics on concrete rheology. *Construction and Building Materials, 25*(3), 1196-1204.

Jackson, E., Mustapha, Z., & Kotey, S. (2019). Compressive strength of concrete produced with proportions of coconut and palm kernel shells. *International Journal of Architecture, Engineering and Construction, 8*(1), 35-41.

Jiang, C., Fan, K., Wu, F., & Chen, D. (2014). Experimental study on the mechanical properties and microstructure of chopped basalt fibre reinforced concrete. *Materials & Design, 58*, 187-193.

Jiang, C., Guo, W., Chen, H., Zhu, Y., & Jin, C. (2018). Effect of filler type and content on mechanical properties and microstructure of sand concrete made with superfine waste sand. *Construction and Building Materials, 192*, 442-449.

Jones, M., Zheng, L., & Newlands, M. (2002). Comparison of particle packing models for proportioning concrete constitutents for minimum voids ratio. *Materials and Structures, 35*, 301-309.

Junaid, M. F., ur Rehman, Z., Kuruc, M., Medveď, I., Bačinskas, D., Čurpek, J., Čekon, M., Ijaz, N., & Ansari, W. S. (2022). Lightweight concrete from a perspective of sustainable reuse of waste byproducts. *Construction and Building Materials, 319*, 126061.

Kabay, N. (2014). Abrasion resistance and fracture energy of concretes with basalt fiber. *Construction and Building Materials, 50*, 95-101.

Kamal, J., & Singh, J. (2015). Experimental Study On Strength Characteristics Of M25 Concrete With Partial Replacement Of Coarse Aggregate By Coconut Shell.

Kanojia, A., & Jain, S. K. (2017). Performance of coconut shell as coarse aggregate in concrete. *Construction and Building Materials, 140*, 150-156.

Karadumpa, C. S., & Pancharathi, R. K. (2021). Developing a novel mix design methodology for slow hardening composite cement concretes through packing density approach. *Construction and Building Materials, 303*, 124391.

Karbhari, V. M., & Strassler, H. (2007). Effect of fiber architecture on flexural characteristics and fracture of fiber-reinforced dental composites. *Dental Materials, 23*(8), 960-968.

Kareem, M., Raheem, A., Oriola, K., & Abdulwahab, R. (2022). A review on application of oil palm shell as aggregate in concrete-Towards realising a pollution-free environment and sustainable concrete. *Environmental Challenges, 8*, 100531.

Khan, M., Cao, M., Chu, S., & Ali, M. (2022). Properties of hybrid steel-basalt fiber reinforced concrete exposed to different surrounding conditions. *Construction and Building Materials, 322*, 126340.

Kockal, N. U., & Ozturan, T. (2011, 2011/04/01/). Strength and elastic properties of structural lightweight concretes. *Materials & Design, 32*(4), 2396-2403.

Kumar, N., & Kumar, D. (2012). Strength Properties of Coconut Shell as Coarse Aggregate In Concrete.

Kumar, V. P., Gunasekaran, K., & Shyamala, T. (2019). Characterization study on coconut shell concrete with partial replacement of cement by GGBS. *Journal of Building Engineering, 26*, 100830.

Kusumawardani, D. M., & Wong, Y. D. (2020). The influence of aggregate shape properties on aggregate packing in porous asphalt mixture (PAM). *Construction and Building Materials, 255*, 119379.

Kwan, A., & Mora, C. (2001). Effects of various shape parameters on packing of aggregate particles. *Magazine of Concrete Research, 53*(2), 91-100.

Kwan, A., Ng, P., & Huen, K. (2014). Effects of fines content on packing density of fine aggregate in concrete. *Construction and Building Materials, 61*, 270-277.

Kwan, A., & Wong, H. (2008). Effects of packing density, excess water and solid surface area on flowability of cement paste. *Advances in cement research, 20*(1), 1-11.

Kwan, A. K. (2000). Use of condensed silica fume for making high-strength, self-consolidating concrete. *Canadian Journal of Civil Engineering, 27*(4), 620-627.

Kwan, A. K., Mora, C., & Chan, H. (1999). Particle shape analysis of coarse aggregate using digital image processing. *Cement and Concrete Research, 29*(9), 1403-1410.

Kwan, A. K., & Wong, H. (2008). Packing density of cementitious materials: part 2—packing and flow of OPC+ PFA+ CSF. *Materials and Structures, 41*, 773-784.

Kwan, A. K. H., Chan, K. W., & Wong, V. (2013). A 3-parameter particle packing model incorporating the wedging effect. *Powder technology, 237*, 172-179.

Kwan, A. K. H., & Fung, W. (2009). Packing density measurement and modelling of fine aggregate and mortar. *Cement and Concrete Composites, 31*(6), 349-357.

Lange, F., Mörtel, H., & Rudert, V. (1997). Dense packing of cement pastes and resulting consequences on mortar properties. *Cement and Concrete Research, 27*(10), 1481-1488.

Lecomte, A., Zennir, A., & De Larrard, F. (1997). Modèle de suspension solide et formulation de bétons calcaires en Lorraine. *Bulletin-Laboratoires Des Ponts Et Chaussees*, 41-52.

Li, L., & Kwan, A. (2014). Packing density of concrete mix under dry and wet conditions. *Powder technology, 253*, 514-521.

Li, L., Lin, C., Chen, G., Kwan, A., & Jiang, T. (2017). Effects of packing on compressive behaviour of recycled aggregate concrete. *Construction and Building Materials, 157*, 757-777.

Li, L., Zhuo, H., Zhu, J., & Kwan, A. (2019). Packing density of mortar containing polypropylene, carbon or basalt fibres under dry and wet conditions. *Powder technology, 342*, 433-440.

Li, L. G., Chen, J.-J., & Kwan, A. K. (2017). Roles of packing density and water film thickness in strength and durability of limestone fines concrete. *Magazine of Concrete Research, 69*(12), 595-605.

Li, Y., Fang, J., Cheng, L., He, X., Su, Y., & Tan, H. (2022). Mechanical performance, hydration characteristics and microstructures of high volume blast furnace ferronickel slag cement mortar by wet grinding activation. *Construction and Building Materials, 320*, 126148.

Li, Y., Lei, W., Zhang, Q., Yang, Q., He, X., Su, Y., Tan, H., Liu, J., & Wang, G. (2022). Synergistic effects of steel slag and wet grinding on ambient cured ground granulated blast furnace slag activated by sodium sulfate. *Construction and Building Materials, 349*, 128661.

Li, Y., Wang, Q., Xu, S., & Song, Q. (2023). Study of eco-friendly fabricated hydrophobic concrete containing basalt fiber with good durability. *Journal of Building Engineering, 65*, 105759.

Lian, H., Sun, X., Yu, Z., Yang, T., Zhang, J., Li, G., Guan, Z., & Diao, M. (2022). Research on the fracture mechanical performance of basalt fiber nano-CaCO3 concrete based on DIC technology. *Construction and Building Materials, 329*, 127193.

Liu, G., Florea, M., & Brouwers, H. (2019). Performance evaluation of sustainable high strength mortars incorporating high volume waste glass as binder. *Construction and Building Materials, 202*, 574-588.

Liu, H., Li, Q., & Wang, P. (2023). Assessment of the engineering properties and economic advantage of recycled aggregate concrete developed from waste clay bricks and coconut shells. *Journal of Building Engineering, 68*, 106071.

Liu, Q., Jia, D., & Miao, J. (2020). Study of the linear and nonlinear packing model based on mixing of quartz sand. *Powder technology, 366*, 382-394.

Lu, J.-X. (2023). Recent advances in high strength lightweight concrete: From development strategies to practical applications. *Construction and Building Materials, 400*, 132905.

Lu, J.-X., Shen, P., Ali, H. A., & Poon, C. S. (2022). Mix design and performance of lightweight ultra high-performance concrete. *Materials & Design, 216*, 110553.

Lu, L., Han, F., Wu, S., Qin, Y., Yuan, G., & Doh, J. H. (2022). Experimental study on durability of basalt fiber concrete after elevated temperature. *Structural Concrete, 23*(2), 682-693.

Lv, J., Zhou, T., Du, Q., & Wu, H. (2015). Effects of rubber particles on mechanical properties of lightweight aggregate concrete. *Construction and Building Materials, 91*, 145-149.

Lyu, Z., Shen, A., & Meng, W. (2021). Properties, mechanism, and optimization of superabsorbent polymers and basalt fibers modified cementitious composite. *Construction and Building Materials, 276*, 122212.

Magrey, T., Malik, B., Akeeb Dar, M., & Bijran, N. (2016). Cocunut shell and Waste Glass based Concrete-A Comparative Study. *International Journal of Engineering Development and Research, 4*(1), 359-371.

Makaratat, N., Jaturapitakkul, C., & Laosamathikul, T. (2010). Effects of calcium carbide residue–fly ash binder on mechanical properties of concrete. *Journal of Materials in Civil Engineering, 22*(11), 1164-1170.

Matias, D., De Brito, J., Rosa, A., & Pedro, D. (2013). Mechanical properties of concrete produced with recycled coarse aggregates–Influence of the use of superplasticizers. *Construction and Building Materials, 44*, 101-109.

Meddah, M. S., Zitouni, S., & Belâabes, S. (2010). Effect of content and particle size distribution of coarse aggregate on the compressive strength of concrete. *Construction and Building Materials, 24*(4), 505-512.

Mehdipour, I., & Khayat, K. H. (2017). Effect of particle-size distribution and specific surface area of different binder systems on packing density and flow characteristics of cement paste. *Cement and Concrete Composites, 78*, 120-131.

Mehdipour, I., & Khayat, K. H. (2018). Understanding the role of particle packing characteristics in rheo-physical properties of cementitious suspensions: A literature review. *Construction and Building Materials, 161*, 340-353.

Mehta, P. K., & Monteiro, P. J. (2014). *Concrete: microstructure, properties, and materials*. McGraw-Hill Education.

Mo, K. H., Alengaram, U. J., & Jumaat, M. Z. (2015). Utilization of ground granulated blast furnace slag as partial cement replacement in lightweight oil palm shell concrete. *Materials and Structures, 48*, 2545-2556.

Mo, K. H., Alengaram, U. J., Jumaat, M. Z., Liu, M. Y. J., & Lim, J. (2016). Assessing some durability properties of sustainable lightweight oil palm shell concrete incorporating slag and manufactured sand. *Journal of Cleaner Production, 112*, 763-770.

Mora, C., & Kwan, A. (2000). Sphericity, shape factor, and convexity measurement of coarse aggregate for concrete using digital image processing. *Cement and Concrete Research, 30*(3), 351-358.

Moutassem, F. (2016). Assessment of packing density models and optimizing concrete mixtures. *Int. J. Civ. Mech. Energy Sci, 2*, 29-36.

Mukharjee, B. B., & Barai, S. V. (2014). Influence of incorporation of nano-silica and recycled aggregates on compressive strength and microstructure of concrete. *Construction and Building Materials, 71*, 570-578.

Nazari, A., & Riahi, S. (2011). The effects of TiO2 nanoparticles on physical, thermal and mechanical properties of concrete using ground granulated blast furnace slag as binder. *Materials Science and Engineering: A, 528*(4-5), 2085-2092.

Neville, A., & Brooks, J. (2002). Concrete Technology Longman Publisher.

Neville, A., & Brooks, J. (2008). Concrete Technology, revised edition.

Ogonowski, S., Wołosiewicz-Głąb, M., Ogonowski, Z., Foszcz, D., & Pawełczyk, M. (2018). Comparison of wet and dry grinding in electromagnetic mill. *Minerals, 8*(4), 138.

Ohemeng, E. A., & Ekolu, S. O. (2020). Comparative analysis on costs and benefits of producing natural and recycled concrete aggregates: A South African case study. *Case Studies in Construction Materials, 13*, e00450.

Oliveira, T. C., Dezen, B. G., & Possan, E. (2020). Use of concrete fine fraction waste as a replacement of Portland cement. *Journal of Cleaner Production, 273*, 123126.

Oliviera, I., Demond, A., & Salehzadeh, A. (1996). Packing of sands for the production of homogeneous porous media. *Soil Science Society of America Journal, 60*(1), 49-53.

Osei, D. Y. (2013). Experimental assessment on coconut shells as aggregate in concrete. *International journal of engineering science invention, 2*(5), 7-11.

Ozkan, A., Yekeler, M., & Calkaya, M. (2009). Kinetics of fine wet grinding of zeolite in a steel ball mill in comparison to dry grinding. *International journal of mineral processing, 90*(1-4), 67-73.

Patel, P., Arora, N., & Vaniya, S. R. (2015). Experiments on partial replacement of coconut shell as coarse aggregate in concrete. *Micron, 332*(694), 40-70.

Patino, F., Talan, D., & Huang, Q. (2022). Optimization of operating conditions on ultra-fine coal grinding through kinetic stirred milling and numerical modeling. *Powder technology, 403*, 117394.

Pavlović, A., Donchev, T., Petkova, D., & Staletović, N. (2022). Sustainability of alternative reinforcement for concrete structures: Life cycle assessment of basalt FRP bars. *Construction and Building Materials, 334*, 127424.

Pelisser, F., Zavarise, N., Longo, T. A., & Bernardin, A. M. (2011). Concrete made with recycled tire rubber: effect of alkaline activation and silica fume addition. *Journal of Cleaner Production, 19*(6-7), 757-763.

Pietsch, W. (1997). *Size enlargement by agglomeration*. Springer.

Polat, R., Demirboğa, R., Karakoç, M. B., & Türkmen, İ. (2010). The influence of lightweight aggregate on the physico-mechanical properties of concrete exposed to freeze–thaw cycles. *Cold Regions Science and Technology, 60*(1), 51-56.

Pordesari, A. J., Shafigh, P., Ibrahim, Z., & Aslam, M. (2021). Engineering properties of coconut shell lightweight concrete: A comparative study. *Advances in concrete construction, 12*(4), 303-316.

Powers, T. C. (1969). The properties of fresh concrete.

Powers, T. C., & Brownyard, T. L. (1946). Studies of the physical properties of hardened Portland cement paste. Journal Proceedings,

Prakash, R., Thenmozhi, R., & Raman, S. (2019). Mechanical characterisation and flexural performance of eco-friendly concrete produced with fly ash as cement replacement and coconut shell coarse aggregate. *International journal of Environment and sustainable Development, 18*(2), 131-148.

Prakash, R., Thenmozhi, R., Raman, S. N., & Subramanian, C. (2020). Fibre reinforced concrete containing waste coconut shell aggregate, fly ash and polypropylene fibre. *Revista Facultad de Ingenieria Universidad de Antioquia*(94).

Prakash, R., Thenmozhi, R., Raman, S. N., Subramanian, C., & Divyah, N. (2020). An investigation of key mechanical and durability properties of coconut shell concrete with partial replacement of fly ash. *Structural Concrete*.

Prakash, R., Thenmozhi, R., Raman, S. N., Subramanian, C., & Divyah, N. (2021). An investigation of key mechanical and durability properties of coconut shell concrete with partial replacement of fly ash. *Structural Concrete, 22*, E985-E996.

Prusty, J. K., & Patro, S. K. (2015). Properties of fresh and hardened concrete using agro-waste as partial replacement of coarse aggregate–A review. *Construction and Building Materials, 82*, 101-113.

Pyo, S., & Kim, H.-K. (2017). Fresh and hardened properties of ultra-high performance concrete incorporating coal bottom ash and slag powder. *Construction and Building Materials, 131*, 459-466.

RA. Dardak , M. R. (2021). Strengthening the Coconut Industry in Malaysia. https://ap.fftc.org.tw/article/2938

Rajeevan, B., & Shamjith, K. (2015). A study on the utilization of coconut shell as coarse aggregate in concrete. *Int. J. Eng. Res. Technol, 4*(07), 77-80.

Ravichandran, G. (2017). An Experimental Study On Strength Parameters Of Steel Or Plastic Fibers Using Coconut Shell Cement Concrete. *Journal of Industrial Pollution Control*, 1381-1386.

Reddy, B. D., Jyothy, S. A., & Shaik, F. (2014). Experimental analysis of the use of coconut shell as coarse aggregate. *J. Mech. Civil Eng, 10*(6), 6-13.

Reed, J. S. (1995). Principles of ceramics processing.

Reisi, M., & Nejad, D. M. (2011). A numerical method to predict packing density of aggregates in concrete. *Advanced Materials Research, 337*, 313-316.

Ren, G., Yao, B., Huang, H., & Gao, X. (2021). Influence of sisal fibers on the mechanical performance of ultra-high performance concretes. *Construction and Building Materials, 286*, 122958.

Roquier, G. (2016). The 4-parameter Compressible Packing Model (CPM) including a new theory about wall effect and loosening effect for spheres. *Powder technology, 302*, 247-253.

Roshavelov, T. (2005). Prediction of fresh concrete flow behavior based on analytical model for mixture proportioning. *Cement and Concrete Research, 35*(5), 831-835.

Roussel, N., Stéfani, C., & Leroy, R. (2005). From mini-cone test to Abrams cone test: measurement of cement-based materials yield stress using slump tests. *Cement and Concrete Research, 35*(5), 817-822.

Safiuddin, M., Kaish, A. A., Woon, C.-O., & Raman, S. N. (2018). Early-age cracking in concrete: Causes, consequences, remedial measures, and recommendations. *Applied Sciences, 8*(10), 1730.

Saidi, T., Hasan, M., Riski, A., Ayunizar, R., & Mubarak, A. (2020). Mix design and properties of reactive powder concrete with diatomaceous earth as cement replacement. IOP Conference Series: Materials Science and Engineering,

Sbia, L. A., Peyvandi, A., Harsini, I., Lu, J., Abideen, S. U., Weerasiri, R. R., Balachandra, A. M., & Soroushian, P. (2017). Study on field thermal curing of ultra-high-performance concrete employing heat of hydration. *ACI Materials Journal, 114*(5), 733-744.

Sedran, T., de LARRARD, F., & Angot, D. (1994). Prévision de la compacité des mélanges granulaires par le modèle de suspension solide-I-Fondements théoriques et étalonnage du modèle. *Bulletin de liaison des Laboratoires des Ponts et Chaussées*(194).

Sekar, A., & Kandasamy, G. (2018). Optimization of Coconut Fiber in Coconut Shell Concrete and Its Mechanical and Bond Properties. *Materials, 11*(9), 1726. https://mdpi-res.com/d_attachment/materials/materials-11-01726/article_deploy/materials-11-01726.pdf?version=1536913793

Sekar, S. (2016). Mechanical and fracture characteristics of Eco-friendly concrete produced using coconut shell, ground granulated blast furnace slag and manufactured sand. *Construction and Building Materials, 103*, 1-7.

Selwyn Babu, J., & Mahendran, N. (2014). Coconut Shell as a Partial Replacement to Coarse Aggregate in Concrete. *Australian Journal of Basic and Applied Sciences, 8*(13), 693-697.

Senik, G. (1995). *Small-scale food processing enterprises in Malaysia*. Food and Fertilizer Technology Center.

Shafigh, P., Mahmud, H. B., Jumaat, M. Z., & Zargar, M. (2014). Agricultural wastes as aggregate in concrete mixtures–A review. *Construction and Building Materials, 53*, 110-117.

Shafigh, P., Nomeli, M. A., Alengaram, U. J., Mahmud, H. B., & Jumaat, M. Z. (2016). Engineering properties of lightweight aggregate concrete containing limestone powder and high volume fly ash. *Journal of Cleaner Production, 135*, 148-157.

Shahbandeh, M. (2023). *Coconut production worldwide in 2021, by leading country*. Statista. Retrieved 25 January 2023 from https://www.statista.com/statistics/1040499/world-coconut-production-by-leading-producers/

Shao, R., Wu, C., Li, J., Liu, Z., Wu, P., & Yang, Y. (2023). Mechanical behaviour and environmental benefit of eco-friendly steel fibre-reinforced dry UHPC incorporating high-volume fly ash and crumb rubber. *Journal of Building Engineering, 65*, 105747.

Shen, P., Zheng, H., Xuan, D., Lu, J.-X., & Poon, C. S. (2020). Feasible use of municipal solid waste incineration bottom ash in ultra-high performance concrete. *Cement and Concrete Composites, 114*, 103814.

Smith, L. (2003). Knowledge based system for powder metallurgy. *Powder Metallurgy, 46*(1), 9-10.

Sobolev, K., & Amirjanov, A. (2007). The simulation of particulate materials packing using a particle suspension model. *Advanced Powder Technology, 18*(3), 261-271.

Sohail, M. G., Alnahhal, W., Taha, A., & Abdelaal, K. (2020). Sustainable alternative aggregates: Characterization and influence on mechanical behavior of basalt fiber reinforced concrete. *Construction and Building Materials, 255*, 119365.

SSEN12620. (2013). Specification for aggregates for concrete.

Stovall, T., De Larrard, F., & Buil, M. (1986). Linear packing density model of grain mixtures. *Powder technology, 48*(1), 1-12.

Subramani, T., & Anbuvel, A. (2016). Experimental behaviour of reinforced concrete beams with coconut shell as coarse aggregate. *International Journal of Application or Innovation in Engineering & Management (IJAIEM), 5*(5), 067-075.

Supit, S. W. M., & Shaikh, F. U. A. (2015). Durability properties of high volume fly ash concrete containing nano-silica. *Materials and Structures, 48*, 2431-2445.

Tan, H., Li, M., He, X., Su, Y., Yang, J., & Zhao, H. (2021). Effect of wet grinded lithium slag on compressive strength and hydration of sulphoaluminate cement system. *Construction and Building Materials, 267*, 120465.

Tao, Y., Hadigheh, S., & Wei, Y. (2023). Recycling of glass fibre reinforced polymer (GFRP) composite wastes in concrete: A critical review and cost benefit analysis. Structures,

Terzić, A., Pezo, L., Mitić, V., & Radojević, Z. (2015). Artificial fly ash based aggregates properties influence on lightweight concrete performances. *Ceramics International, 41*(2), 2714-2726.

Toufar, W., Born, M., & Klose, E. (1976). Contribution of optimisation of components of different density in polydispersed particles systems. *Freiberger booklet A, 558*, 29-44.

Ünal, M., Gökçe, H., Ayough, P., Alnahhal, A., Şimşek, O., & Nehdi, M. (2023). Nanomaterial and fiber-reinforced sustainable geopolymers: A systematic critical review. *Construction and Building Materials, 404*, 133325.

Ünal, M. T., & Şimşek, O. (2021). Çimento harçlarında optimum uçucu kül ve PVA lif oranının belirlenmesi. *Politeknik Dergisi, 25*(2), 477-489.

Wang, D., Wang, H., Larsson, S., Benzerzour, M., Maherzi, W., & Amar, M. (2020). Effect of basalt fiber inclusion on the mechanical properties and microstructure of cement-solidified kaolinite. *Construction and Building Materials, 241*, 118085.

Wang, J., Tan, H., He, X., Zhang, J., Jian, S., Du, C., & Deng, X. (2022). Influence of wet grinded slag on the hydration of phosphogypsum-slag based cement and its application in backfill tailings. *Construction and Building Materials, 360*, 129509.

Wang, J., Zheng, K., Cui, N., Cheng, X., Ren, K., Hou, P., Feng, L., Zhou, Z., & Xie, N. (2020). Green and durable lightweight aggregate concrete: the role of waste and recycled materials. *Materials, 13*(13), 3041.

Wang, X., Yu, R., Song, Q., Shui, Z., Liu, Z., Wu, S., & Hou, D. (2019). Optimized design of ultra-high performance concrete (UHPC) with a high wet packing density. *Cement and Concrete Research, 126*, 105921.

Wang, Y., He, X., Su, Y., Tan, H., Yang, J., Lan, M., Ma, M., & Strnadel, B. (2018). Self-hydration characteristics of ground granulated blast-furnace slag (GGBFS) by wet-grinding treatment. *Construction and Building Materials, 167*, 96-105.

Wang, Y., Zhang, S., Niu, D., Su, L., & Luo, D. (2020). Strength and chloride ion distribution brought by aggregate of basalt fiber reinforced coral aggregate concrete. *Construction and Building Materials, 234*, 117390.

Westerholm, M., Lagerblad, B., Silfwerbrand, J., & Forssberg, E. (2008). Influence of fine aggregate characteristics on the rheological properties of mortars. *Cement and Concrete Composites, 30*(4), 274-282.

Wong, H. H., & Kwan, A. K. (2005). Packing density: a key concept for mix design of high performance concrete. Proceedings of the materials science and technology in engineering conference, HKIE materials division, Hong Kong,

Wong, H. H., & Kwan, A. K. (2008). Packing density of cementitious materials: part 1—measurement using a wet packing method. *Materials and Structures, 41*, 689-701.

Wong, V., & Kwan, A. (2014). A 3-parameter model for packing density prediction of ternary mixes of spherical particles. *Powder technology, 268*, 357-367.

Wong, V., Wai Chan, K., & Kwok Hung Kwan, A. (2013). Applying theories of particle packing and rheology to concrete for sustainable development. *Organization, technology & management in construction: an international journal, 5*(2), 844-851.

Wu, M., Zhang, Y., Liu, G., Wu, Z., Yang, Y., & Sun, W. (2018). Experimental study on the performance of lime-based low carbon cementitious materials. *Construction and Building Materials, 168*, 780-793.

Wu, T., Yang, X., Wei, H., & Liu, X. (2019). Mechanical properties and microstructure of lightweight aggregate concrete with and without fibers. *Construction and Building Materials, 199*, 526-539.

Xiaopeng, L. (2005). Structural lightweight concrete with pumice aggregate.

Xie, Y., Liu, B., Yin, J., & Zhou, S. (2002). Optimum mix parameters of high-strength self-compacting concrete with ultrapulverized fly ash. *Cement and Concrete Research, 32*(3), 477-480.

Xu, Z., Gao, J., Zhao, Y., Li, S., Guo, Z., Luo, X., & Chen, G. (2022). Promoting utilization rate of ground granulated blast furnace slag (GGBS): Incorporation of nanosilica to improve the properties of blended cement containing high volume GGBS. *Journal of Cleaner Production, 332*, 130096.

Yang, J., Huang, J., He, X., Su, Y., Tan, H., Chen, W., Wang, X., & Strnadel, B. (2019). Segmented fractal pore structure covering nano-and micro-ranges in cementing composites produced with GGBS. *Construction and Building Materials, 225*, 1170-1182.

Yang, J., Huang, J., Su, Y., He, X., Tan, H., Yang, W., & Strnadel, B. (2019). Eco-friendly treatment of low-calcium coal fly ash for high pozzolanic reactivity: A step towards waste utilization in sustainable building material. *Journal of Cleaner Production, 238*, 117962.

Yang, J., Zeng, J., He, X., Hu, H., Su, Y., Bai, H., & Tan, H. (2021). Eco-friendly UHPC prepared from high volume wet-grinded ultrafine GGBS slurry. *Construction and Building Materials, 308*, 125057.

Yang, J., Zeng, J., He, X., Su, Y., Tan, H., & Strnadel, B. (2020). Nano-carbide slag seed as a new type accelerator for Portland cement. *Materials Letters, 278*, 128464.

Yang, J., Zeng, J., He, X., Zhang, Y., Su, Y., & Tan, H. (2022). Sustainable clinker-free solid waste binder produced from wet-ground granulated blast-furnace slag, phosphogypsum and carbide slag. *Construction and Building Materials, 330*, 127218.

Yaşar, E., ATIŞ, C. D., & Kiliç, A. (2004). High strength lightweight concrete made with ternary mixtures of cement-fly ash-silica fume and scoria as aggregate. *Turkish Journal of Engineering and Environmental Sciences, 28*(2), 95-100.

Yazıcı, H., Yardımcı, M. Y., Aydın, S., & Karabulut, A. Ş. (2009). Mechanical properties of reactive powder concrete containing mineral admixtures under different curing regimes. *Construction and Building Materials, 23*(3), 1223-1231.

Yerramala, A., & Ramachandrudu, C. (2012). Properties of concrete with coconut shells as aggregate replacement. *International journal of engineering inventions, 1*(6), 21-31.

Yıldırım, M., & Özhan, H. B. (2023). Durability properties of basalt fiber-reinforced mortars with different mineral admixtures exposed to high temperatures. *Construction and Building Materials, 400*, 132574.

Yoo, D.-Y., Oh, T., & Banthia, N. (2022). Nanomaterials in ultra-high-performance concrete (UHPC)–A review. *Cement and Concrete Composites*, 104730.

Yu, R., Spiesz, P., & Brouwers, H. (2015). Development of an eco-friendly Ultra-High Performance Concrete (UHPC) with efficient cement and mineral admixtures uses. *Cement and Concrete Composites, 55*, 383-394.

Zeng, Y., & Tang, A. (2021). Comparison of effects of basalt and polyacrylonitrile fibers on toughness behaviors of lightweight aggregate concrete. *Construction and Building Materials, 282*, 122572.

Zhang, J., An, X., & Nie, D. (2016). Effect of fine aggregate characteristics on the thresholds of self-compacting paste rheological properties. *Construction and Building Materials, 116*, 355-365.

Zhang, J., An, X., Yu, Y., & Nie, D. (2019). Effects of coarse aggregate content on the paste rheological thresholds of fresh self-compacting concrete. *Construction and Building Materials, 208*, 564-576.

Zhang, J., Tan, H., He, X., Yang, W., & Deng, X. (2020). Utilization of carbide slag-granulated blast furnace slag system by wet grinding as low carbon cementitious materials. *Construction and Building Materials, 249*, 118763.

Zhang, J., Tan, H., He, X., Yang, W., Deng, X., Su, Y., & Yang, J. (2019). Compressive strength and hydration process of ground granulated blast furnace slag-waste gypsum system managed by wet grinding. *Construction and Building Materials, 228*, 116777.

Zhang, M.-H., & GjorvI, O. E. (1990). Development of high-strength lightweight concrete. *Special Publication, 121*, 667-682.

Zhou, M., Wu, Z., Ouyang, X., Hu, X., & Shi, C. (2021). Mixture design methods for ultra-high-performance concrete-a review. *Cement and Concrete Composites, 124*, 104242.

Zhu, C., Tan, H., Du, C., Wang, J., Deng, X., Zheng, Z., & He, X. (2023). Enhancement of ultra-fine slag on compressive strength of solid waste-based cementitious materials: Towards low carbon emissions. *Journal of Building Engineering, 63*, 105475.

Zou, R., & Yu, A.-B. (1996). Evaluation of the packing characteristics of mono-sized non-spherical particles. *Powder technology, 88*(1), 71-79.

Zulcão, R., Calmon, J. L., Rebello, T. A., & Vieira, D. R. (2020). Life cycle assessment of the ornamental stone processing waste use in cement-based building materials. *Construction and Building Materials, 257*, 119523.